N7035954

MEASUREMENT AND CORRELATION OF HELIUM AND FLUID LEAK RATES

BOEING CO., WASHINGTON, D. C

29 JUL 1970

THE [redacted]

CONTRACT NO. 9120

NUMBER D2-114258-1

TITLE: MEASUREMENT AND CORRELATION OF HELIUM AND FLUID LEAK RATES

ORIGINAL RELEASE DATE 7/29 FOR THE RELEASE DATE OF SUBSEQUENT REVISIONS, SEE THE REVISIONS SHEET. FOR LIMITATIONS IMPOSED ON THE DISTRIBUTION AND USE OF INFORMATION CONTAINED IN THIS DOCUMENT, SEE THE LIMITATIONS SHEET.

MODEL Apollo CONTRACT NASW-1650

ISSUE NO ISSUED TO

Boeing-Houston

Concurrence
C. A. Prier
5-2962

J. M. Carter
5-2940

A. W. Blair

PREPARED BY
Allen E. Senear

SUPERVISED BY
C. D. Burns

APPROVED BY
E. E. Bauer

APPROVED BY

PREPARED FOR
NATIONAL AERONAUTICS AND SPACE ADMINISTRATION
MANNED SPACECRAFT CENTER
HOUSTON, TEXAS

ABSTRACT

This document reports the results of an extensive series of fluid leak correlation tests performed at The Boeing Space Center, Kent; during 1963. Helium leakage was correlated with leakage of Apollo Propellants nitrogen tetroxide, monomethylhydrazine, and Aerozine-50 and Apollo ECS fluids water, water/glycol (several proportions), hydrogen, oxygen, and nitrogen. In addition, several currently used methods of helium leak detection were evaluated. Detailed descriptions of the apparatus and procedures used, test results obtained, theoretical interpretation of these results and conclusions and recommendations drawn from the program are presented. Summary graphs relating fluid leak rates to helium leak rates are presented but must be used with caution (as discussed in Section 5.0). This work was prepared for the NASA Manned Spacecraft Center, Houston, Texas, in coordination with Boeing-Houston, as part of Apollo TIE Contract NASw-1650.

KEY WORDS

Apollo	ECS Fluids
Leak	Methods
Testing	Correlation
Helium	Analysis
Propellants	

TABLE OF CONTENTS

TABLE OF CONTENTS (Continued)

TABLE OF CONTENTS (Continued)

THE BOEING COMPANY

LIST OF FIGURES

LIST OF FIGURES (Continued)

LIST OF FIGURES (Continued)

LIST OF TABLES

LIST OF TABLES (Continued)

LIST OF TABLES (Continued)

LIST OF REFERENCES

1. Memo 5-2746-HOU-080, N. D. Boring to T. P. Nelson, November 16, 1967.

2. IDWA-HOU-5-2-1-074, February 7, 1968.

3. Memo 5-2746-HOU-23-036, C. A. Krier to E. E. Bauer, February 9, 1968.

4. Memo 5-2746-HOU-23-056, C. A. Krier to E. E. Bauer, April 8, 1968.

5. Specification MSC-SPEC-C-6A, "Apollo Spacecraft - Fluid Cleanliness, Specification for", October 15, 1965.

6. Specification MSC-PPB-2, "Propellant, Inhibited Nitrogen Tetroxide", February 1, 1966.

7. Specification MIL-P-27402, "Propellant, Hydrazine-uns-Dimethylhydrazine (50% N_2H_4-50% UDMH), 25 August 1961.

8. B. E. Saltzman, "Colorimetric Microdetermination of Nitrogen Dioxide in the Atmosphere", Anal. Chem. 26, 1949 (1954).

9. F. Fiegl, "Spot Tests in Inorganic Analysis, 5th Ed.", Elsevier Publishing Co., Amsterdam, 1958.

10. M. K. Pinkerton, et al, "A Colorimetric Determination of 1, 1-Dimethylhydrazine in Air, Blood and Water", ASD Tech. Report 61-708 (December 1961).

11. E. Elvove, "A Note on the Detection and Estimation of Small Amounts of Methyl Alcohol", Ind. Eng. Chem. 9, 295 (1917).

12. Belcher, "Submicro Methods of Organic Analysis", Elsevier Publishing Co., Amsterdam, 1966.

13. North American-Rockwell Corporation Drawing No.'s R-213291-101 through R-213291-108.

14. Ace Rubber Company, Southgate, California, Part No.'s SMD-9-0439-5 and SMD-9-0439-10.

15. J. W. Marr, "Leakage Testing Handbook", Report 3-67-1014, prepared by the General Electric Corp. for the Jet Propulsion Laboratory under Contract NAS7-396.

16. J. Amesz, "Conversion of Leak Flow-Rates for Various Fluids and Different Pressure Conditions", EUR 2482.e, published by European Atomic Energy Community, 1966.

17. H. Jamison, "An Investigation of the Correlation Between Helium and Apollo Propellant Leak Determinations", NASA Internal Note #MSC-EP-T-67-29, December 22, 1967.

ACKNOWLEDGEMENTS

The majority of the experimental work in this program was performed by Messrs. A. E. Senear, A. W. Blair, N. J. Munsey, and D. J. Ottestad of this laboratory, directed by Mr. C. D. Burns. Support in metallographic examination of plugged leaks was provided by Dr. E. C. Roberts and personnel of the Metallurgical Laboratory. Mr. J. Hall of the Quality Control Development organization performed the mass spectrometric measurements and assisted in the fluid leak correlation tests. Mr. E. Strobelt of the Quality Control Development organization assisted in the initial planning of the program and provided direction in set-up of the mass spectrometer and analysis of the resulting data.

This report was prepared by Dr. A. E. Senear and Mr. A. W. Blair with the assistance of Messrs. D. J. Ottestad and N. J. Munsey. Guidance was provided by Messrs. J. M. Gunderson, P. S. Holman, C. A. Krier and J. M. Carter of Boeing-Houston.

Mr. H. Brasseaux NASA/MSC collaborated in establishing the testing sequence and techniques for this program. The results of the earlier work (Reference 17) done by H. Jamison, H. Brasseaux and P. K. McCheehy, Propulsion and Power Division NASA Manned Spacecraft Center, provided baseline techniques.

1.0 INTRODUCTION

This document reports the results of a test program on leak testing, and correlation of fluid leak rates, carried out at the Boeing Space Center during the first half of 1968. Several methods of helium leak rate measurements were tested, and compared. Experimental correlations were developed between measured helium leak rates and leak rates observed for nine fluids used in the Apollo spacecraft, three propellants (nitrogen tetroxide, monomethylhydrazine and Aerozine-50); five fluids related to the environmental control system (oxygen gas, three water/glycol solutions, and potable water); and two additional gases (nitrogen and hydrogen). The purpose of this study was to furnish data bearing on the practical implications of helium leak testing of Apollo systems; e.g., to enable a decision to be made concerning what level of helium leakage, measured by some specific technique, would indicate a potentially dangerous leakage rate for one of the spacecraft fluids. An additional objective was to assess the applicability of theoretical leakage calculations to the correlation of helium and Apollo fluid leak rates. The work was designed to support efforts of Boeing-Houston and MSC personnel in developing adequate leakage measurement methods for the Apollo spacecraft

1.1 Program Origin

This work was initiated as a result of a request from Boeing-Houston (Reference 1) and authorized according to Reference 2.

The original program plan was set up during a meeting in Houston in December 1967, attended by Mr. Austin Blair and Mr. Douglas Ottestad of this laboratory. The original detailed statement of work is contained in Reference 3, and a revised work statement is contained in Reference 4 This report includes data dealing with each item of the test plan, with a few minor variations in detail.

1.2 Program Objectives

The primary objective of this program was to correlate measured helium leakage rates and measured leakage rates of several Apollo spacecraft fluids for various types of small leaks. Secondary objectives included:

1. To compare the experimentally observed correlations between helium and fluid leakage rates with the predictions of theoretical correlations.

2. To compare the available methods for measuring helium leak rates from spacecraft components and systems, in order to support Boeing-Houston personnel in the preparation of adequate spacecraft leakage specifications.

3. To gain experience with changes in leak rates of various fluids with exposure time, and to determine the effects of contamination, corrosive attack on the leak, etc. to aid in understanding actual hardware leak situations.

1.2.1 Helium Leak Testing Methods

Two basic instruments were utilized; a Bendix mass spectrometer and a CEC Leak Detector.* The latter was used in several configurations, with the leak plumbed directly into its inlet, with a hand-held pumped probe moving across the container surface while the container was filled with helium, and with the leak area surrounded by an alligator boot, which was directly connected to the leak detector. These test methods were briefly compared with each other in regards to accuracy and sensitivity, and were also compared with application of leak detecting fluid to a pressurized system.

1.2.2 Correlation of Helium and Fluid Leak Rates

This effort comprised the major portion of the laboratory work. As described in the experimental techniques section, three types of metal leaks as well as glass leaks were tested. The general procedure was to measure a helium leak rate by an appropriate technique (depending on the size of the leak), to fill a reservoir attached to the leak with test fluid, pressurize to several pressures, and measure fluid leak rates. After completion of this test the helium leak rate was then remeasured to determine whether the leak had been altered by exposure to the fluid. Separate graphs are presented for each leak-fluid combination, and a summary graph for each fluid is presented.

Each graph contains a curve of the theoretically expected leak rate for the test fluid, calculated from the observed helium leak rate. These calculations are described in Section 5 of this report. Where the helium leak rates before and after fluid exposure are quite different, theoretical curves corresponding to both conditions are presented.

1.2.3 Data Applicable to Hardware Leaks

The chief conclusion applicable to actual hardware derived from these experiments is the very great susceptibility of small leaks (10^{-1} cc/sec of helium and lower) to partial or complete blockage. We found it necessary to take very careful precautions, both in system cleanliness, and in fluid filtration, in order to obtain reproducible data. This suggests that any leak criteria based upon these results would probably be conservative. Several "historical" graphs are included, detailing the type of changes observed with time

*Referred to as MSLD (Mass Spectrometer Leak Detector).

in leak rates of propellants in metal leaks. These probably have no scientific value, but do represent the type of phenomenon which can be anticipated in actual hardware. In order to overcome the difficulty with plugging, we have made extensive use of glass capillary leaks. This was not done to avoid fluid-metal interactions, but to enable us to use a visual criteria for leakage which allowed us to run tests with microgram quantities of test fluid, thus cutting down greatly the potential for blockage.

2.0 EXPERIMENTAL TECHNIQUES

The techniques used for preparing test leaks, for measuring fluid leak rates, for cleaning and assembling leak testing hardware, and for purifying test fluids underwent an evolutionary process throughout the test program. In the section on specific test results an attempt has been made in each instance to identify the experimental conditions in sufficient detail so that data interpretation can be meaningful. In the following paragraphs an attempt is made to describe how our techniques evolved, and to express our thoughts on the most satisfactory test procedures.

The major experimental difficulty which became apparent immediately upon beginning the program was the very great susceptibility of these small leaks to becoming blocked or plugged. Although care had been taken to assemble a clean pressure system, the first few attempts to measure nitrogen tetroxide leakage resulted in rapid loss of flow. Subsequently the leaks were found to be clogged with a combination of bright metal chips, inorganic particles, and a resinous substance. The latter, according to infrared spectroscopy, contained both Kel-F grease and some organic compound containing both aliphatic carbon-hydrogen and carbonyl bonds.

The entire system was checked, with negative results, to ascertain the source of Kel-F and organic contamination. It may have been carried into the leak from gages and valves in the high pressure helium leak setting system, or leached by N_2O_4 from gages, valves and fittings in the test manifold. The metal chips were assumed to have come from torquing unlubricated stainless steel fittings.

As a result of this experience the entire apparatus was disassembled. All of the plumbing involved in leak calibration or testing was cleaned with great care. The welded or formed metal parts were degreased and cleaned using standard methods and then flushed with filtered solvents. The valves, gages and other hardware were cleaned with filtered solvents and the systems utilizing these parts were assembled in a clean bench. The assembled systems were then solvent-flushed again and evacuated to insure the removal of all of the solvent vapors. The use of Millipore filters on the gas inlet side of all of the systems insured against recontamination.

The entire system was rebuilt and all the valves replaced between the N_2O_4 and hydrazine tests. In spite of this care contamination was again encountered when work on monomethylhydrazine was begun. The fuel removed from the apparatus after the test was brown in color, and left a residue on evaporation. This difficulty was traced, in part, to the use by the manufacturer of Kel-F grease in inserting a plug into the valve body which compressed a Teflon seal against the ball. The Kel-F was trapped in a dead volume between two Teflon seals, where ordinary cleaning did not reach it, yet valve disassembly after the test showed that monomethylhydrazine had leaked past the Teflon seals into this volume.

In spite of taking every possible precaution, short of shifting the entire operation into a clean room, leak plugging and blocking continued to be a major problem. We have not reported all cases of blocked leaks in the data section, but have included a representative sample.

2.1 Measurement of Helium Leak Rates

The primary objective of these measurements was to calibrate experimental leaks to be used for studying leak rates of other fluids. Two major approaches were used. Early in the program we used a helium leak detector for measuring helium leak rates wherever possible. In cases where our leaks were so large that the detector was saturated we used volumetric water displacement techniques. Towards the end of the program our viewpoint shifted, and we used volumetric techniques wherever possible, using the leak detector only for very small leaks in the 10^{-5} and 10^{-6} cc/sec helium range. This reversal in attitude was based upon the versatility of volumetric procedures, and the time required in calibrating the leak detector. This opinion would probably not hold in the case of a program of routine repetitive testing.

Several other helium leak detection methods were investigated briefly in order to assess their value for leak testing actual hardware. These included use of leak testing fluid, use of a probe and the helium leak detector, and use of an alligator boot with the helium leak detector, all in connection with a helium pressurized leaking system.

Leak rates in this report are given in cubic centimeters per second (cc/sec). Leak rates were actually measured in milliliters per second (ml/sec), in standard centimeters per second (scc/sec), or in atmosphere-cubic centimeters per second (atm-cc/sec), depending upon the leak test method used, and the units used in calibrating the reference standard leaks. In comparison with the accuracy of the measurements and the scale on which the data is plotted, the differences between these units are inconsequential.

In the body of this report leaks are referred to as being within some range such as 10^{-2} to 10^{-4}. In all cases this refers to leak rates in cc/sec of helium.

2.1.1 Helium Leak Detector

Two helium leak detectors were used in this program. A schematic diagram of the testing manifold is shown in Figure 1. At times during the program a CEC Model 24-120B was substituted for the Model 24-120A instrument shown. This latter model has two additional attenuation factors of 5,000 and 10,000, beyond the maximum attenuation available from the Model A; thus allowing much larger leaks to be studied. This advantage,

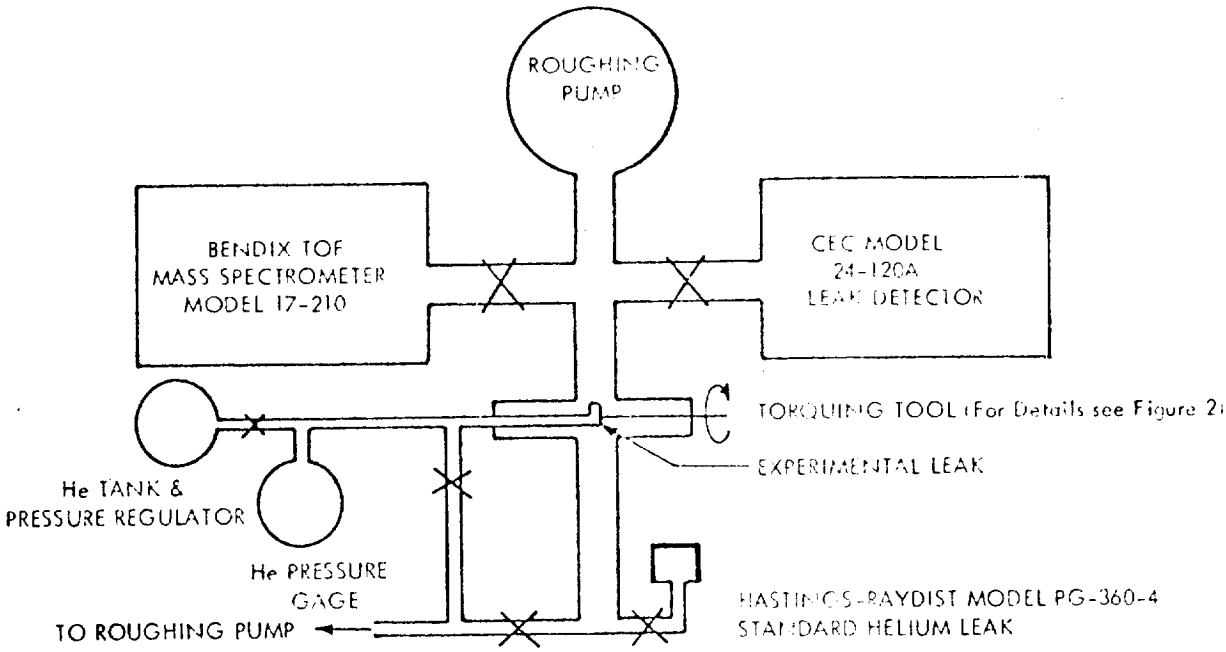

FIGURE 1. VACUUM MANIFOLD FOR SETTING AND CALIBRATING HELIUM LEAKS

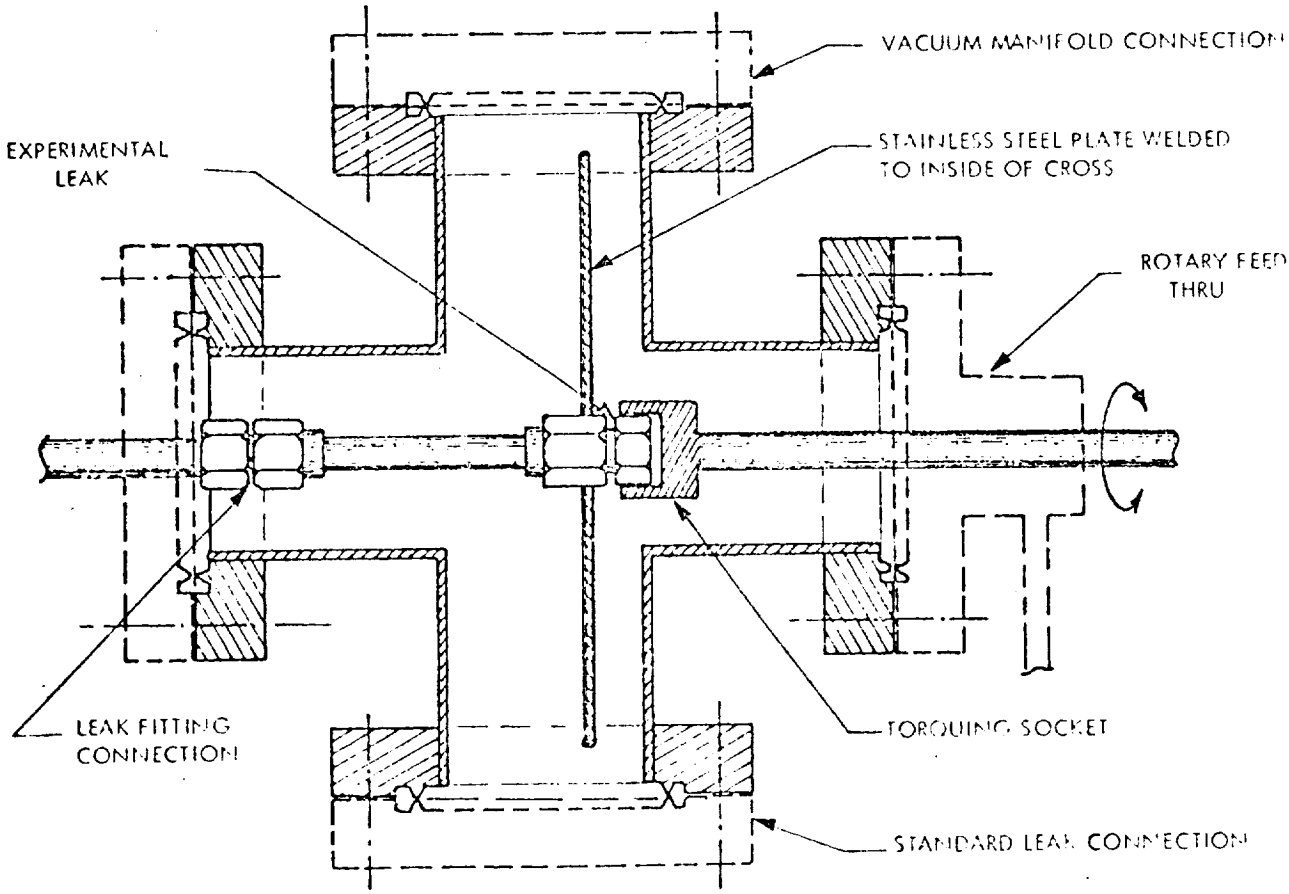

FIGURE 2. DETAIL OF TORQUING TOOL FOR ADJUSTING HELIUM LEAKS WITHIN VACUUM PLENUM

however, was somewhat negated by the observation that the amplifiers for the high and low ranges were sufficiently different so that the instrument could not be balanced and calibrated to use both sets of ranges at the same time.

An experimental leak was set at the desired value as follows: The leak was mounted within the vacuum manifold in the special torquing tool (Figure 2). The leak detector background reading was recorded. A Hastings-Raydist, Inc. Model PG-360-4 standard helium leak was valved into the manifold. This leak had been calibrated at the Boeing Primary Standards Laboratory and found to possess a leak rate of 5.70×10^{-6} atm cc/sec, while leaking from 1 atm to vacuum at 84°F. The leak detector response was noted, and a sensitivity factor calculated in terms of atm-cc of helium/second/leak detector scale division.

Two other fixed rate standard leaks were used for calibrating low helium leak rate leaks. A variable leak rate glass capillary standard leak was fabricated and calibrated by the Boeing Primary Standards Laboratory for use in calibrating relatively large test leaks.

The experimental leak was then supplied with helium at the desired pressure, and the increase in instrument reading noted. From this reading increase and the previously calculated sensitivity factor, the helium leak rate was calculated as follows:

$$\text{Leak rate} = (\text{atm-cc/sec}) = \frac{A - B}{B} \cdot R$$

where A = instrument reading with both standard and test leaks in system.

B = instrument reading with standard leak only in system.

R = leak rate of standard leak in atm-cc/sec.

The leak was then slowly compressed in the torquing tool until a detector response corresponding to the desired leak rate was attained. At this point the leak rate of the experimental leak was measured at each pressure value. The leak detector zero reading and sensitivity factors were checked periodically during these measurements.

2.1.2 Volumetric Techniques

Several types of equipment were used for these measurements at different times. In every case helium was allowed to leak from the test leak, pressurized on the upstream side with filtered gas, into a short length of Tygon vacuum tubing directly attached to the top of a water-filled burette. Burettes ranging in volume from fifty microliters to 100 ml were used for various sized leaks. A leveling bulb was attached to the bottom of the burette, and the time required to collect a known volume of gas at room temperature and pressure was measured with a stopwatch. All volumes presented in the data sheets are uncorrected, representing helium volumes at ambient pressure, at room temperature, and partly or completely saturated with water vapor. Room temperature remained quite constant at 70-72°F during these tests, except for the last few runs in June, when temperatures as high as 82°F were encountered.

The metal leaks used with hydrazine and nitrogen tetroxide were attached to the pressure manifold shown in Figure 3, with the leak placed inside the small glass chamber shown. This permitted measurement of the helium leak rate by attaching the gas burette to one of the glass side arms, introduction of test liquid into the reservoir, pressurization, measurement of the liquid leak rate by sweeping, followed by removal of residual liquid by evacuation, and a measurement of the final helium leak rate, with minimum exposure of the system or leak to the laboratory environment.

Initially leaks in the 10^{-4} cc/sec of helium range were measured using the CEC leak detector, due to the very long time period required to collect sufficiently large volumes of helium to measure accurately. Later in the program the simple apparatus shown in Figure 4 was developed using a 50 microliter Hamilton syringe as a gas burette. This proved to be very suitable for measuring helium leak rates in the 10^{-4} cc/sec range, and with a little patience could be used at 10^{-5} cc/sec of helium.

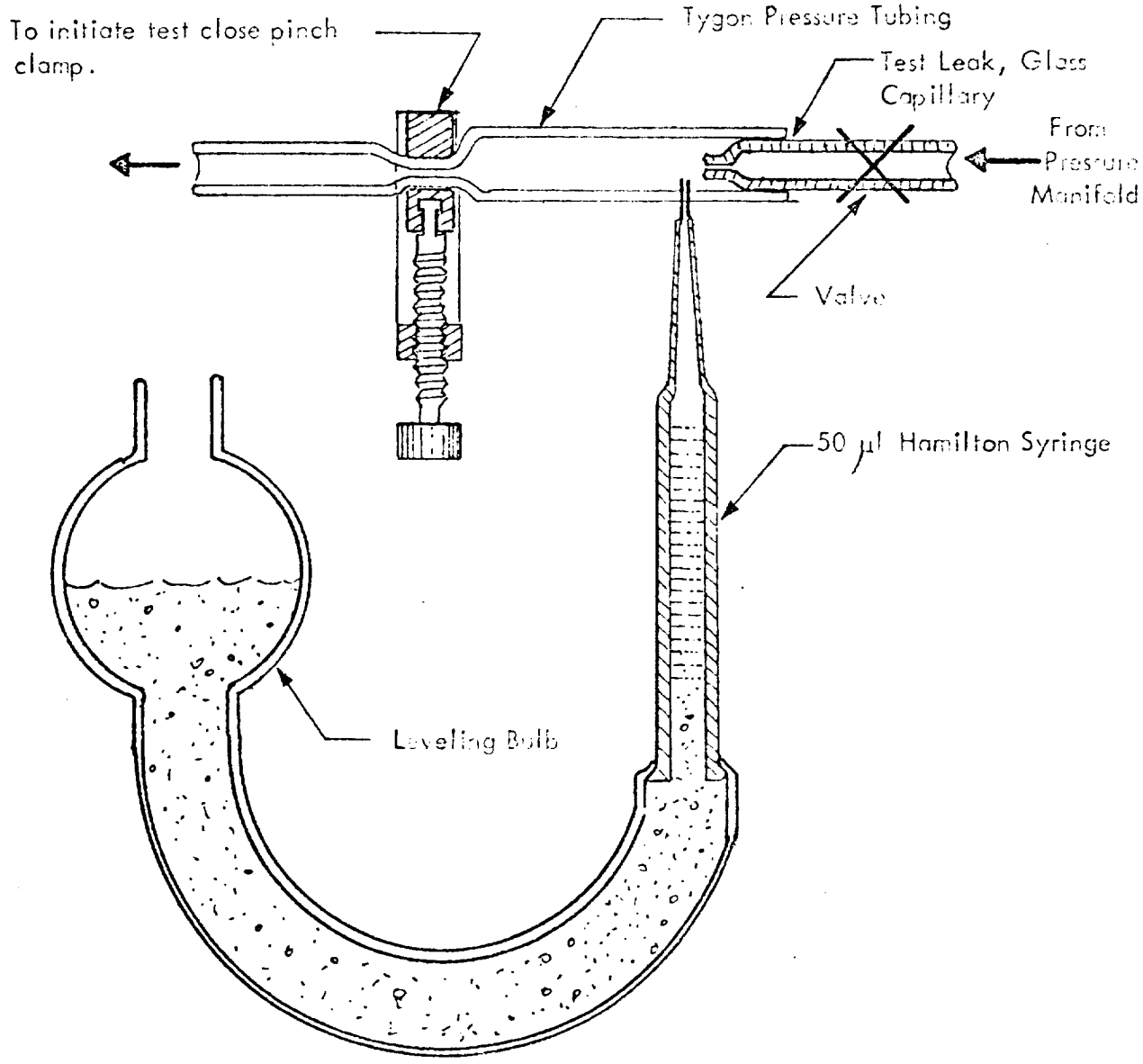

FIGURE 4 MICROVOLUME TECHNIQUE FOR MEASURING HELIUM LEAK RATES

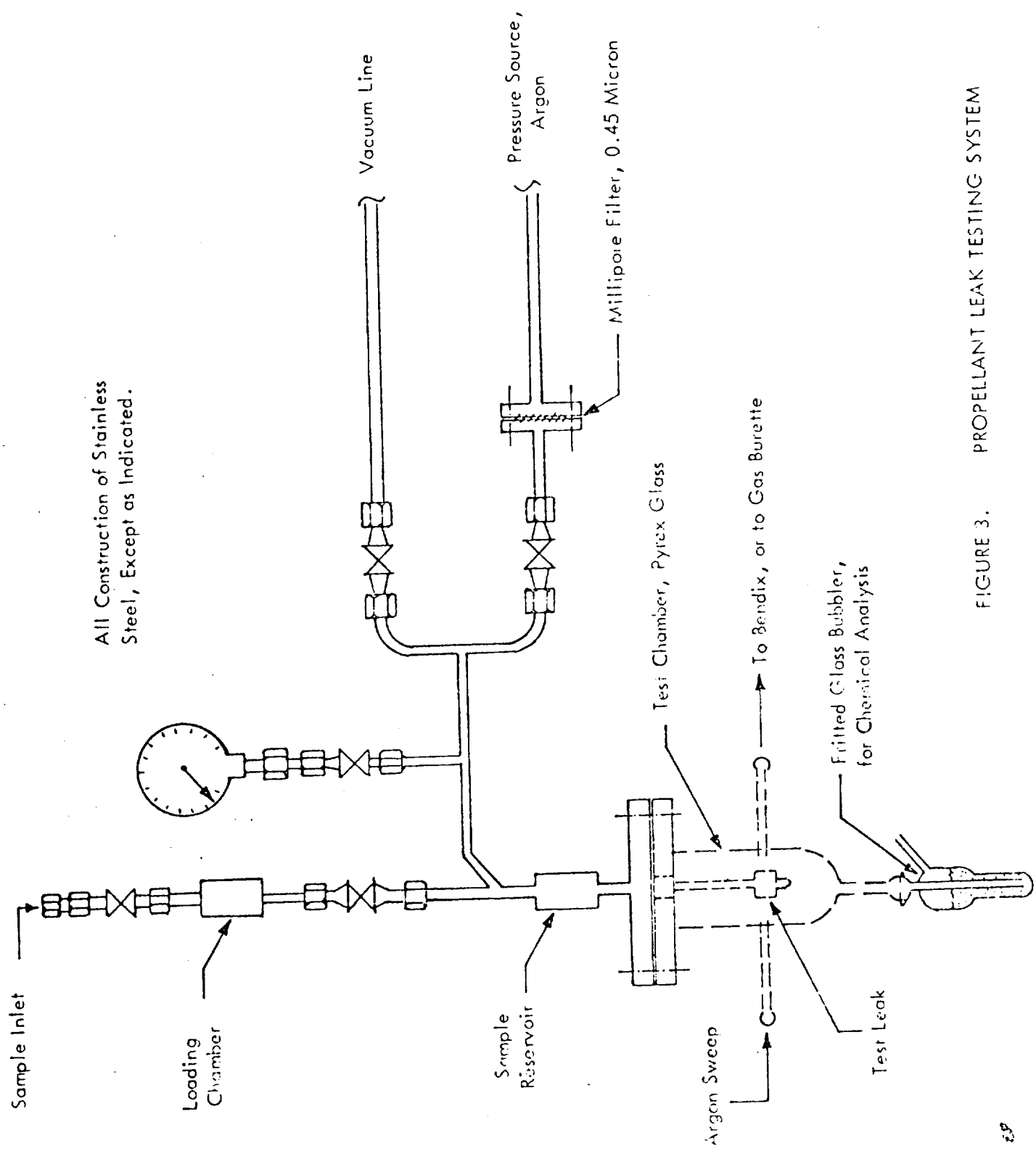

FIGURE 3. PROPELLANT LEAK TESTING SYSTEM

2.2 Leak Types

Data is presented on four types of leaks. Initially we studied a channel type leak, prepared by scribing a leak path across the mating surface of a stainless steel plug. When this type of leak proved to be very susceptible to blockage b, metal chips due to galling as the leaky fitting was torqued down, attention shifted to a crushed tubing leak. For the ECS liquids a glass capillary leak was utilized, and when it proved to give satisfactory data it was also used for the hydrazine fuels. Finally leakage of the two hydrazine fuels was studied through a loosely torqued stainless steel plug. Details of the preparation of these leaks are given in the following paragraphs.

2.2.1 Scribed AN Plugs

These leaks were prepared by scribing a small channel across the mating surface of a 1/4-inch AN-806-4S plug of type 304 stainless steel, using a diamond scribe. These plugs were then sealed to mating flares in 1/4-inch stainless steel tubing, which was attached to a helium filled pressure manifold. The assembly was mounted within the special tool in the entrance chamber of the leak detector (Figures 1 and 2) and the plug torqued down against the fixed backing nut until the desired leak rate was indicated by the detector.

Scribes were made in "as-received" plugs, in plugs which had been polished with 400 grit abrasive to a mirror finish (and whose flares had been so polished), and in plugs which had been lapped into the flares utilizing 400 grit abrasive, by rotating the plugs in a drill chuck, until a highly polished mating surface at least a millimeter across had been developed. In every case the scribes were examined at 40 to 500 magnifications, and metal chips, dirt, and loose metal particles observed in the scribe were removed by brushing and washing with reagent grade ethanol.

Test leaks which required excessive torque in order to reach low leak rates were found to be galled when disassembled and observed microscopically. Such galled plugs appeared to leak in areas in addition to the scribe and, in some instances, the scribed path was galled shut. Looping of the fitting allowed a reduction of the sealing force required, and decreased the galling observed No lubrication of the mating surface could be used, since the fluids to be tested would have reacted with any lubricant.

One major drawback of this leak configuration was the fact that fluid, having leaked across the mating surface through the scribed channel, was still trapped within a dead volume, and could not immediately evaporate into the sweep gas. Attainment of an equilibrium value by the apparent leak rate thus required considerable time. The same criticism applies to the loosely torqued AN fitting leaks described below. Data from one of these latter leaks (Figure 15) suggests that it may take several hours to reach equilibrium. This not only makes experimentation extremely time-consuming, but also makes measurement impossible if the leak is simultaneously becoming plugged by some deposit.

2.2.2 Crushed Tubing Leaks

These leaks were tried because of the time required (approximately one day/leak) to prepare, set, and calibrate scribed leaks. Crushed tubing leaks were found to be equally satisfactory for testing, and required approximately one-half as long to prepare.

These leaks were prepared by smashing the end of 1/16-inch outside diameter thin-walled stainless steel tubing. In order to attain a channel type leak a 0.001-inch hard steel wire was placed inside the tubing and the tubing was first crimped as flat as possible in a vise. By rotating the crimp 90° and closing the vise the crimp was opened enough to allow withdrawal of the wire, thus leaving a channel impressed in the flattened walls of the crimp. The crimped tubing was then placed in a special tool for additional compression.

An AN plug and nut were modified to crush the crimped tube inside the vacuum chamber of the leak detector, using the special tool of Figure 2. This arrangement performed adequately, and was used to set the crushed tubing leaks in the N_2O_4 test series. However, applying enough torque to crush the leak sufficiently was difficult. In addition the geometry was unsatisfactory for hydrazine fuels, leaking at fairly rapid rates, where unevaporated drops of liquid could form at the leak outlet.

For the hydrazine tests a nut and bolt clamp was fabricated (Figure 5) which was suitable; however, it would not fit the torquing device (Figure 2) in the vacuum chamber of the leak detector, so that the leak had to be removed from the chamber each time the leak rate was adjusted. Crushed tubing leaks made in the Figure 5 fixture were, therefore, confined to the relatively large leak rates which could be calibrated by volumetric displacement.

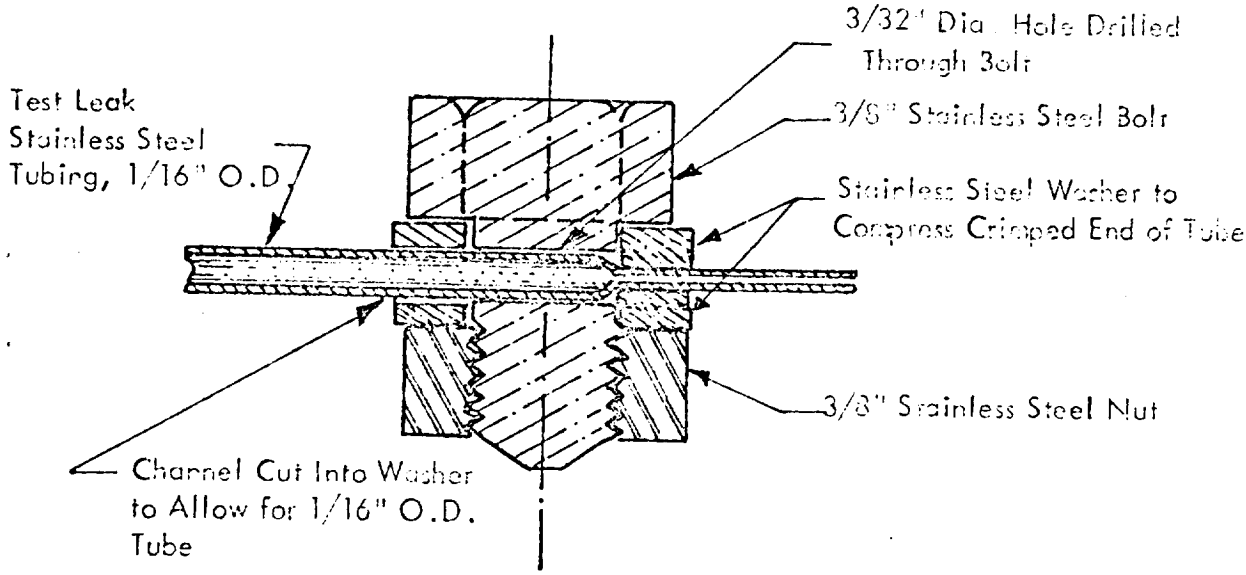

FIGURE 5 LEAK-RATE ADJUSTING TOOL FOR CRIMPED TUBING LEAKS

The fluid emerging from this leak path was not expelled directly into the sweep gas stream, since there was a small dead volume of 1/16-inch tubing beyond the leak. However the sweep gas stream was directed at the exit of the tubing and tended to aspirate vapors from the tubing, and the configuration was much more satisfactory geometrically than the AN plug leaks.

2.2.3 Glass Tubing Leaks

The difficulties experienced with the various metal leaks led to the use of glass leaks for the later MMH and Aerozine-50 tests, as well as for the ECS fluids. These leaks were prepared by softening and drawing down Pyrex glass tubing to form fine capillary orifices. In most cases the desired helium leak rates could be reached by selecting orifices with leak rates higher than required, very carefully flaming the tip, and remeasuring the leak rate until the desired value had been obtained. Occasionally a leak was fused closed; however, with practice it was possible to fabricate glass leaks of 10^{-1} to 10^{-3} range quite readily. Because of the measurement time needed, and the danger of flaming the leak shut, 10^{-4} and 10^{-5} cc/sec leaks required several hours apiece to prepare.

For the low pressure ECS fluid leak tests at 30, 60 and 90 psig, the glass leaks were attached to the pressure manifold with 1/4" x 1/8" Tygon pressure tubing. For the fuel system fluids, tested at 50, 150, and 250 psig, the glass leaks were attached to a metal pressure manifold using 1/4" nylon Swagelock ferrules and backing nuts Care in selection of the glass tubing was required, since variations in glass diameter afforded some undersized tubing which slipped out of the ferrules, and some oversized tubing which cracked. No difficulty was encountered from tubing shattering at 250 psig, and several leaks were successfully pressure checked up to 900 psig. Nevertheless all tests were observed through a heavy Plexiglass safety screen.

Figure 6 shows a series of photomicrographs of the cross-section of a typical glass leak. The cross-section was prepared by embedding the glass tubing and carefully grinding it down until the center of the leak was reached. This is the 10^{-3} cc/sec helium leak used to measure the leak rate of 25 percent glycol/water (see data Table 49 and Figure 41). Note that the leak actually does approach a long, cylindrical channel. The channel diameter is 0.0002-inch, and the length of the narrowest cylindrical section is approximately 0.04-inch, so that the ratio of length to diameter is greater than 100:1. For this leak at the maximum liquid flow rate of 2.65×10^{-5} cc/sec (observed at 90 psig pressure difference) the Reynolds number is 3 while for the maximum helium flow rate of 8.5×10^{-3} cc/sec it is 17. Therefore both liquid and gaseous flow through this leak would be expected to be essentially laminar.

It is not known whether this geometry was present in all of the glass leaks tested. Particularly in the case of the 10^{-4} cc/sec helium leaks microscopic examination of the intact leak appeared to indicate that the low flow rate had been obtained by shrinking the outer end of the channel so that the leak restriction may have actually more closely resembled an orifice than a channel. This was even more likely for a 10^{-5} cc/sec helium leak, since very little heating was required to reduce a 10^{-4} to a 10^{-5} cc/sec leak.

THE BOEING COMPANY

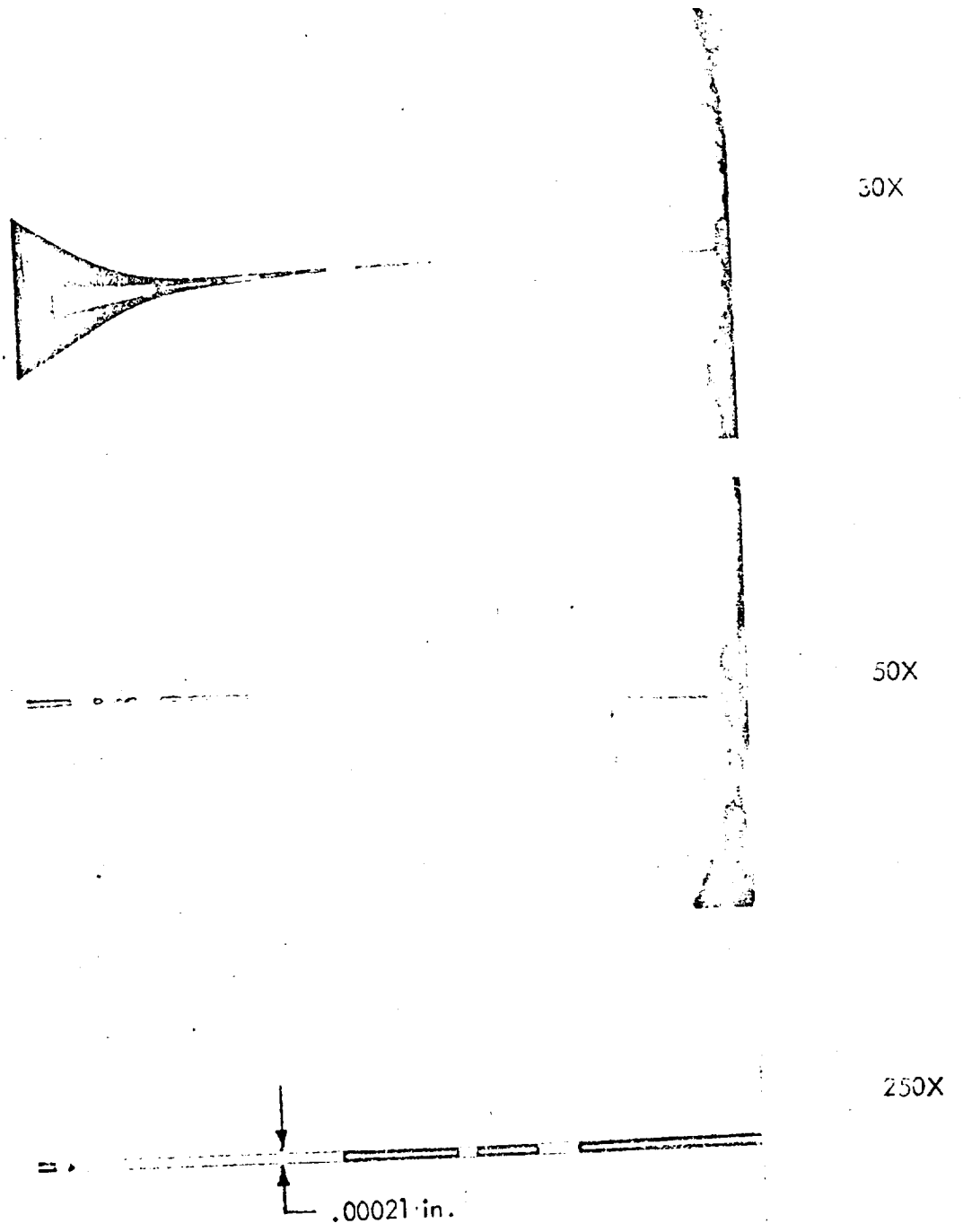

FIGURE 6. PHOTOMICROGRAPHS OF 10^{-3} CC/SEC HELIUM GLASS LEAK

2.2.4 AN Flared Fittings with Lightly Torqued Plugs

These consisted of a 1/4" steel plug, Type AN-806-4S, attached to a 1/4" flared stainless steel tube. Leakage was produced by failing to torque the backing nut sufficiently to produce sealing. This type of leak was tested late in the program, following completion of the glass leak testing, as it was felt to be more representative of the type of leakage which might be encountered in an actual spacecraft. It obviously shares with the scribed plug leaks the drawback of reaching an equilibrium flow rate to the surrounding atmosphere very slowly.

2.3 Fluids Tested

The fluids tested were those called out in Reference 4, and included three liquid propellants (nitrogen tetroxide, Aerozine-50, and monomethylhydrazine), four fluids used in the environmental control system (oxygen gas; 35 percent glycol-water; 62 percent glycol-water, Type II water/glycol, and water), and three additional gases; hydrogen from the fuel cells, and nitrogen and helium used as leak test gases. NASA-SPEC-C-6A (Reference 5) was used as a guide in selecting materials, although no effort was made to qualify the fluids to this specification.

A great deal of effort was expended in obtaining fluids as free as practicable from particulate contamination. All fluids were carefully filtered through the finest filter practical, using glassware previously rinsed carefully with filtered solvents. Contamination by dust or atmospheric particles was avoided rigorously. Even with this care, leak plugging, producing erratic leakage rates, was a major problem throughout the test program. Due to the meticulous care taken, the objection could be raised that the leakage results might not be representative of the results to be expected in actual Apollo hardware. However working with less carefully filtered fluids would probably have made the program impossible.

2.3.1 Nitrogen Tetroxide

The nitrogen tetroxide used in the majority of these tests came from a large storage tank located at the Boeing Remote Hazardous Test Site at Tulalip, Washington. Nine pound samples were transferred to the Kent Site in steel pressure bottles. Standard precautions in handling and transfer were taken to prevent access of atmospheric moisture, resulting in conversion to nitric and nitrous acid.

One test run was made using "green" nitrogen tetroxide, that is nitrogen tetroxide containing approximately 0.5 percent nitric oxide, as described in the NASA specification MSC-PPB-2 (Reference 6). No difference in the behavior of red or green fluid was observed.

A great deal of leak blockage was observed, especially in the early tests. An evaporation test showed that the N_2O_4 contained less than 0.01 percent non-volatile solids. Since the liquid evaporates at the exit of the leak, it was felt that even traces of non-volatile constituents could form leak plugs. For this reason the N_2O_4 was distilled in an all glass apparatus, which had been carefully washed and rinsed with solvents which had, themselves, passed through a 0.45 millipore filter. The distillation equipment contained an ultra-fine ground glass fritted filter so-located that the N_2O_4 vapor passed through it before being condensed. According to the manufacturer, the nominal pore size for a UF glass filter is 0.9-1.4 microns.

2.3.2 Monomethylhydrazine

The fuel sample used was furnished to us from stock by the storeroom at the Boeing Tulalip Test Site. It was a colorless, clear liquid purchased from the Olin-Matheson Company. To remove any particles it was passed through an ultra-fine fritted glass filter in an all glass apparatus designed for the preparation of sterile solutions. The apparatus had been previously washed, rinsed with solvents which had passed a 0.45 micron Millipore filter, and dried by evacuation. After filtration the fuel sample was stored under a helium blanket to preclude reaction with atmospheric CO_2

Evaporation of a 50 ml sample of the filtered fluid under a stream of dry argon left no visible residue. No change in weight of the beaker was observed using an analytical balance, indicating a residual weight of less than 0.2 mg, or a non-volatile content of less than 4 ppm.

The viscosity and density of this fluid are reported in Table 1. The values checked literature values very closely. These measurements were made after completion of the leak testing, indicating that opening the bottle for removing liquid samples periodically had not degraded the material

2.3.3 Hydrazine-Unsymmetrical dimethylhydrazine

This fuel was furnished to us by the storeroom of the Boeing Tulalip Test Site, and labeled Aerozine-50*. It was manufactured by the Olin-Matheson Company. It was freed of particulate impurities by the filtration technique described above for monomethylhydrazine. The density of the test fluid checked the literature value. The viscosity, however, was approximately 5 percent below the literature value.

2.3.4 Distilled Water

Distilled water was used as a reasonable substitute for potable water according to MSC-SPEC-C-21A. The water used was distilled in our laboratory in an all glass apparatus, and filtered through a Millipore filter stated to retain particles exceeding 0.45 microns in size.

*Aerozine-50 is a trademark of the Aerojet-General Corporation applied to a material meeting the requirements of MIL-P-27402 (Reference 7).

TABLE I

APOLLO TIE LEAK DETECTION DATA

PHYSICAL PROPERTIES OF HYDRAZINE FUELS

Density measured using Sargent No. S-41885 hygrometers, calibrated at 60°/60°F. Viscosity measured using a modified Ostwald viscosimeter, size 50, tube A-20, calibration constant 0.002504 at 77°F, 0.002502 at 100°F.

Test Temperature: 73°F

	Monomethyl-hydrazine	Unsymmetrical dimethylhydrazine, hydrazine 50-50	Comments
Density, experimental, gm/cc	0.873	0.901	
Density, literature, gm/cc	$0.874^{77°}$	$0.901^{73°}$	
Viscosimeter flow time, sec.	351, 341, 354, avg. = 349	357, 356, 356, avg. = 356	Slight bubbling in MMH runs.
Viscosity, experimental, centistokes	0.873	0.891	
Viscosity, literature, cs.	$0.882^{77°}$	0.94	
Viscosity, experimental, cps	0.762	0.804	

Literature values for MMH from "Handling Hazardous Materials", D. R. Cloyd and W. J. Murphy. NASA SP-5032, Sept. 1965.

Literature values for Aerozine-50 from "Storable Liquid Propellants", Aerojet-General Corporation Report No. LRP 198, June 1962.

2.3.5 Water/Glycol Solutions

Three water/glycol solutions were used in this test program. The first was a solution furnished to us by R. Holman of Boeing-Houston, labeled Type II water/glycol, Apollo, inhibited, 62.5 glycol, 37.5 water. The solution was somewhat cloudy, and a small amount of very fine brown precipitate had settled to the bottom of the bottle. It immediately became apparent that this material in the as-received condition would plug any small leak almost immediately. Therefore the mixture was passed through a Millipore filter capable of retaining particles of 0.45 micron and larger. The entire surface of the filter became covered with a brown precipitate. The physical properties (Table 2) indicated that the ethylene glycol concentration of this solution was slightly high compared to the specification value, being 67 percent. This solution is referred to subsequently in this report as Type II water/glycol.

The second water/glycol solution was also furnished by Boeing-Houston, and labeled water/glycol, Type I, Apollo, uninhibited, 67.5% glycol, 32.5% water. It was a clear, colorless, sediment-free solution. Analytical data, as shown in Table 2, indicated that this material had an actual glycol concentration of 62 percent, very close to that of Type II fluid. It is referred to subsequently in this report as 62 percent glycol/water. This material was tested in order to determine the effect of the presence or absence of inhibitor in producing leak plugging. It was also filtered through the 0.45 micron Millipore filter before use.

The third fluid was a solution of 35 weight percent ethylene glycol in distilled water, prepared in this laboratory from C.P. ethylene glycol. It was also filtered through the Millipore filter before use. It is subsequently referred to as 35 percent glycol/water.

The viscosities and densities of these three fluids were measured. The data is shown in Table 2, and the physical properties and composition of these fluids are compared with the specification values for Type I and Type II water/glycol in Table 3.

2.3.6 Fixed Gases

Oxygen, nitrogen, and hydrogen were used in the gas leakage correlation. Helium was used as the reference gas for all leakage correlation tests. Argon was extensively used in the program both as a pressurizing gas and as a sweep gas during chemical analysis.

Standard cylinder gases were used, procured from the Boeing Kent bottle yard. In all cases where gases were attached to a system upstream of a leak a cartridge containing a Millipore 0.45 micron filter was placed in the line between the bottle and the pressure manifold.

TABLE 2

APOLLO TIE LEAK TEST DATA

PHYSICAL PROPERTIES OF WATER-GLYCOL SOLUTIONS

1. Density: Measured using a glass pycnometer.

	Fluid I (35% glycol, similar to Type I, uninhibited)	Fluid II (62% glycol, similar to Type II, uninhibited)	Fluid III (65% glycol, Type II, inhibited)	Comments
Weight fluid, grams	26.9696	24.7106	24.7513	
Pycnometer volume	25.367	22.906	22.906	
Temperature, °C	24.2	24.4	25.6	
Density, gm/cc	1.043	1.079	1.081	At test temperature.
			1.082	At 75°F
Glycol concentration, wt. %, calculated		64.1	67.2	Calculated for fluids II & III(1).

2. Viscosity: Measured using a modified Ostwald viscosimeter, Tube H-53, Size 150, calibration constant 0.03384 at 100°F, 0.03365 at 200°F.

Test Temperature = 72°F.

Flow time, sec.	66.4, 66.4	122, 122	151, 151	Duplicate runs.
Viscosity, cs	2.24	4.14	5.12	Flow time x 0.0339.
Viscosity, cps	2.34	4.47	5.53	Vis., cs x d.
Glycol concentration, wt. %, calculated		60.5	67.3	By interpolation from literature data(2).

(1) Data taken from Timmerman's "Physical Constants of Binary Mixtures".

(2) Data from International Critical Tables.

TABLE 3. COMPARISON OF TEST WATER/GLYCOL SOLUTIONS WITH SPECIFICATION

	Specification Values		Fluid III	Fluid II	Fluid I
	Type I	Type II	Type II Water/Glycol	62% Glycol/Water	35% Glycol/Water
Ethylene Glycol, (% by weight)	35.00±0.50	62.50±0.50	67.2	62.3*	34.67
Distilled Water	As required	As required			65.33
Triethanol phosphate (% by weight)	1.60±0.04	1.60±0.04	Present	None	None
Viscosity, cs (75°F ±0.5°F)	2.25cs ±0.15	No require.	5.12	4.14	2.24
Specific Gravity (75°F ±0.5°F)	1.048±0.002	1.082±0.002	1.083	1.079	1.043
Color	Clear, light straw	-	Straw	Clear	Clear
Silting	None	None	Yes	None	None

*Obtained by averaging results calculated from density and viscosity data.

2.4 Fluid Leak Testing Methods

Four general methods were tried for measuring leakage rates of the test fluids through experimental leaks after the helium leak rate had been determined. Brief descriptions of each method are given below; since modifications were required for particular fluids these methods are elaborated as necessary in Section 4 where specific test results are described. The test methods were:

1. Direct weighing of the expelled fluid.

2. Quantitative chemical analysis of the leaked fluid.

3. Measurement of the time required for passage of a known microliter volume of liquid.

4. Mass spectrometer measurement of the downstream concentration of fixed gases under steady state leakage conditions.

2.4.1 Direct Weighing of the Expelled Fluid

This very simple test method was used only in the case of the glycol/water and water fluids. The liquid was placed in the glass tubing with the leak mounted vertically and pointed down. The leak was attached to a glass pressure manifold with Tygon pressure tubing, held in place by a hose clamp. The desired pressure was applied and the formation of drops observed until a steady drip rate had been reached. At this point a weighed ten-milliliter volumetric flask was placed directly below the leak, so that the glass leak extended into and almost blocked the neck of the flask. This was done as quickly as possible after a drop had fallen from the capillary tip.

The flask was removed when a sufficient weight of liquid had dropped into the volumetric flask, immediately after a drop had fallen. The total collection time, and the weight of the collected liquid were noted, and the leak rate calculated. A test experiment showed that evaporation loss from the volumetric flask under these conditions was negligible.

At least ten drops were collected in each test. The weighing error of ±0.4 mg was less than 1 percent in every instance. With the care taken to duplicate the relationship between drop time and the time of flask placement and insertion, we believe that the error of timing was definitely less than one-fifth of the interval between drops. This corresponds to a maximum timing error of ±2 percent, if only ten drops are collected; the minimum number collected in any experiment. Therefore we believe the average leak rate measured by this technique is accurate within ±5 percent. Unfortunately, it could be used only with larger leaks (10^0, 10^{-1} cc/sec helium) for non-toxic liquids.

2.4.2 Quantitative Analysis of Leaked Fluid

Chemical analytical techniques are readily applicable to leak measurement when the fluid tested has sufficient volatility so that it can be evaporated into a moving gas stream as rapidly as it emerges from the leak. This criteria is met by both hydrazine fuels leaking at below 10^{-4} cc/sec of liquid and by nitrogen tetroxide leaking at below 10^{-1} cc/sec of gas.

The test leak is attached to the pressurization manifold as shown in Figure 3. A sweep gas is passed into the chamber surrounding the leak, and exited through the glass bubbler containing a solution capable of quantitatively removing the test fluid vapor from the gas stream. The bubbler is attached to the system for a known time period, removed, and the concentration of test fluid measured by an appropriate quantitative microchemical analysis. The specific methods are described in the following paragraphs.

The sensitivity of the analytical methods permitted measurement of liquid flow rates down to 10^{-7} cc/sec with a one minute collection period. Much higher leak rates were measured by suitable dilution of the bubbler samples. Since sampling could be done periodically almost at will, this method permitted us to follow changes as the leak rate initially increased, remained steady, or decreased due to blockage.

One drawback of this technique is the time delay between collecting the sample and obtaining the leak rate. This delay is inherent both in the chemical analysis itself, since color development usually takes some time, and also in the logistics of running many samples in a small time period. It would certainly be desirable to readout the leak rate directly on some analytical instrument.

A consideration of the factors involved in making this measurement, including bubbler efficiency, instrumental error, errors due to dilution techniques, and calibration uncertainties suggest that any given determination may be in error by ±10 percent. Additional variation in observed leak rates are seen under steady state conditions; these can be attributed to geometrical factors in the leaks tested.

An attempt was made to use this method for glycol/water leak rate testing. The test method for ethylene glycol described below was developed for measuring microgram quantities. A trial experiment showed that the volatility of water/glycol mixtures is much too low for practical sweeping.* Therefore the tip of the leak was rinsed with distilled water, the fluid was allowed to leak out for ten minutes, and the tip then rinsed again, collecting the washings in a volumetric flask.

*See Table 4.

TABLE 4

APOLLO TIE LEAK TEST DATA

SWEEP RATE OF ETHYLENE GLYCOL

Date: 2/6/68

Experimental Set-Up:

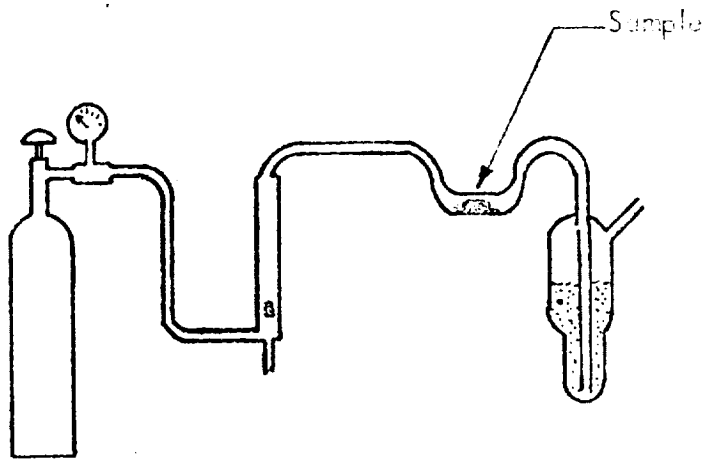

Glycol Weight: 27 mg

Glycol Surface Area: Approximately 1/32 square inch.

Sweep Rate: 200 cc argon/minute.

Elapsed Time: 27 hours

Weight Loss Observed: 0.35 mg

Glycol Collected in Bubbler: 0.1 mg (by chemical analysis).

Glycol Transfer Rate: $1\text{-}4 \times 10^{-9}$ cc/sec.

2.4.2.1 Nitrogen Tetroxide (Nitrogen Dioxide) Analysis

Nitrogen dioxide was determined colorimetrically using the sulfanilic acid diazotization method of Saltzman (Reference 8). This method is the standard procedure used in the industrial hygiene field for measurement of parts per million to parts per billion concentrations of NO_2 in air.

We utilized the method by argon sweeping the effluent NO_2 through a fritted glass midget scrubber filled with the Saltzman reagent (a mixture of sulfanilic acid, N-1-Naphthylethylenediamine dihydrochloride and acetic acid) and reading the color developed in the diazosulfanilic acid containing solution either directly or after suitable dilution. Our procedure allowed the detection of at least one microgram of NO_2 in the collection solution. Since we utilized a maximum sweep time of 25 minutes this gave a lower detectable limit of about 2×10^{-7} cc of gaseous NO_2 per second. The efficiency of the scrubbers used was found to be above 98% in the collection concentration range we used.

Standardization was against sodium nitrite solution. Past experience has shown replication of well within 1% in this procedure. $NaNO_2$ does not of course form nitrous and nitric acids in water as does NO_2, and therefore produces more color per gram than does NO_2. We utilized the Saltzman equivalence factor of 0.72 rather than go through the laborious and uncertain process of preparing standard NO_2 gas samples. This usage may have introduced an error of as much as 5%, which is probably the limiting error in this analysis.

2.4.2.2 Monomethylhydrazine Analysis

MMH was determined colorimetrically by its reaction with p-dimethylamino-benzaldehyde in an acid medium. The procedure is an adaptation of the test given by Feigl for hydrazine determination (Reference 9) but in this instance the reaction mechanism is not as well known and the procedure is several times less sensitive than for hydrazine.

We argon swept the effluent MMH through a water filled midget scrubber and subsequently reacted the aqueous MMH solution, or a suitable dilution thereof, with a hydrochloric acid containing alcoholic solution of the aldehyde. In our procedure we could with confidence detect 5 micrograms of MMH in our total scrubbing solution, or 4×10^{-9} cc of liquid MMH per second averaged over a 25 minute sweep period. Where possible, sweep times were kept down to 1 minute. The scrubber efficiency, measured by placing several in series, was found to be above 98%.

Standardization was against the same MMH used in the test series. All checks on standardization points, performed on different days, fell within 1%.

The major source of error is probably not in the analytical procedure itself but in the sample collection. Unlike the N_2O_4, which was essentially at its boiling point and thus readily removed by the sweep gas, the MMH is a relatively low vapor pressure fluid

whose removal by the sweep gas is directly related to exposed droplet area. Due to the necessary geometry of the pinched tube and AN-flare leaks, it was possible to build up significant amounts of fluid beyond the actual leak orifice but before exposure to the sweep stream. This could happen especially at higher leak rates and would be a source of rather erratic results. Obviously, any run where droplets were actually seen to be growing was invalidated. Overall error due to this problem of geometry might well be 25%.

2.4.2.3 Aerozine-50 Analysis

Aerozine-50 is an approximate 50-50 weight mixture of hydrazine and unsymmetrical dimethylhydrazine. For analytical purposes we chose to detect the former and assume the latter. The method for hydrazine, an adaptation of the Feigl p-dimethylaminobenzaldehyde spot test (Reference 9) is more sensitive, simpler, and more rapid than the standard trisodium pentacyanoamino-ferrate colorimetric method for UDMH (Reference 10).

The hydrazine method was exactly the same as that used for MMH, but with hydrazine the sensitivity is several times greater.

Sample sweeping and collection procedures were the same as for MMH. In our procedure we could with confidence detect 1 microgram of hydrazine in our total scrubber solution, or 1.5×10^{-9} cc of liquid Aerozine-50 per second averaged over a 25 minute sweep period Sweep periods were normally kept to one minute. Scrubber efficiency was found to be greater than 98%.

Standardization was against pure hydrazine. Tests were run to ascertain that UDMH did not interfere, and no interference was detected at UDMH concentrations 500 times that of N_2H_4.

As with MMH, the major source of error, again probably as much as 25%, was the sample collection problem due to the peculiar, but rather practical, leak geometry.

2.4.2.4 Ethylene Glycol Analysis

Ethylene glycol solutions were analyzed by periodic acid oxidation, followed by colorimetric determination of the formaldehyde formed. Initially the formaldehyde was determined by the Schiff-Elvove method (Reference 11), a modification of Schiff's reaction in which formaldehyde reacts with a bisulfite decolorized solution of parafuchsin to form the formaldehyde-bisulfite addition product and thus allow the dye coloration to be regenerated. The method was fairly satisfactory, but the color development was slow, and the intensity changed slowly, so that very careful control of development time was required for accuracy.

For this reason the use of chromotropic acid (4 5-Dihydroxy-2,7-naphthalene-disulfonic acid, disodium salt) for determining formaldehyde was investigated. As periodate interferes with this reaction, it is necessary to destroy excess oxidant by the addition of arsenous acid solution before color development. The method finally used was a slight modification of one reported in Belcher (Reference 12)

Standardization was carried out by analysis of known solutions of C.P. ethylene glycol in distilled water. Details of the method are given in the Appendix. The final method was capable of detecting a glycol concentration of 1 microgram/ml in 5 milliliters of solution. When it became apparent that chemical analysis would not be used for water/glycol leak rate determinations work on this method was abandoned. The method could be developed to yield greater sensitivity if required.

2.4.3 Microvolume Expulsion

This technique was developed when early attempts to study water/glycol flow rates led to extensive leak plugging. Since the water/glycol was not expected to react with the walls of the leak, this plugging was attributed to washing of extraneous particles from the tubing walls into the leak. It was felt the probability of placing particles into the leak with the test fluid could be minimized by working with a minimum volume of test fluid. This would also avoid contact of the test fluid with the capillary walls.

Sample volumes were injected into the glass capillary leaks using a 10 microliter syringe*. These syringes are stated to possess a delivery accuracy of ±1 percent. A volume of between 1 and 10 microliter was injected, to give an effluent time suitable for accurate measurement. The tip of the syringe was placed as far down as possible within the capillary, so that the sample forms a plug at the top of the capillary, and the syringe needle was carefully withdrawn. A calculation indicated that the error, should any of the sample be drawn into the leak by capillary action, was negligible.

The glass capillary containing the fluid was then attached to a pressure manifold, with the valve closed. With the glass leak in place the pressure valve was rapidly opened, applying the preset helium pressure to the fluid plug in the capillary leak. Timing was begun as the valve was turned, and ended when helium broke through the capillary. Observations of the latter required care, and use of a magnifying lens or a small microscope for smaller leaks.

For the water and water/glycol tests at 30, 60 and 90 psig the glass leak was attached to the pressure manifold by 1/4 inch Tygon pressure tubing, and secured by a hose clamp. For the hydrazine fuels run at 50, 150 and 250 the glass leak was attached

*Syringe manufactured by Hamilton Co., Whittier, California.

to a 1/4 inch stainless steel manifold, using Swagelock fittings with nylon ferrules. The leak was directed down into a bucket of water, and observed behind a safety screen. No difficulties with glass failures occurred; in fact these leaks were pressure checked without rupture up to 900 psig. An occasional leak slipping out of the fitting and hitting the water effectively wet down the experimenter.

Data on the quantitative nature of the transfer from the microliter syringe is given in Table 5 for ECS liquids and in Table 6 for Aerozine-50. Unfortunately the syringe used for monomethylhydrazine was broken before it could be calibrated. Based upon the manufacturer's specifications for these syringes, and the nature of the fluid, we are confident that the transfer errors for monomethylhydrazine were comparable to those observed for Aerozine-50. The water and water/glycol liquids were expelled into a flat, microbalance container. The maximum deviation between volume expelled and weight observed was 21 percent, the average deviation is 6 percent. For Aerozine-50 the transfer was into actual glass capillary leaks. Here the observed deviations were large (16-27 percent) for 2 microliter samples, and small (1-8 percent) for 4 and 6 microliter samples. In view of the high leak rates, compared to theory, measured for all fluids by this technique, we believe that a tendency must exist for some portion of the fluid to remain on the walls of the leak at the time of gas breakthrough.

2.4.4 Mass Spectrometer Measurement of Leaked Fluids

Initially we had anticipated using the Bendix Time-of-Flight mass spectrometer as an analytical tool for the detection of the leaked volatile liquids such as nitrogen tetroxide, the hydrazines, and water, either alone or evaporated from water/glycol solutions. At that time we were considering testing leaks in the 10^{-8} cc/sec of helium range, where the sensitivity of chemical analysis would not have sufficed. This motive disappeared when we restricted our interest to helium leaks of 10^{-6} cc/sec and larger. We had hoped not only to be able to detect emergence of the vapors of these liquids as the liquids initially came through the leak, but also to be able to measure their rate of emergence quantitatively by suitable calibration of the mass spectrometer.

A number of operational problems with the instrument were encountered. In addition the problem of obtaining known, sufficiently dilute gaseous concentrations of these liquids for calibrating the instrument seemed onorous. For this reason, and because the chemical analytical techniques developed for the propellants proved to be sufficiently sensitive, and reasonably convenient, the use of the mass spectrometer for this purpose was dropped, after one abortive attempt to use it for the detection and analysis of N_2O_4.

The mass spectrometer was used for measuring the leak rates of helium hydrogen, nitrogen and oxygen through 10^{-4} and 10^{-5} cc/sec helium leaks. These measurements were made by allowing the test gas to pass through the experimental leak into a plenum, pumped at a constant speed, connected to the ion source of the Bendix Time-of-Flight mass spectrometer through a constant pin-hole leak. The response of the Bendix in scale divisions was then recorded for each combination of gas and pressure.

TABLE 5

APOLLO TIE LEAK TEST DATA

CALIBRATION OF MICROLITER SYRINGE TRANSFER

Date: 5/24/68

Method: The test fluid was expelled from the syringe into a microbalance pan with a crimp-on type cover. The closed container was weighed immediately on a Cahn Electrobalance.

Syringe: Hamilton Manufacturing Co 10 Microliter Style.

Data:

Fluid	Fluid Density gm/ml	Weight Deposited mg	Volume Deposited Gravimetric (w/d) µl	Volumetric µl	Deviation Actual (Grav-Vol) µl	Deviation Percent %
Water, Distilled	0.998	2.00	2.004	2.1	-0.096	5
		0.945	0.947	1.0	-0.053	5
		0.845	0.847	1.0	-0.153	15
		0.975	0.977	1.1	-0.123	11
		0.955	0.957	1.0	-0.043	4
Water-Glycol nominal 62% glycol	1.079	1.210	1.121	1.0	0.121	12
		1.085	1.006	1.0	0.006	0.6
		1.005	0.931	1.0	-0.069	7
		1.095	1.015	1.0	0.015	2
		1.305	1.209	1.0	0.209	21
		5.675	5.26	5.0	0.26	5
Water-Glycol, Type II	1.080	1.075	0.995	1.0	-0.005	1
		2.185	2.02	2.0	0.02	1
		1.100	1.019	1.0	0.019	2
		0.985	0.912	1.0	-0.088	9
		3.160	2.926	3.0	-0.074	2

TABLE 6

APOLLO TIE LEAK TEST DATA

CALIBRATION OF MICROLITER SYRINGE AND TRANSFER TECHNIQUE

Date: 6/12/63

Method: The test fluid (Aerozine-50 - density 0.901 gm/ml) was expelled from the syringe into tared glass leaks in the same manner used for measuring A-50 leakage through glass leaks. The weights were taken using a Sartorius semi-microbalance.

Syringe: Hamilton Mfg. Co., 10 Microliter Style

Data:

Volume Delivered, (μl)	Weight Delivered (grams)	Volume Delivered (Calculated from weight ÷ d)	Deviation Actual (grav.-vol.)	Percent
2	0.001513	1.68	-.32 μl	-16.0
2	0.001331	1.48	-.52	-26.0
2	0.001314	1.46	-.54	-27.0
2 (Avg.)	0.001386	1.54	-.46	-23.0
4	0.003629	4.03	+.03	+0.7
4	0.003370	3.74	-.26	-6.5
4	0.003653	4.05	+.05	+1.3
4 (Avg.)	0.003551	3.94	-.06	-1.5
6	0.005469	6.07	+.07	+1.2
6	0.005273	5.85	-.15	-2.5
6	0.004952	5.50	-.50	-8.3
6 (Avg.)	0.005231	5.81	-.19	-3.2

Scale readings were converted to actual helium leak rates as follows. On each day of testing the actual helium leak rate of the experimental leak was measured by attaching it directly to a CEC helium leak detector, which had previously been calibrated using a commercial helium leak as a standard. Measurement of the response of the Bendix to this same leak under the same conditions established a daily sensitivity factor for helium.

To convert scale readings for the other gases to actual leak rates, the following measurement was made. An experimental leak was shown to pass helium at 1.14×10^{-4} atm cc/sec at 250 psig, by the CEC leak detector method described in Section 2.1.1. It was assumed that flow through this leak at 250 psig would follow Poiseuille's law for all four gases. The response of the Bendix to each of these gases was measured at 250 psig, and the actual leak rates of each gas calculated by Poiseuille's law, as in the example:

$$Q_{H_2} = Q_{He} \cdot \frac{n_{He}}{n_{H_2}} = 1.14 \times 10^{-4} \cdot \frac{0.0197}{0.0089} = 2.52 \times 10^{-4} \text{ atm cc/sec}$$

From the observed instrumental response, sensitivity factors were calculated, and from these the ratios of the sensitivity factor for each gas to that for helium. It was assumed that the relative sensitivity of the measuring system to these gases would be free of fluctuations from day to day. These sensitivity factor ratios were, therefore, used to reduce data for these gases for each day.

TABLE 7. SENSITIVITY FACTORS FOR H_2, O_2, N_2 RELATIVE TO HELIUM

Gas	Leak Rate x 10^{-4} (atm cc/sec)	Bendix Response (Scale Divisions)	Sensitivity Factor x 10^{-7} Atm cc/sec/div	Ratio, Sensitivity Factor to Helium Factor
Helium	1.14	1086	1.05	(1.00)
Hydrogen	2.52	1715	1.47	1.40
Oxygen	1.08	6130	0.177	0.169
Nitrogen	1.26	7700	0.164	0.156

3.0 EVALUATION OF FIELD LEAK DETECTION TECHNIQUES

Brief evaluations were made of several currently used techniques of leak detection. Sensitivity, ease of operation, reproducibility, and accuracy were among the parameters studied. The techniques evaluated were bubble fluid, helium sniffer probe, and rubber boots. Total immersion was not studied.

3.1 Bubble Fluid

The bubble fluid selected for evaluation was FM Inert Leak Detection Liquid manufactured by American Gas and Chemicals, Inc.

The bubble fluid was applied to a calibrated scribed plug leak in such a manner as to produce no bubbles during the application. The helium pressure on the fitting was raised to 400 psig to produce a leak rate of 1×10^{-5} cc/sec. A small bubble appeared, grew to approximately 3/32 inch diameter, and remained at that diameter for 5 minutes. One more bubble, 1/16 inch diameter, then formed and both burst. No further bubbles formed. The leak was then recalibrated with helium and was found to have plugged to 1/2 its original leak rate. The leak was then pressurized to 500 psig (this should have produced a leak rate of 4×10^{-5} cc/sec) and the actual leak rate at this pressure was found to be 4.7×10^{-6} cc/sec. After 30 minutes at this pressure the leak had opened to 5.7×10^{-6} cc/sec. The leak was tested several days later at 100 psig and gave no leak indication (the original rate at this pressure was 6.1×10^{-7} cc/sec). When the pressure was increased to 112 psig the leak again opened. Several cycles were repeated in which it was demonstrated conclusively that the bubble fluid contaminated leak was acting as a check valve, with no detectable leak between about 0-110 psig, leakage starting around 120 psig, and cutting-off again when the pressure was lowered below 112 psig.

It would seem obvious from the data presented in the preceding paragraph that the use of bubble fluid for leak testing on a system will not only provide inadequate detection of existing leaks but will probably compound future leak detection problems by turning constant leaks into erratic leaks.

3.2 Sniffer Probe

The helium sniffer probe attached to a CEC helium leak detector with 5 feet of Tygon tubing and fitted with a 1/8" ID Tygon tip (per Grumman Specification LSP-1A-50121A) was used to test an AN scribed fitting leaking at a rate of 1×10^{-5} cc He/sec at 380 psig applied helium pressure. The absolute sensitivity of the leak detector at the end of the probe had previously been determined to be 3.4×10^{-10} atm cc/sec/division. When tested in the open laboratory and when holding the probe perpendicular to the axis of the leaking fitting a very large variation was obtained dependent upon precise positioning, with

over an order of magnitude difference recorded 60° either side of the top of the fitting. Variations of about 50% at any one position were also noted. The maximum indicated leak rate detected during this experiment (265 divisions) was 9×10^{-8} cc/sec, by an operator with prior knowledge of the location of the leak.

Experiments were also attempted with discouraging results, using the fingers to hood the leak in order to improve sensitivity. These readings proved quite unstable and non-reproducible although an increase in sensitivity level was produced. Checking in the open air, if relatively still, seems to be the best, most reproducible method.

Table 8 gives the results obtained by four different operators on four different leaks utilizing both the hooded-by-fingers and open still air probing techniques. These operators had no prior knowledge of the location of the leaks. Examination of the data will reveal that the sniffer probe technique is not a quantitative leak measurement method. It is, to be sure, quite useful as a screening technique for locating relatively large leaks ($> 1 \times 10^{-6}$ cc/sec of helium).

3.3 Alligator Boots

Two alligator boots were tested. These were constructed of rubber, according to a North American Rockwell drawing (Reference 13) and manufactured by the Ace Rubber Company (Reference 14). These were designed to accommodate respectively 3/8" and 1-1/2" unions of a type which we did not have. We therefore manufactured chambers into which our standard and test leaks might vent, possessing holes leading to the interior of the boots, as shown in Figure 7.

A scribed AN fitting leak (5.7×10^{-5} cc/sec) was calibrated with the scribed leak and a standard leak closely coupled to the leak detector. The leak detector was then calibrated with the inlet valve throttled 15X. The alligator boot tests were subsequently performed with the valve in this position.

The boots were cleaned by wiping lightly with acetone saturated gauze followed by an application of a very thin coat of vacuum grease on the mating surfaces. It was not always possible to reduce the boot pressure to the 3 or 4×10^{-1} torr minimum required to avoid excessive throttling of the leak detector without significant recleaning and adjusting the boot. The boot was attached immediately adjacent to the standard leak, and separated from the leak detector by a 10 foot length of 1/2" Tygon tubing (see Figure 7).

With this test configuration quite quantitative results were obtained as evidenced by the data of Table 9 and the graph of Figure 8.

It is apparent that this method is completely quantitative if the MSLD is calibrated with a known (standard) leak attached as closely as possible to the boot. The leak rate of the standard leak should be about equal to the maximum allowable leak rate of the item to be tested (e.g., 1×10^{-5} atm cc He/sec for many of the Apollo propulsion and ECS

TABLE 8
APOLLO TIE LEAK TEST DATA

SNIFFER PROBE EVALUATION RESULTS

Known Leak Rate (cc/sec)	Operator	Leak Indication (divisions) w/hood	Leak Indication (divisions) w/o hood	L.D. Sensitivity (cc/sec/div)	Apparent Leak Rate (cc/sec) w/hood	Apparent Leak Rate (cc/sec) w/o hood
1×10^{-5}	A	212	18	3.62×10^{-10}	7.67×10^{-8}	6.51×10^{-9}
	B	695	14	3.73×10^{-10}	2.59×10^{-7}	5.22×10^{-9}
	C	219	17	"	8.16×10^{-8}	6.35×10^{-9}
	D	265	16	3.40×10^{-10}	9.01×10^{-8}	5.45×10^{-9}
5×10^{-6}	A	84	17	3.62×10^{-10}	3.04×10^{-8}	6.18×10^{-9}
	B	339	8	3.73×10^{-10}	1.26×10^{-7}	2.98×10^{-9}
	C	69	6	"	2.67×10^{-8}	2.24×10^{-9}
	D	180	14	"	6.70×10^{-9}	5.22×10^{-9}
1×10^{-6}	A	16	2	3.62×10^{-10}	5.8×10^{-9}	7.5×10^{-10}
	B	62	2	3.73×10^{-10}	2.31×10^{-8}	7.45×10^{-10}
	C	10	1	"	3.73×10^{-9}	3.73×10^{-10}
	D	13	3	"	4.85×10^{-9}	1.12×10^{-9}
5×10^{-7}	A	10	2	3.62×10^{-10}	3.62×10^{-9}	7.5×10^{-10} (1)
	B	30 (1)	(1)	3.73×10^{-10}	1.12×10^{-8}	(1)
	C	3	(1)	"	1.12×10^{-9}	(1)
	D	14 (2)	3 (2)	"	5.22×10^{-9} (2)	1.1×10^{-9} (2)

(1) Could not possibly identify the number of divisions (if any).

(2) Questionable.

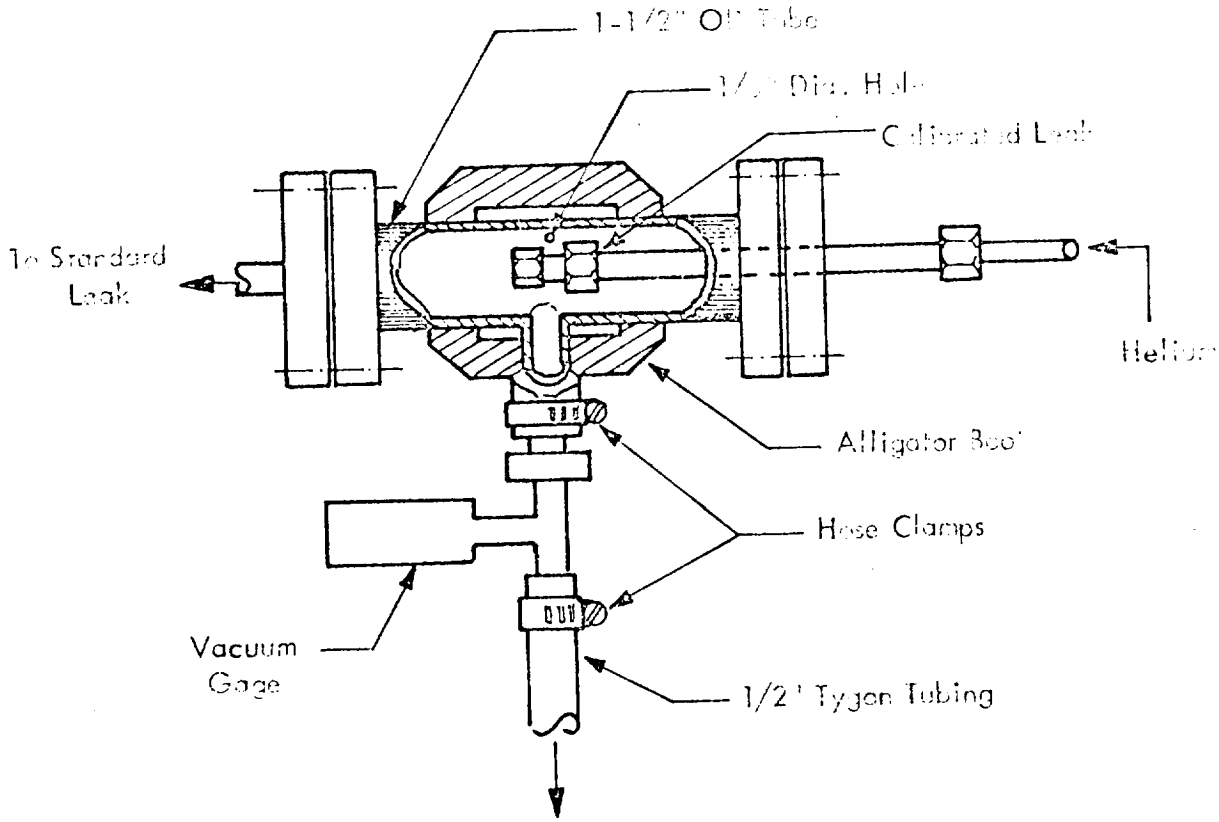

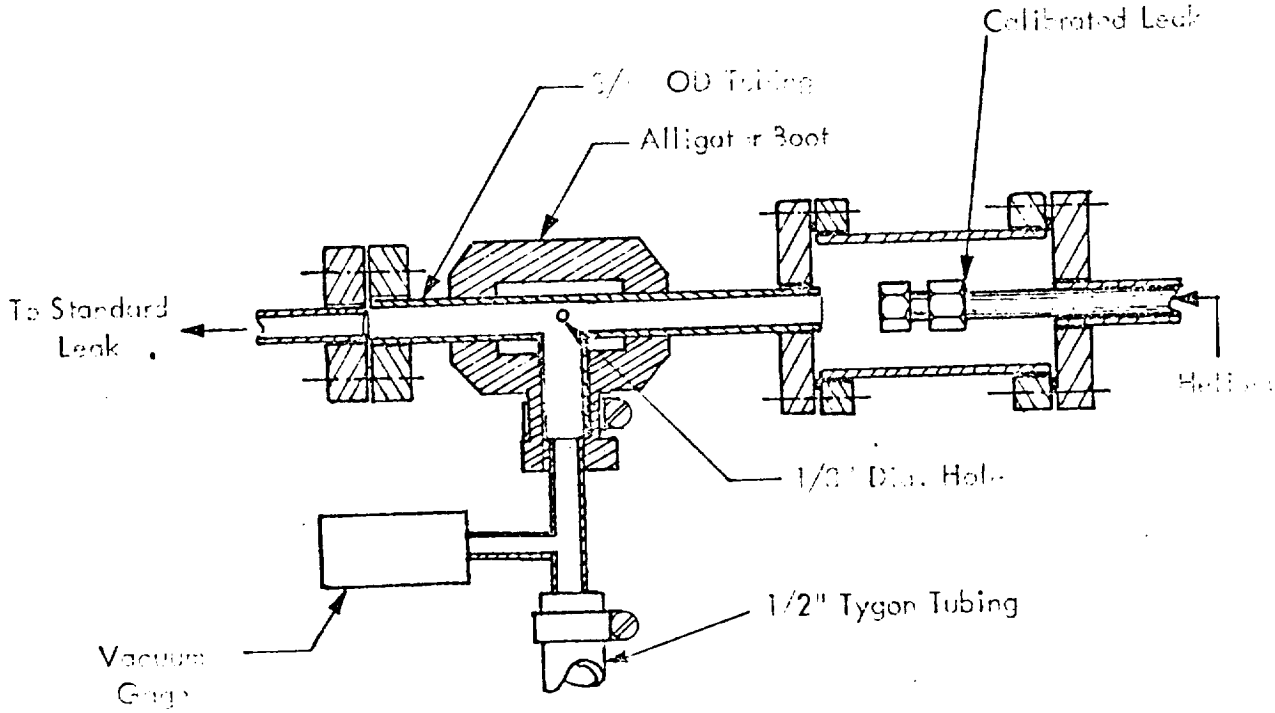

FIGURE 7. SCHEMATIC OF USE OF ALLIGATOR BOOTS FOR LEAK TESTING

TABLE 9

APOLLO TIE LEAK TEST DATA

ALLIGATOR BOOT TEST DATA

Date: 3/7/68

Event	Psig	Divisions Std.	Divisions Std + Leak	Leak Rate, (cc/sec)
Using 1.12×10^{-6} cc/sec Standard				
Quantitative Method - No Throttling				
	10	3800	26,000	6.54×10^{-6}
	20	3900	35,000	8.93×10^{-6}
	30	4050	43,250	1.08×10^{-5}
	60	4000	73,000	1.93×10^{-5}
Quantitative Method - Throttled 15X				
	60	300	6,000	2.13×10^{-5}
	120	300	14,000	5.12×10^{-5}
	200	300	23,500	8.66×10^{-5}
Small Boot - Throttled 15X				
	30	290	3,450	1.22×10^{-5}
	60	290	6,000	2.21×10^{-5}
	120	290	13,000	4.91×10^{-5}
	200	290	25,000	9.54×10^{-5}
Large Boot - Throttled 15X				
	10	295	1,900	6.09×10^{-6}
	30	295	3,300	1.14×10^{-5}
	60	295	5,800	2.09×10^{-5}
	120	295	12,000	4.45×10^{-5}
	200	295	21,000	7.86×10^{-5}

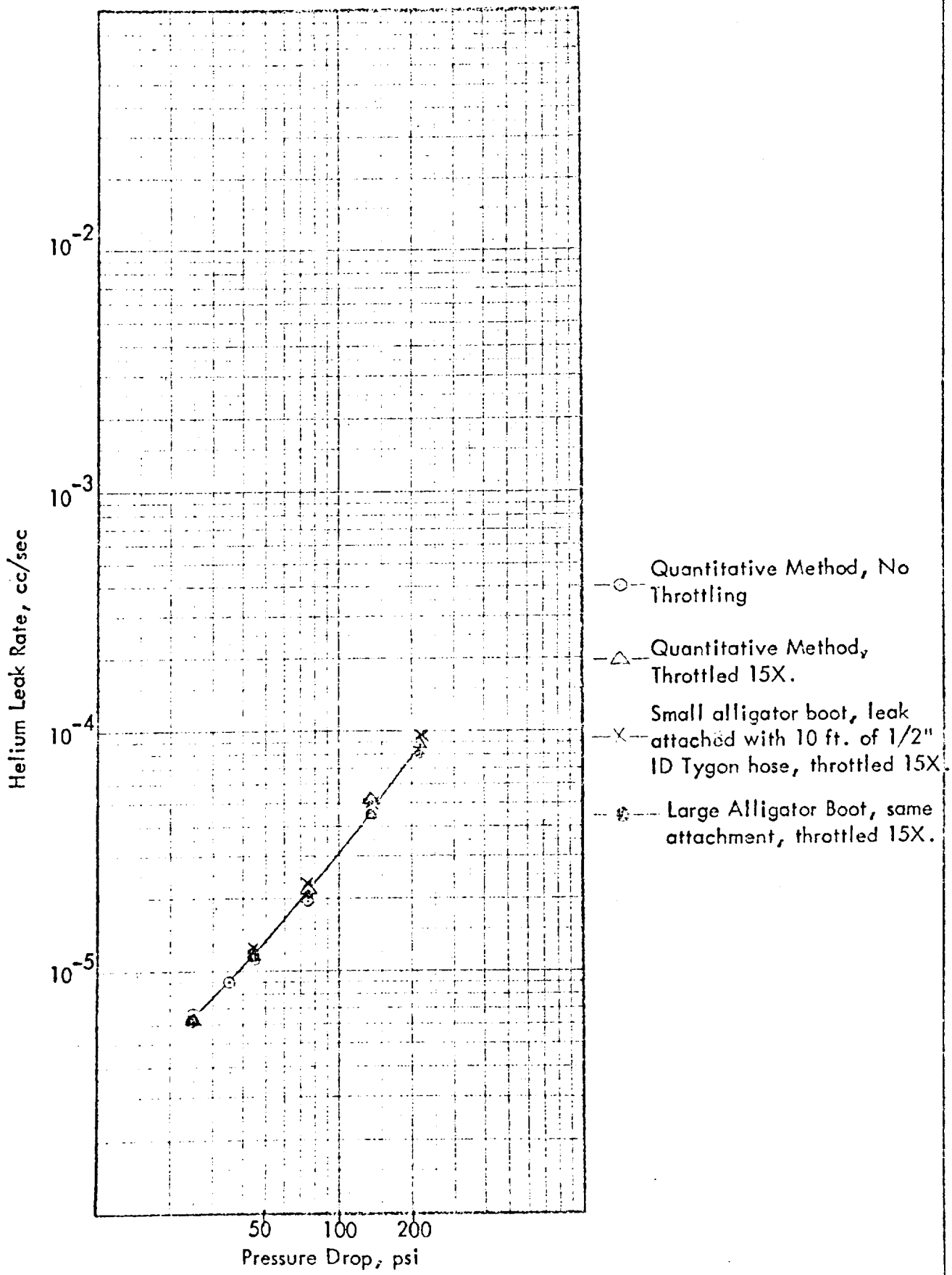

Figure 8. Comparison of Alligator Boot Vs. Quantitative Helium Leak Rate Measurement

fluid system joints, fittings, etc.). The standard leak can be attached so that it is in constant communication with the leak detector, or appropriate valving can be provided to allow periodic monitoring.

The test results indicated that the sensitivity of the alligator boot method is unaffected by boot pressure ranging between 9×10^{-3} and 3×10^{-1} torr. In addition, spraying the outside of the boot with helium for a few minutes, and allowing helium to leak into the area around the test bench for several hours, resulted in no change in sensitivity. Attaching the boot to the MSLD with a 10 ft. length of Tygon increased the response time slightly (20-30 seconds) but had no affect on sensitivity.

The alligator boot method is considered ideal for Apollo use from the standpoints of sensitivity and ability to quantitatively measure individual joint leak rates. Its major disadvantage is the need to fabricate a specific boot configuration for each different joint configuration. The speed of leak testing, although initially slower, perhaps, than the sniffer probe and bubble fluid systems, may prove faster in the long run because of the inherent reliability of the method.

4.0 TEST RESULTS ON INDIVIDUAL FLUIDS

This section contains the experimental data, both in tabular and graphical form, for each leak tested in which significant results were obtained. These individual figures and tables are grouped at the end of the report. In the case of the ECS liquids the same leaks were used to determine leak rates for water and two of the three water/glycol solutions. Summary curves of helium leak rates versus liquid leak rates for each liquid tested are given at the end of this report, and may be referred to for an overall view of the test results. We caution, however, against indiscriminate use of these curves without referring to the specific data and test conditions used in their generation.

4.1 Nitrogen Tetroxide Test Results

Nitrogen tetroxide was the first of the propellants tested. Learning to make satisfactory measurements proved to be a very lengthy process. Some five leaks were discarded before a winning combination of leak construction and cleaning, apparatus configuration and cleanliness, oxidizer purification and handling, and test procedure was put together.

Cleanliness far beyond that originally envisioned in the program, and quite possibly beyond that found in operational systems, was found necessary to prevent leak plugging. The oxidizer used was distilled and vapor filtered. It was found that trace but plugging amounts of contaminants could be obtained from such sources as valves and fittings that had been "LOX cleaned", the NO_2 cylinder valve itself, Teflon thread dope, and from the galling process by which our early scribed plug leaks were made. It appeared that even tightening an AN flared tube fitting upstream of the leak could generate contaminants. In these cases we found it advantageous to use gold gaskets.

All leaks were metal, either of the scribed plug or crushed tube variety, the latter proving the more satisfactory. No measurements using glass or loosely torqued AN plug leaks were attempted.

Of the 10 leaks exposed to N_2O_4 only 5 did not plug completely. Stable NO_2 leak rates were achieved with four leaks. These are tabulated below:

Leak rates for NO_2 are expressed in cc/sec of gas at its 70°F density. This material undoubtedly exists in the leak in the form of liquid N_2O_4, and evaporates at the exit from the leak.

TABLE 10. SUMMARY OF NITROGEN TETROXIDE LEAK DATA

Leak Type	Nominal Helium Leak Rate, cc/sec	Result Summary	Location of Data Table	Location of Graph Figure
Scribed Plug, mated surfaces	10^{-2}	Partially plugged, plug partially removed during post-test helium measurements. Good agreement with theory prior to removal of plug during helium test.	13	10
Scribed Plug	5×10^{-2}	Plugged severely initially, but plug was mostly removed by use of high heat and surges of high pressure. Run took 9 days.	11	9
Crushed Tube	5×10^{-6}	No significant plugging observed during NO_2 measurements but plugging of one order of magnitude obvious from helium-after results.	16	12
Crushed Tube	5×10^{-5}	This, the last NO_2 leak, performed faultlessly during NO_2 testing, but plugged absolutely prior to helium-after tests. Excellent theoretical agreement with helium-before data.	15	11

Figure 45 summaries the results of the above four leaks. It may be seen from Figure 45 that for each leak the NO_2 and helium leakage are roughly similar. Under ideal conditions (true Poiseuille flow at low pressure), it is theoretically possible for the NO_2 rate to be nearly an order of magnitude higher than the corresponding helium rate. The ideal leak geometry required for true Poiseuille flow was not achieved in this program, primarily because the test leaks tended to plug with precipitated solids on exposure to N_2O_4. However, if the actual leak geometry is considered to consist of numerous small capillaries through an area blocked by a precipitated solid, the resulting helium flow can be treated as a combination of Poiseuille flow and Knudson (molecular) flow. Then, if it is assumed that the leak geometry remained unchanged during the helium measurements after the N_2O_4 tests, the variation of the helium leak rate with pressure reflects the geometry of the leak and the relative contributions of Poiseuille and molecular flow to the total flow. The calculated NO_2 leak rates of Figures 9 through 12 were based on these assumptions, and agree fairly well with the measured NO_2 rates.

4.2 Monomethylhydrazine Test Results

Monomethylhydrazine for these tests is described in paragraph 2.3.2. Care was taken to prevent contact between the fuel and air, and as the viscosity measured at the end of the tests checked the literature value closely, it was concluded that no fuel degradation from contact with atmospheric carbon dioxide had occurred.

Data on four metal and eleven glass leaks is reported. In addition several early tests were run on scribed plug metal leaks. The data on these was very poor, and following the test the monomethylhydrazine from the reservoir was brown in color. This was attributed to system contamination, even though the components had been carefully cleaned prior to assembly. When the equipment was disassembled, carefully cleaned, and re-assembled this problem disappeared.

TABLE 17. SUMMARY OF MONOMETHYLHYDRAZINE LEAK DATA

Leak Type	Helium Leak Rate cc/sec	Summary of MMH Test Results	Location of Data Table	Location of Graph Figure
Smashed Tubing	10^{-2}	Flow rate initially 10-fold below theory, decreased 1500-fold further.	18	13
Smashed Tubing	5×10^{-3}	Initial flow rate 100-fold below theory, decreased 10-fold further.	19	14
AN Plug, Lightly Torqued	10^{-2}	Slow increase of leak rate up to 1/10th theory, then decreased.	20	15
AN Plug, lightly Torqued	10^{-3}	Initial leak rate 1000-fold below theory and then decreased.	21	16
Glass, No. 2	4×10^{-2}	Leak rate 2 times theory.	22	17

TABLE 17. (Continued)

Leak Type	Helium Leak Rate cc/sec	Summary of MMH Test Results	Location of Data Table	Location of Graph Figure
Glass No. 7	10^{-3}	Plugged after one point.	23	19
Glass No.'s 8 & 9	10^{-3}	Plugged after one point.	24	19
Glass No. 11	10^{-4}	Leak rate 30%> theory.	25	20
Glass No. 5	10^{-5}	Leak rate 30%> theory.	23	18
Glass No.'s 1 & 3	10^{-2} to 10^{-3}	Plugged after one point.	26	
Glass No.'s 4, 6 and 10	10^{-4}	Plugged during initial points.	27	

Monomethylhydrazine produced very severe plugging problems. After the early scribed plug tests a brown, gummy deposit was found on the plug. This was attributed to the system contamination previously mentioned. No such deposit was observed in the lightly torqued AN plug tests, when clean, colorless MMH was recovered from the reservoir. MMH from the reservoir of the smashed leak tests was also colorless. Nevertheless these tests also showed evidence of leak plugging.

All four metal leaks exhibited leak blocking. In every case the initial flow observed was far below the value predicted by applying simple theory to the observed helium flow rates. In addition the MMH flow rates continued to decrease with time. At the ends of these experiments the MMH flow rates were 3-1/2, 3, 2-1/2, and 3 orders of magnitude below the predicted values.

In each of these experiments the helium flow rates through the leak were decreased by exposure to MMH. The two smashed tubing leaks were decreased by factors of 1/30 and 1/100, the two AN plug leaks by factors of 1/2 and 1/4. This decrease, however, was far too small to account for the tremendously low MMH leak rates observed. A leak blocking mechanism which is partially removed when fuel is pumped out of the system must be invoked.

By contrast the MMH leak rates through the glass leaks were reasonably close to the theoretically calculated values. In every case they were high, between 30 and 100 percent high. Similar results were observed for water, water/glycol, and for the mixed hydrazine fuel. Possible explanations for this discrepancy are discussed in Section 2.4.3.

Blocking of the glass leaks was a major problem; in only three of eleven trials was it possible to run MMH leak rates at three pressure drop values, and then rerun helium calibrations. We could not tell whether the plugging was due to adventitious particles, or to some inherent property of the monomethylhydrazine. For this reason it is not possible to conclude that we were successful in obtaining leak rates close to theory in the glass leaks due to the chemical ineriness of glass as compared to stainless steel; our success may have been due entirely to our ability to use microliter quantities of fluids in the glass leaks.

The data of Figure 15 on the 10^{-2} cc/sec AN plug leak are interesting because of the slow increase in observed leak rate for the first two hours of the test. If this is due to slow seepage of MMH through the threads of the backing nut, it indicates the difficulty of obtaining accurate data in such a system, since the leak obviously must be plugging up while the equilibrium flow to the exterior of the test piece is being established.

4.3 Aerozine-50 Test Results

The Aerozine-50 used for these tests is described in paragraph 2.3.3. Helium blanketing was used to prevent reaction of the fuel with the components of the air. The viscosity of the fluid was measured after the test series, and the value obtained, while 5% below the literature value, indicated no significant reaction with aimospheric carbon dioxide. Reaction with CO_2 would markedly increase fuel viscosity and lead to much lower observed leak rates.

Data is reported on nine glass and three metal leaks. The metal leaks were all of the paragraph 2.2.4 AN lightly torqued plug type. No crushed tubing or scribed plug leaks were attempted.

TABLE 28. SUMMARY OF AEROZINE-50 LEAK DATA

Leak Type	Nominal Helium Leak Rate, cc/sec	Summary of A-50 Test Results	Location of Data Table	Location of Graph Figure
AN Plug, Lightly Torqued	10^{-2}	Gradual increase in flow rate within 1/2 order of magnitude of theory.	31	23
AN Plug, Lightly Torqued	5×10^{-3}	Gradual increase in flow rate to about 1/10 theory.	30	22, 23
AN Plug, Lightly Torqued	10^{-3}	Gradual increase in flow rate to within 1/10 theory.	29	21, 23
Glass No. 1	10^{-2}	Leak rate 1-1/2 times theory	32	24
Glass No. 2	10^{-3}	Plugged after 1 point.	35	-

TABLE 28. (Continued)

Leak Type	Nominal Helium Leak Rate, cc/sec	Summary of A-50 Test Results	Location of Data Table	Location of Graph Figure
Glass No. 3	10^{-4}	Plugged on first point.	35	-
Glass No. 4	10^{-3}	Leak rate about 30%> theory.	33	25
Glass No 5	$5x10^{-4}$	Leak rate about 20%> theory.	33	26
Glass No. 6	10^{-5}	Plugged after 1 point.	35	-
Glass No. 7	10^{-5}	Leak rate about 30%> theory.	34	27
Glass No. 8	10^{-4}	Plugged after 1 point.	35	-
Glass No. 9	10^{-4}	Leak rate about 1-1/2 times theory.	34	28

The consistent plugging phenomena by MMH noted with metal leaks was not noted in the three metal leaks tested with Aerozine-50. Indeed, two of the three showed significant increase in post-test helium leak rates while the intermediate size leak showed some plugging. This latter test was performed on a fixture which did not have the same quality of workmanship as the other two and may indeed have contained some residual contamination. In all cases the Aerozine-50 recovered after test appeared clean and colorless.

Higher than 50 psig data could not be taken on the 10^{-2} metal leak as the leak rate became so high that it started to drip.

Figures 21 and 22 give the results of the 5×10^{-3} and 10^{-3} metal leaks. Figure 23 gives a historical plot of the three metal leaks. It can be seen that, as in the case of MMH leaking through similar leaks, time to reach some sort of equilibrium is rather long. The marked data scatter at "equilibrium" is undoubtedly due to erratic fluid movement in the leak configuration downstream of the actual leak orifice.

Comparing only the MMH filled AN flared leaks with similar A-50 filled leaks, it would seem that the blocking mechanism prevalent in the MMH case is not so severe or absent in Aerozine-50.

By contrast, Aerozine-50 in glass leaks performed reasonably like MMH. Again results were some 30-50% above theoretically predicted, and a high incidence of plugging occurred. As in the case of the MMH glass leaks, when plugging occurred it was absolute and no post-test helium runs were possible.

A series of hypodermic syringe calibrations (Table 6) were performed subsequent to the Aerozine-50 glass leak tests in which the 10-microliter syringe used in the leak tests was utilized to inject various volumes of Aerozine-50 into tared simulated leaks. The leaks were then weighed and actual delivery volume calculated. The purpose of the experiment was to simultaneously calibrate the syringe-delivery technique. It was suspected from visual observation that some Aerozine-50 tended to adhere to the outside of the syringe needle when it was withdrawn from the leak. The data obtained seems to confirm this suspicion in the case of the smallest delivery volumes (2 microliters). Errors in larger volume deliveries were found negligible. This data can therefore not be used to support any sensible explanation of the actual vs. theoretical results discrepancy.

4.4 Water and Water/Glycol Test Results

The four test fluids, water, 35-percent glycol/water, 62-percent glycol/water and Type II water/glycol are described in paragraph 2.3.4 and 2.3.5. Leak rates for these fluids were measured using glass capillary leaks only. The low volatility of the glycol/water solutions precluded the use of the sweeping techniques required for low leak rate metal leaks. The data in Table 4 illustrate the very slow transfer rate of ethylene glycol from a glass surface into a bubbler. Therefore the microvolume expulsion method, which depends on seeing through the leak, was used in most of the tests. Weighing or chemical analysis of expelled liquids was used in some experiments.

Location of the data and graphs for these liquids is summarized below:

TABLE 36. SUMMARY OF WATER & WATER/GLYCOL LEAK DATA

			Water		35% Glycol/ Water		62% Glycol/ Water		Type II Water/Glycol	
Leak No.	Leak Size	Test Method	Data Table	Graph Figure	Data Table	Graph Figure	Data Table	Graph Figure	Data Table	Graph Figure
	10^{-1}	1			47	39				
	10^{-2}	1			48	40				
	10^{-3}	1			49	41				
2-1	10^{-1}	1	37	29			37	29	37	29
1	10^{-2}	1	38	30			38	30	38	30
3-1	10^{-3}	1	39	31			39	31	39	31
	10^{-4}	1	40	32			40	32	40	32
6	10^{0}	2							44	36
1	10^{-1}	2							45	37
11	10^{-3}	3							46	38
4	10^{0}	2	41	33						
12	10^{-3}	1	42	34						
16	10^{-3}	1	43	35						

Test Methods:
1. Microliter Expulsion
2. Weighing of Expelled Fluid
3. Chemical analysis of expelled fluid.

It will be noted that it was possible to measure leak rates for three of these fluids through the same glass leaks (the fourth fluid studied, 52 percent glycol/water was done at a later date, or it could also have been done in the same leaks). Plugging occurred with all four fluids, however it was much more prevalent and persistent with the Type II fluid. In fact it was necessary to run this last; in three out of four cases with small leaks this fluid plugged the leak irreversibly, preventing re-measurement of the helium leak rate after the experiment was completed. A number of additional leaks were tested, for which data has not been presented, in which leak plugging occurred so soon that no significant data could be obtained.

The much greater tendency for Type II fluid to plug the leak was attributed to its corrosion inhibiter content. As noted above, in the as-received condition, this liquid contained a great deal of suspended solid. Even though this was removed by filtration, it seemed that additional solids could form and block the leaks. This may be a very significant factor in assessing the applicability of this data to Apollo hardware situations.

Extreme care was required with these fluids to get satisfactory data. All testing was accomplished working at a laminar flow clean bench. The solvents used for cleaning leaks, syringes, tubing, and the pressurization system were all filtered through a 0.45 micron Millipore filter. The Tygon pressure tubing used was carefully blown out with helium which had passed through a similar filter. When leak plugging did occur an attempt to remove the blockage was made, by forcing solvents or detergent through the leak by pressure back flushing, or by forcing a jet of solution through a fine syringe tip up into the leak. Sometimes it was possible to clean out a plugged leak and reach the original helium leak rate, at other times this proved to be completely impossible.

The data of Table 46 and Figure 38 for Type II water/glycol through a 10^{-3} cc/sec helium leak, measured using the chemical analytical technique, show how leak plugging with this fluid made use of the visual technique mandatory. In this experiment it appears that the initial group of data points at 30, 60, and 90 psig represent leakage through a partially blocked leak, at a rate less than 0.1 percent of theory. Furthermore the slope of the data, if plotted, suggests that the leak was becoming more obstructed during the test.

The leak was then "cleaned out" at which point the leak rate became too low to measure by this analytical method. The leak was again cleaned out, at which time a third run was initiated. This apparently gave three reasonable data points, and then began to close up again. At no time did the observed leak rate reach within an order of magnitude of theory, based upon the initial helium leak rate, even though several of the points were close to the theoretical value based upon the final helium leak rate observed for the partially plugged leak. When this kind of changeable leak rate is observed, a test method giving leak rates immediately, instead of after several hours of mixing, standing, and analytical work, is a must.

The microliter volume data shows the same trend as the similar data for the hydrazine fuels. The observed leak rates are higher than theory, by between 30 percent and 100 percent. The results are consistent enough so that this probably represents some systematic bias in the experiment. Two explanations are immediately apparent:

1. The theory used for prediction is too unsophisticated. In particular, it does not make allowance for retention of fluid in a stationary film on the walls of the leak.

2. The fluid wetting the leak just above the capillary does not all move down into the leak during the expulsion time. This error would be larger for a large leak, where smaller expulsion times are encountered.

The data measured by weighing the expelled Type II water/glycol from a 10^{-1} cc/sec helium leak checked theory accurately. This would appear to confirm the conclusion that the high results for fluids obtained by the microliter expulsion method contain some experimental bias.

From this data the following conclusions can be drawn:

1. Water/glycol solutions and water plug small leaks rapidly, unless care is taken to use filtered fluids.

2. Inhibitor increases the plugging tendency of water/glycol solutions.

3. The predicted leak rate, using Poiseuille theory, through glass capillary leaks of 10^{-1} to 10^{-3} cc/sec of helium is between 20 and 50 percent below the observed leak rate by the microliter volume method.

4.5 Fixed Gas Test Results

Leak rates of four gases (helium, hydrogen, oxygen, and nitrogen) were measured through metal leaks of 10^{-2}, 10^{-4}, and 10^{-6} cc/sec of helium. Data is given in Tables 50, 51, 52, and 53, and graphed in Figures 42, 43, and 44. The volumetric water displacement method was used for the 10^{-2} cc/sec leak, and the mass spectrometric method described in paragraph 2.4.4 was used for the 10^{-4} and 10^{-6} cc/sec leaks. Helium and oxygen were measured between 20 and 900 psi pressure difference, and hydrogen and nitrogen between 20 and 250 psi pressure difference. A discussion of the results, and of the relationship between actual values and values derived from gas flow theory, is given in Section 5.4 below.

One possible source of deviation in the experimental data should be pointed out The actual test data on the two smaller experimental leaks was taken using the Bendix mass spectrometer on April 8 and April 9 Calibration of the mass spectrometer sensitivity ratios for these gases was done on April 10. The validity of the results depends on the assumption that the ratio of the sensitivity of the system for a test gas such as oxygen, to its sensitivity for helium was invariant over this three day period, even though the helium sensitivity on these three days was 1.63, 0.59 and 1.05 x 10^{-7} atm-cc/sec/div (on the 10^{-11} scale) respectively.

Normally this assumption would be quite accurate for a given mass spectrometer. However, the instrument was subject to drift in the electronic control circuits; apparently triggered by a momentary line voltage surge in our laboratory. This drift caused the alignment of the ion beam to vary slightly from day to day, and was considered to be the cause of the differing daily helium sensitivities. Variation of ion beam alignment could cause the instrument to respond differently to different mass numbers (i.e., the sensitivity factor ratio of two gases would vary from day to day). This effect is considered to be the cause of the 50 percent higher than expected leak rate data for hydrogen discussed in Section 5.4.

5.0 DATA CORRELATION AND THEORY

No attempt will be made in this report to carry out any extensive discussion of the theory and practice of leakage measurement, or of the extensive theoretical treatments which have been made of fluid flow through small leaks of various configurations. This subject is adequately covered in available publications. In particular we have found the leakage testing handbook of Marr (Reference 15) to be exceedingly useful.

5.1 General Discussion of Fluid Leakage

Flow rate through a leak is controlled by a great many parameters. Among the most important of these are the geometry of the leak path, including its length, cross-sectional area, and its tortuosity, the pressure differential across the leak which acts as a driving force, the phase of the leaking fluid (e.g. gaseous or liquid) not only on both sides of the leak but also within the leak, and the type of flow at every position within the leak. Three types of flow are commonly encountered, molecular or Knudsen flow in which the molecular mean free path is greater than a typical flow path cross-sectional length, laminar viscous flow in which the flowing particles follow constant stream lines, and turbulent viscous flow in which the stream line flow breaks down due to the formation of eddys in the flow. A fourth type of flow, choked flow, occurs when a fluid encounteres a large pressure differential when flowing through a short orifice and reaches sonic velocity. Sonic flow is not considered to be present commonly during normal leakage conditions.

The particular flow mode encountered in a given leak depends on the parameters enumerated above. Theoretical analysis of flow through small leaks is complicated by three facts. Firstly, the transition between two flow modes is not sharp and as one flow mode is giving way to a second the theoretical treatment becomes complicated. Many theoretical equations describing such transition flow are available. Secondly the flow mode may change within the length of the leak path of a single leak due to changing pressure or changing geometry. In particular a gas leaking from a high pressure to vacuum could undergo laminar flow until a pressure small enough to permit molecular flow is encountered. Cross-sectional variation can result in both laminar and turbulent flow in the same leak. And thirdly it is possible for two different leaks to exhibit the same leak rate for a given

fluid at the same pressure difference, while undergoing two different modes of leakage. One leak might consist of a single channel, while another leak consists of multiple fine capillaries. In the latter case flow through some capillaries might be molecular, through others might be laminar, and through still others could be transitional between molecular and laminar.

The following table, assembled from Marr's handbook, lists some of the conditions under which different leakage modes may be anticipated.

TABLE 54. FLOW RELATIONS INVOLVED WITH VARIOUS FLUID LEAKAGE MODES

Leakage Type	Leakage Region (cc/sec)	Gaseous Leakage Flow-Press. Relation $Q \propto$	Flow Prop. $Q \propto$	Liquid Leakage Region Reynolds No.	Liquid Leakage Flow-Press. Rel.
Turbulent	$>10^{-2}$	$(P_1^2-P_2^2)^{1/2}$	$\sqrt{1/M}$	>2100	$\sqrt{P_1-P_2}$
Laminar	10^{-1}-10^{-6}	$(P_1^2-P_2^2)$	$1/\eta$	<1200	P_1-P_2
Molecular	$<10^{-5}$	P_1-P_2	$\sqrt{1/M}$	Not Applicable	

In order to correlate leak rates of different fluids, especially when comparing the leak rate of a gas and a liquid through the same leak, it is necessary to know the applicable leak mode. This is frequently difficult to discover.

The majority of our measurements have been made with fluids leaking from an elevated pressure to one atmosphere. Under these conditions, and with the size of leaks with which we have dealt, the majority of our leakage has occurred in the laminar mode.

For laminar flow of a gas through a cylindrical leak the Poiseuille equation is applicable:

$$Q_G = \frac{\pi}{8} \cdot \left(\frac{D}{2}\right)^4 \cdot \frac{1}{L} \cdot \frac{1}{\eta_G} \cdot P_a (P_1 - P_2) \qquad \text{(Eq. 1)}$$

Q_G = gaseous leak rate = quantity/unit time.

D = diameter of leak path

L = length of leak path

η = absolute viscosity of gas

P_a = average pressure of gas within the leak = $(P_1 + P_2)/2$

P_1 = pressure at high side

P_2 = pressure at low side.

By algebra we get $Q_G = \frac{\pi}{8}\left(\frac{D}{2}\right)^4 \cdot \frac{1}{2 \cdot \eta_G \cdot L}\left(P_1^2 - P_2^2\right)$ (Eq. 2)

For laminar flow of a liquid through a cylindrical leak path the following equation applies:

$$Q_L = \frac{\pi}{8}\left(\frac{D}{2}\right)^4 \cdot \frac{1}{L} \cdot \frac{1}{\eta_L}\left(P_1 - P_2\right) \qquad \text{(Eq. 3)}$$

Q_L = liquid leak rate = quantity/unit time

η_L = liquid absolute viscosity

Since the geometrical factor of $\pi/8 \cdot (D/2)^4 \cdot 1/L$ is the same in equations 1 and 3, the ratio of Q_L to Q_G is given by:

$$Q_L = Q_G \cdot \frac{\eta_G}{\eta_L} \cdot \frac{1}{P_a} \qquad \text{(Eq. 4)}$$

If the leak path departs from the strictly cylindrical geometry used in deriving equations 1 and 3, it is still probable that the geometry will produce similar effects on gaseous and liquid flow. For this reason equation 4 has been used in this report for calculating theoretical liquid flow rates from observed helium flow rates, even though it is recognized that the procedure rests on a shaky theoretical foundation.

Information concerning the flow mode in a leak may be obtained from a log-log plot of pressure difference against flow rate, as shown by the following derivations:

Equation 3 for liquids reduces to the form:

$$Q_L = K \cdot \Delta P \qquad \text{(Eq. 5)}$$

$$\log Q_L = \log K + \log \Delta P \equiv C + \log \Delta P \qquad \text{(Eq. 6)}$$

This implies that data relating leak rate to pressure differential should produce a straight line with a slope equal to one if plotted on log-log paper if the flow is laminar.

Equation 2, for gases, reduces to:

$$Q_G = K' (P_1^2 - P_2^2) \qquad \text{(Eq. 7)}$$

For leakage to a vacuum $P_2 = O$, $P_1 \equiv \Delta P$, and if logs are taken

$$\log Q_G = \log K' + 2 \log P_1 = C' + 2 \log \Delta P \qquad \text{(Eq. 8)}$$

This implies that a log-log plot of leak rate data vs. pressure difference should again be linear, with a slope of 2 for laminar flow.

If $P_2 \neq 0$ one would no longer expect a straight line plot with a slope of 2 for a plot of log Q against log ΔP. However if $P_2 \ll P_1$ the data should still closely approximate this form.

For some of the larger leaks studied in this program, which have been in the range of 10^{-2}–10^{0} cc/sec of helium, we have either moved from the region of laminar flow into the region of turbulent flow, or are in the process of so doing. For gases in the turbulent flow region, the appropriate equation is:

$$Q_G = D^{5/2} \left[\frac{RT (P_1^2 - P_2^2)}{16 FM \cdot L} \right]^{1/2} \cdot \pi \qquad \text{(Eq. 9)}$$

where the symbols are as defined previously, R, T, and M have their usual kinetic theory meanings, and F is a factor related to the frictional characteristics of the leak walls.

This equation, for the case of $P_2 = 0$, reduces to:

$$Q_G = K'' \cdot \Delta P_1 \qquad \text{(Eq. 10)}$$

$$\log Q_G = \log K'' + \log \Delta P = C'' + \log \Delta P \qquad \text{(Eq. 11)}$$

and again a log-log plot will be linear with a slope of one. As long as $P_2 \ll P_1$ the plot will still be close to linear, with this same slope. Thus as the gaseous flow mode changes from laminar to turbulent, the change should be indicated by a change in the slope of a log-log plot from two to one.

The applicable equation for liquid leaking by the turbulent mode is:

$$Q_L = \frac{\pi}{4} D^{5/2} \left[\frac{P_1 - P_2}{2 \cdot \rho \cdot F \cdot L}\right]^{1/2} \qquad \text{(Eq. 12)}$$

From this equation, with the usual assumption that $P_2 \ll P_1$ it follows that a plot of log Q_L against log ΔP would give a straight line with a slope of 1/2. It is not probable that any of our liquid leak rates were high enough to be in the turbulent range.

The final case to be considered is that of a combination of laminar and Knudsen gas flow. This will occur when a gas is leaking from a relatively high pressure to a vacuum. At the leak inlet flow is obviously laminar unless the leak is so large that turbulent flow can take place. As the pressure drops through the leak a position will be reached when the pressure is low enough so that the molecular mean free path of the gas will be of the same order of magnitude as the diameter of the leak. This is the condition required for the onset of Knudsen flow, and from this point to the outlet Knudsen flow will occur. For very fine capillaries this may occur at a reasonably high pressure; a leak consisting of many capillary channels in parallel may exhibit this behavior with a reasonably high flow rate.

An equation fitting this situation has been given by J. Amesz (Reference 16) as follows:

$$Q_G = 10^{-6} \frac{D^3}{L} \left[0.093 \frac{D}{\eta_G}(P_1^2 - P_2^2) + 2.88 \sqrt{\frac{T}{M}}(P_1 - P_2)\right] \qquad \text{(Eq. 13)}$$

Equation 13 expresses the gas flow rate in micron-liters/sec instead of atm-cc/sec. This equation, as noted below, was used as a basis for predicting liquid flow rates from helium leak rate data obtained from the helium leak detector.

5.2 Discussion of Observed Helium Leakage

Helium leak rates through leaks, with leak rates ranging between 2.3 cc/sec and 5.2×10^{-7} cc/sec are plotted in this document. Almost all of these, with the exception of the lightly torqued AN plug leaks, approximate cylindrical leaks to some degree. The theory discussed in the previous section suggests that log-log plots of leak rate against pressure difference for small leaks should lie on various parts of a generalized curve. This curve has an initial slope of one for very small leak rates, corresponding to molecular flow, with the slope changing through a transition region to two for viscous laminar flow at moderate leak rates, and finally in a second transition region changing back to one again at the onset of turbulent flow.

A log-log plot for a single leak could lie partially in two of these portions of the generalized curve, since with a higher pressure differential and the resulting higher flow rate, the primary flow mode through the leak could be different from the primary flow mode at a lower pressure differential. Whether the downstream side of the leak is at a vacuum, or at ambient pressure, can also affect the flow mode strongly.

The primary mode of leakage exhibited by the majority of the leaks studies in this program seemed to be laminar, with slopes close to two for log-log plots of leak rate against pressure differentials. For the larger leaks a change of slope toward one can be seen, indicative of the onset of turbulent flow. Similarly for the smallest leaks a change of slope toward one can be seen, especially where the downside pressure is close to zero.

As an example, consider Figure 9, for a 5×10^{-2} cc/sec leak. A line connecting the 35 and 50 psi points, with leak rates of 2×10^{-2} and 4×10^{-2} has a slope of 1.7, while a line connecting the 250 and 350 psi points at 5×10^{-1} and 8×10^{-1} cc/sec has a slope of 1.4. Thus in both cases we appear to observe transitional flow, with the laminar mode predominating at low pressure differences and turbulent flow at high pressure differences.

The data graphed in Figure 20, for a 10^{-4} cc/sec leak, gives a slope of 2.0. This leak rate is in the middle of the laminar region, and the flow is probably laminar at all pressure differences.

The transition to molecular flow can be seen in Figure 12 for a 5×10^{-6} cc/sec leak. A change in slope from 1.5 at the high pressure difference to 1.3 at the low pressure difference indicates an increasing contribution of molecular flow to the observed flow rate. After the test the leak rate of the partially blocked leak had dropped by a factor of three, and the slope for the two lowest points was 1.0, indicating essentially molecular flow throughout the leak.

In applying this theory to explain the observed helium leak rates, it is important to recognize the possible effect of experimental data scatter on the observed leak rates and slopes. Also, it should be re-emphasized that the same leak rate can occur by different modes in two leaks with quite different geometries.

5.3 Discussion of Liquid Leakage

Leakage data for each individual fluid through a series of test leaks is given in both tabular and graphical form at the rear of this report. For every experiment a theoretical liquid leak rate has been calculated from the observed helium gas leak rate, and compared on the graph with the observed liquid leak rate. In the instances where the helium leak rate changed during the test the calculated curve was generally based upon the helium leak rate as observed at the end of the experiment. This choice is, in a measure, arbitrary since it was not usually possible to tell at what stage of the experiment partial blockage of the leak occurred. Where complete blockage took place, the theoretical curve was perforce calculated from the helium rate observed before the liquid was introduced.

Three techniques were used for calculating the theoretical curves. For small N_2O_4 leaks, where the helium leak rates were measured using the CEC leak detector, so that the downstream pressure was close to zero, an equation given by Amesz (Reference 16) was used. This equation allows one to predict liquid leak rates from gaseous leak rate data taken at three pressures leaking to a vacuum, even if both molecular and laminar flow modes are important in the gaseous flow.

$$Q_L = 2.0 \frac{\eta\, G}{\eta\, L} \Delta P_L \left[\frac{(P_B - P_A)(Q_{GC} - Q_{GB}) - (P_C - P_B)(Q_{GB} - Q_{GA})}{(P_C - P_A)(P_C - P_B)(P_B - P_A)} \right] \qquad \text{(Eq. 14)}$$

where Q_L = liquid leak rate in cc/sec

η = absolute viscosity

ΔP_L = pressure drop for the liquid leak

A, B, C = refer to three upper pressures for helium leaking to vacuum

P = pressure

Q_G = gas leak rate in atm cc/sec

For small helium leak rates measured volumetrically, so that the downstream pressure was 1 atmosphere, equation 4, as given in Section 5.1, was used. This included all of the tests for the hydrazine fuels, and the water/glycol fluids in which the slope of the log-log plots of helium leak rate against pressure drop approached 2.

For large helium leak rates, greater than 10^{-2} cc/sec of helium, where turbulent flow became important, so that the slope of the log-log plots approached 1, the liquid leak rate was predicted by multiplying the observed helium leak rate by the ratio of the viscosity of helium to the viscosity of the liquid. This approach was taken since it maintains the same slope for both curves, and since insufficient information is available in this leak rate region to allow more sophisticated calculation.

In general, the observed differences between predicted and observed values are within a factor of two of each other, provided the helium leak rate is measured under the same conditions of blockage as the fluid leak rates. For metal leaks this latter condition can be very difficult to fullfil, as extreme excursions of liquid leak rates were observed during the tests. It would appear that the use of these theories to predict liquid leak rates from observed helium leak rates is a reasonable procedure, which generally will err on the side of conservatism.

In the case of glass leaks measured by the mic volume expulsion technique, the observed liquid leak rates appear to be uniformly high, usually between 20 and 100 percent. As indicated previously, this probably represents a systematic experimental deviation, which could possibly be compensated for analytically, based upon enough calibration data.

Figures 45 to 51 present summaries of the relationships between observed helium and liquid leak rates for each liquid tested. They can be used for order of magnitude predictions, provided that it is remembered that each line represents an individual leak, with its own geometry, and that another leak with the same helium leak rates might possess somewhat different liquid leak rates.

It is interesting to compare the summary curves of Figures 50 and 51, since they deal with two quite similar fluids, glycol/water solutions with 62 and 67 percent glycol, with viscosities of 4.46 and 5.53 cps respectively. If these figures are overlaid, the leak rates for the 62% glycol/water are approximately 50% higher than those for the 67% glycol/water (Type II water/glycol). While this difference is somewhat larger than the difference in viscosities, the check is still fairly close.

5.4 Discussion of Fixed Gas Leakage

The objective of the fixed gas leakage tests was merely to determine whether the leak rates generally correlated with theory; thus extreme care was not taken in these measurements, and the resulting experimental error was correspondingly higher than would have been obtained if time-consuming sophisticated methods had been employed.

The results (Figures 42, 43 and 44) do indicate a general agreement with theory. Leakage through the largest test leak (Figure 42) was roughly proportional to the inverse of the gas viscosities at the low test pressures, and to the inverse of the square root of the gas molecular weights at the high test pressures. Also, the slope of the leakage curves for this test leak showed a decreasing trend with increasing pressure. It would therefore appear that the flow mode in this leak was in transition from viscous laminar to turbulent flow, with the flow at low pressure mostly laminar, and that at high pressure mostly turbulent.

Leakage through the medium-sized test leak (nominal 1×10^{-4} cc He/sec, Figure 43) appeared to be predominately in the laminar flow mode, except at the lowest test pressures at which a slight transition to molecular flow was observed. At the higher pressures, the slope of the leak rate plot approached 2, and the relative positions of the curves for the four gases indicate that the leak rates were roughly proportional to the inverse of the gas viscosities, although the hydrogen curve was about 50% higher than would be expected. At the lowest test pressures, the effect of the gas viscosity on the leak rates appeared to be reduced slightly in favor of the effect of the gas molecular weight.

The transition from molecular to laminar flow was much more strongly apparent in the smallest test leak (nominal 1×10^{-6} cc He/sec, Figure 44). At the lowest test pressures, the slope of the leak rate curves was very nearly one, and their relative displacement was approximately proportional to the square root of the gas molecular weights. Again, the curve for hydrogen was somewhat higher than would be expected, relative to those of the other gases. At the highest test pressures, the curves reflected the reducing influence of molecular weight and the increasing effect of gas viscosity, along with a gradual increase in slope, indicating the increasing contribution of the Poiseuille flow mode to the total leak rate.

It can be concluded that, as predicted by kinetic theory, the leak rates of the four gases are not greatly different under any conditions, and those of helium, oxygen, and nitrogen in the viscous laminar flow regime are quite similar because their viscosities are quite similar. Hydrogen leaks at a somewhat higher rate than the other gases because both its viscosity and molecular weight are lower than those of the other gases; this fact should be taken into account in assigning allowable leakage rates for other tracer gases in a system which will contain hydrogen.

6.0 DISCUSSION OF EXPERIMENTAL ERRORS

The reason for discussing experimental errors is to establish a confidence level for the experimental data presented. A completely rigorous discussion is not warranted because the measurement errors were estimated rather than being assessed statistically. The estimated errors of the individual measurements are reported in Table 55 together with the approximate probable error for each fluid correlation. (The probable error is that number which the actual error may, with equal probability, be greater than or less than.)

Table 55 shows that the estimated contribution of random errors to the probable error is relatively small (2.2 to 4.5%). The validity of this estimate is illustrated by the internal consistency of the data.

The estimated contribution of systematic or biased errors is generally greater than the contribution of random errors. In the case of the volumetric displacement measurements on the fixed gases no significant systematic errors are anticipated. The MSLD and mass spectrometer systematic errors arise from the 10% uncertainty of the rate of the standard helium leak used to calibrate the MSLD and the 6% error in the mass spectrometer detector factor for oxygen and nitrogen gases and the factor error for hydrogen, which is even greater. It should be noted that systematic errors in the helium measurements influence all correlations of liquid with helium leakage.

The N_2O_4 liquid leakage data is the most accurate with a probable systematic error of 5% due to the analytical standard. The probable correlation error of N_2O_4 vs. helium for the leaks used is 11.4%.

Systematic errors in the other liquid leakage data arise from difficulty in collecting materials of low volatility for chemical analysis or from inaccuracy in introducing known volumes of liquids into glass capillaries and liquid hold-up in the capillary when gas breakthrough occurs. These errors are systematic in the sense that the chemical analysis indicates lower than actual leakage rates in these cases while the microvolume expulsion indicates higher than actual values. They are also systematic in the sense that the influence on the leakage rate determined varies with leakage rate or sample volume, however, they are random in the sense that they are not quantitatively reproducible.

Systematic errors in the MMH and A-50 measurements may result in leakage rates determined by chemical analysis or microvolume expulsion which are as much as 25% low, causing helium correlation errors of the same magnitude. Systematic errors in the water and water glycol measurements result in leakage rates by the microvolume expulsion technique which are believed to be of the order of 10% high producing helium correlation errors of approximately 14%.

The foregoing discussion deals only with the accuracy of the experimental work done in this program. The difference between the experimental and theoretical correlations can be influenced by:

1. Systematic experimental errors.
2. Non-ideality of the leak path geometry.
3. Interaction of the leaking fluid and the material of construction of the leak.
4. Deficiencies in the theory applied.

TABLE 55

EXPERIMENTAL ERRORS

Fluid	Measurement Method	Error	Percent Error [1]	Type of Error [2]
Helium	MSLD	Upstream Pressure	±2	R
		Instrumental	±1	R
		Calibrating Leak	±10	S
		Probable Random [3]	±4.1	R
		Systematic [4]	±10	S
	Volumetric Displacement	Upstream Pressure	±2	R
		Gas Burette Volume	±1	R
		Time	±1	R
		Probable Random [3]	±4.2	R
		Systematic [4]	0	S
N_2O_4 (Liquid)	Chemical Analysis	Upstream Pressure	±2	R
		Sample Collection	-<2	S
		Time	±2	R
		Sample Dilution	±2	R
		Analytical Standard	±5	S
		Analytical Determination	±1	R
		Probable Random [3]	±3.6	R
		Helium Calibration [5]	±11.4	S
MMH and A-50	Chemical Analysis	Upstream Pressure	±2	R
		Sample Collection	25	S
		Time	±2	R
		Sample Dilution	±2	R
		Analytical Standard	±1	S
		Probable Random [3]	±3.6	R
		Helium Correlation [5]	<26.7	S
	Microvolume Expulsion	Upstream Pressure	±2	R
		Sample Volume	-<25	S
		Time	±1	R
		Probable Random [3]	±2.2	R
		Helium Calibration [5]	-< 26.7	R
H_2O and Water/Glycol	Microvolume Expulsion	Upstream Pressure	±2	R
		Sample Volume	-<10	S
		Time	±1	R
		Probable Random [3]	±2.2	R
		Helium Correlation [5]	-<14.1	S

TABLE 55 (Continued)

Fluid	Measurement Method	Error	Percent Error (1)	Type of Error (2)
Nitrogen Oxygen	Mass Spectrometer	Upstream Pressure	±2	R
		Detector Error	±6.3 (6)	S
		Instrumental	±2	R
		Probable Random (3)	±4.5	R
		Helium Correlation (5)	±18.1	S
	Volumetric Displacement	Upstream Pressure	±2	R
		Gas Burette Volume	±1	R
		Time	±1	R
		Probable Random (3)	±4.2	R
		Helium Correlation (5)	0	S

(1) Estimated Error

(2) R is Random, S is Systematic (See Text).

(3) Probable Random Error in Absolute Leak Rate (Assuming Laminar Flow).

(4) Systematic Error or Bias in Absolute Leak Rate.

(5) Probable Systematic Error or Bias in Fluid vs. Helium Correlation.

(6) Detector Factor Error is Greater for Hydrogen (See Text).

NOTE: (3), (4) and (5) Estimated as the Root Sum Square of the Contributing Errors.

7.0 CONCLUSIONS AND RECOMMENDATIONS

7.1 Conclusions

1. Leaks in the 10^{-1}-10^{-6} cc/sec of helium range are extremely susceptible to plugging and partial blockage during liquid flow conditions.

2. In view of the unpredictability of plugging effects, application of laboratory experimental data to actual hardware liquid leaks should be done with caution.

3. Poiseuille flow theory satisfactorily predicts liquid flow rates through unblocked glass leaks in the 10^{-2}-10^{-5} cc/sec of helium range.

4. Poiseuille flow theory predicts propellant flow rates through metal leaks which are in general higher than the actual rates experienced. In no case were liquid flow rates encountered significantly higher than predicted.

5. Extreme care in cleaning system components, and the assembled system, and in purifying and filtering test fluids reduces but does not prevent leak plugging.

6. This program did not study leakage due to permeation. Such leakage is generally not susceptible to plugging or blockage.

7. Chemical analytical techniques, based upon sweep methods, are a convenient and accurate way of measuring liquid leak rates providing the liquid is sufficiently volatile.

8. N_2O_4 flow rates through leaks in the 10^{-2} to 10^{-6} cc/sec of helium range can be predicted from measured helium leak rates within 50%, using transition flow theory, and assuming N_2O_4 liquid leakage. This is providing the helium flow rates are measured under the same blockage conditions as the N_2O_4 flow rates.

9. In every case N_2O_4 passing through a metal leak decreased the leak rate of helium to some extent.

10. The leak rate of MMH through metal leaks continued to decrease with exposure time.

11. In two out of three cases exposure of metal leaks to Aerozine-50 resulted in an increase in the helium leak rate.

12. Aerozine-50 does not appear to produce blockage of metal leaks as exposure time increases.

13. The presence of inhibitor in water/glycol solutions is a major factor in producing leak plugging.

14. Bubble leak fluid detection is inadequate for detecting small leaks ($<10^{-5}$ cc/sec helium), and may interfere with subsequent leak testing using better methods.

15. The sniffer probe method is of qualitative value only. The observed leak rates are approximately three orders of magnitude lower than the actual leak rate, and variations of ±300% are found between different operators, and different probe attitudes.

16. The alligator boot method, properly applied, can measure helium leak rates accurately.

7.2 Recommendations

1. We recommend that allowable helium leak rates be established, based upon allowable fluid leak rates, by assuming the appropriate theoretical relationship between the two. For liquids flowing through leaks of 10^{-2} cc/sec of helium and lower assume Poiseuille flow. The resulting permissible helium leak rates will be conservative in view of the probability of partial or complete blockage in actual hardware leaks.

2. We recommend use of the alligator boot method for measuring helium leak rates where it is geometrically feasible

3. When it is desired to study propellant leakage from a loaded system or assembly, we recommend use of sweep gas techniques combined with colorimetric chemical analytical methods.

4. In connection with recommendation 3, a chamber surrounding the leak is required. We recommend development of propellant resistant chambers similar to alligator boots, for this purpose.

5. We recommend additional study, aimed at developing the use of the mass spectrometer as a detector for continously monitoring propellant vapor concentrations during leak testing studies with sweep gases.

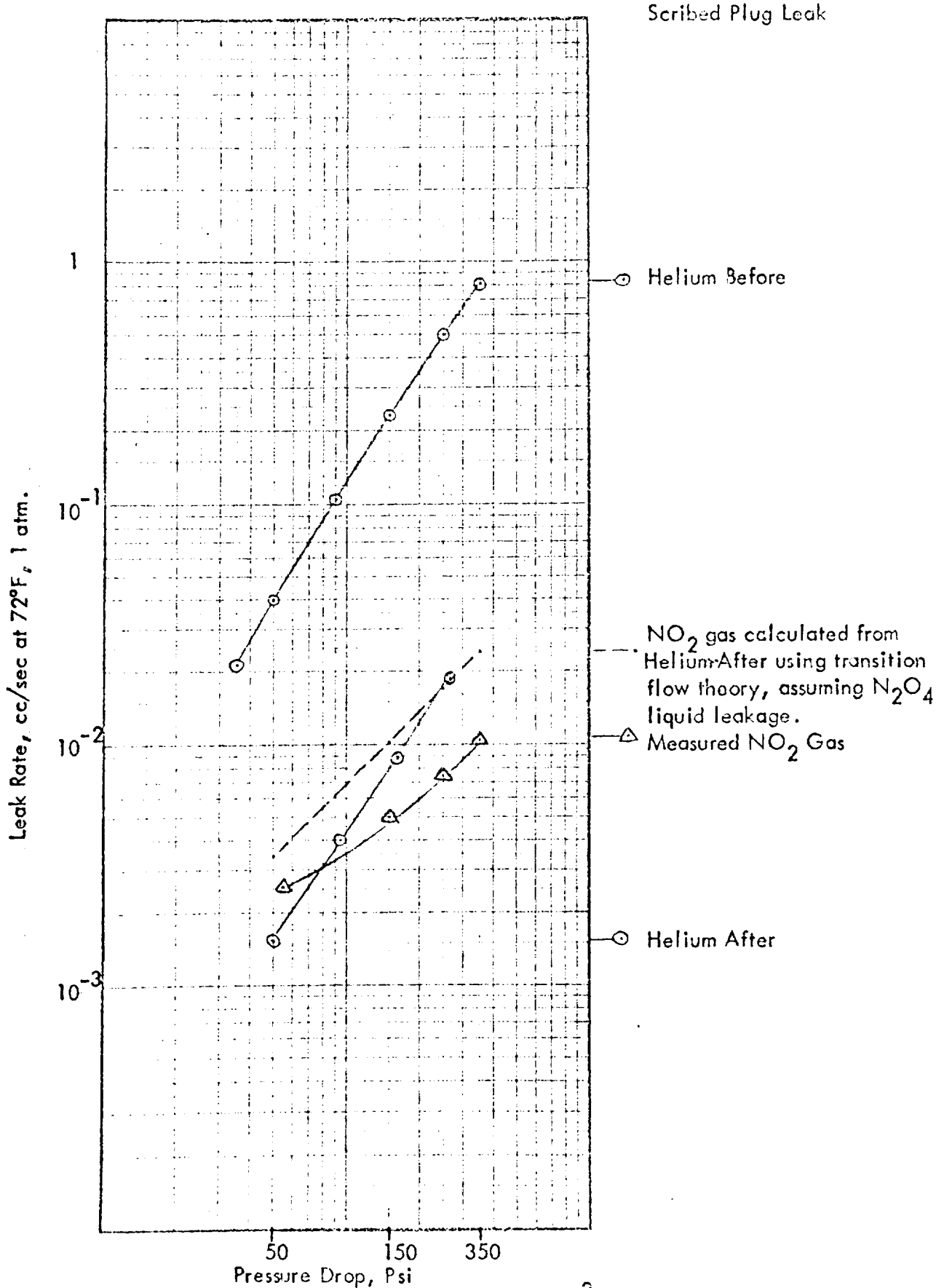

FIGURE 9. NO_2 LEAK RATES THROUGH A 5×10^{-2} cc/sec HELIUM LEAK

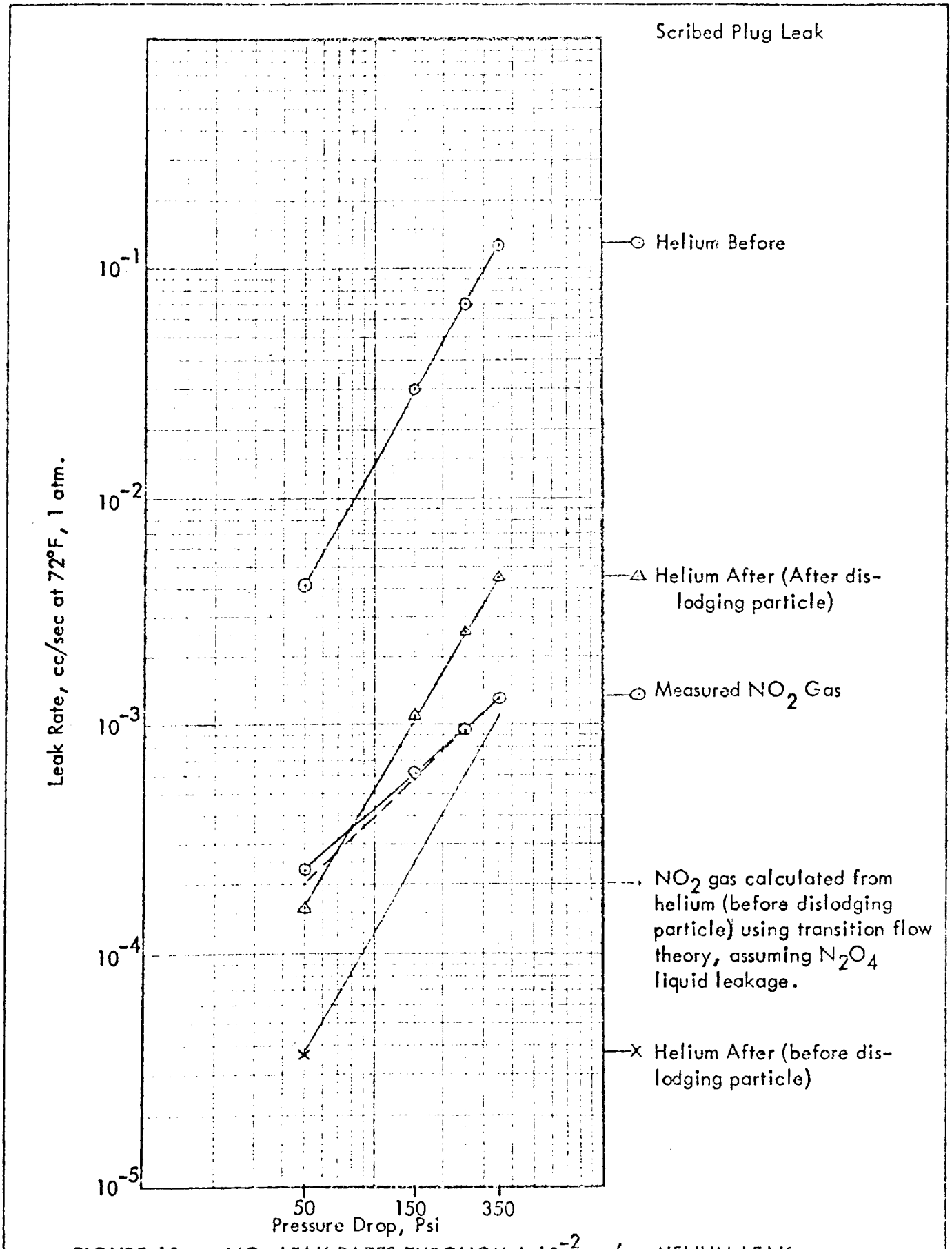

FIGURE 10. NO_2 LEAK RATES THROUGH A 10^{-2} cc/sec HELIUM LEAK

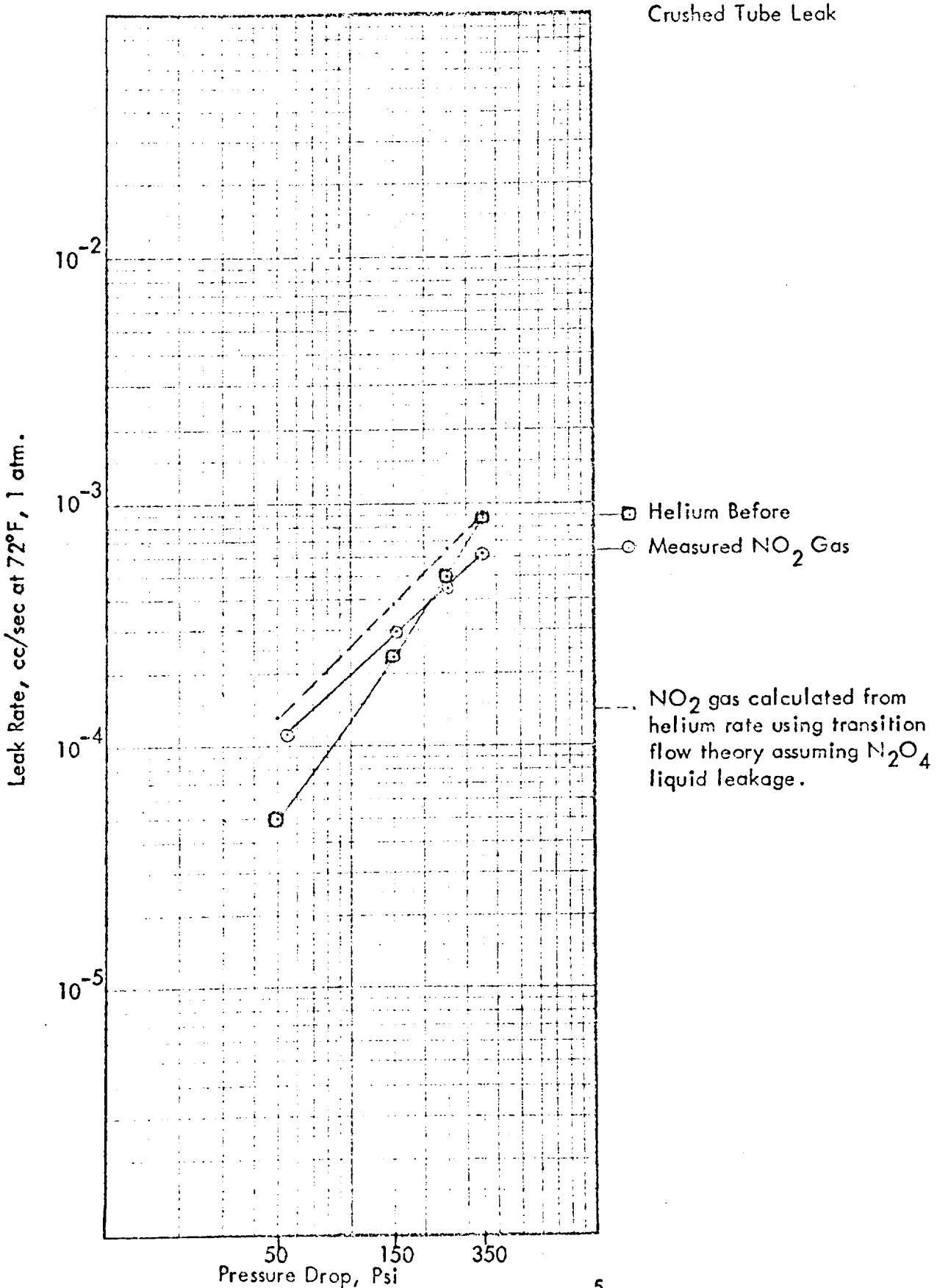

FIGURE 11. NO_2 LEAK RATES THROUGH A 5×10^{-5} cc/sec HELIUM LEAK

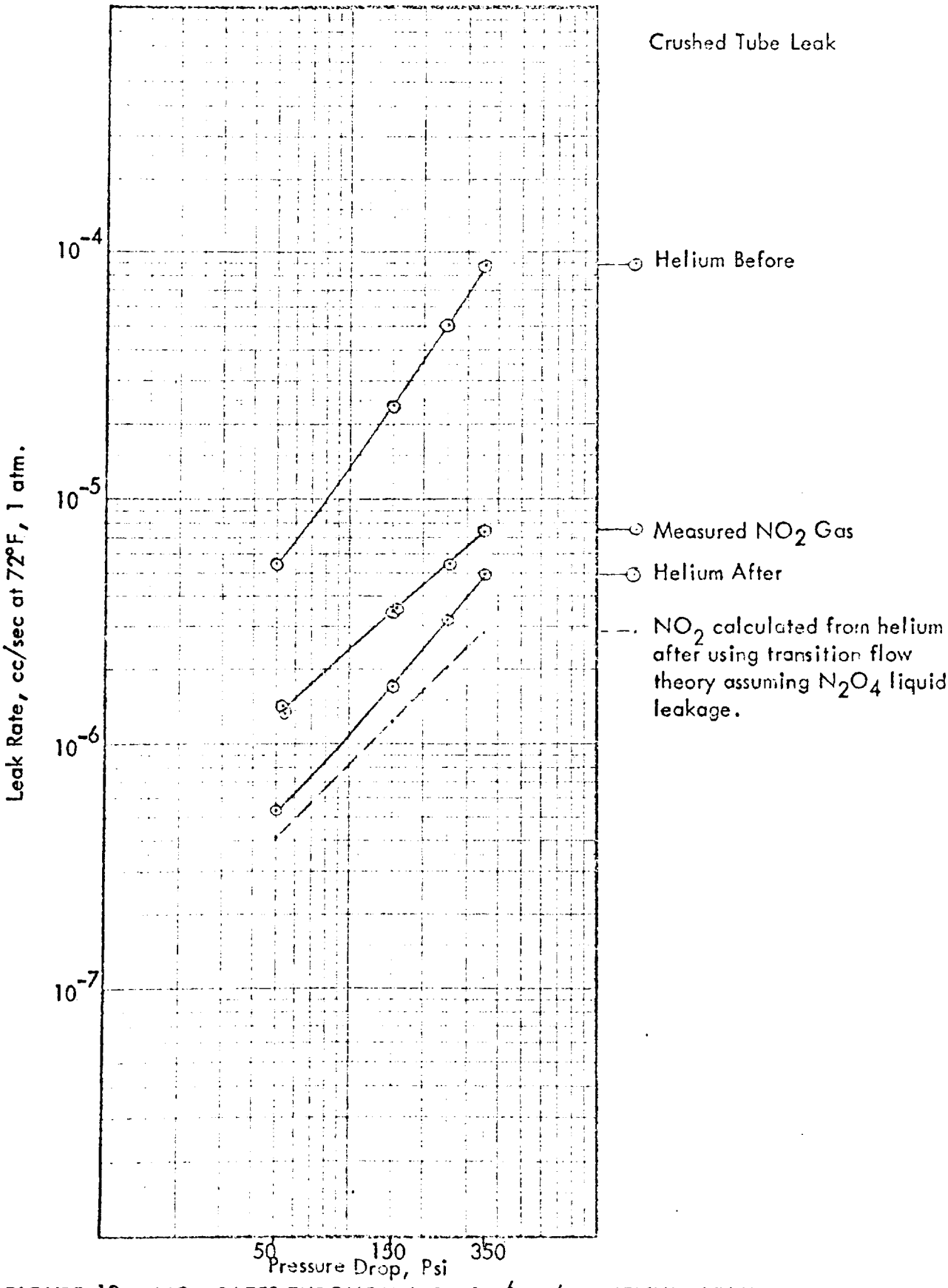

FIGURE 12. NO_2 RATES THROUGH A 5×10^{-6} cc/sec HELIUM LEAK

FIGURE 13. MONOMETHYLHYDRAZINE LEAK THROUGH A 10^{-2} cc/sec SMASHED TUBING HELIUM LEAK

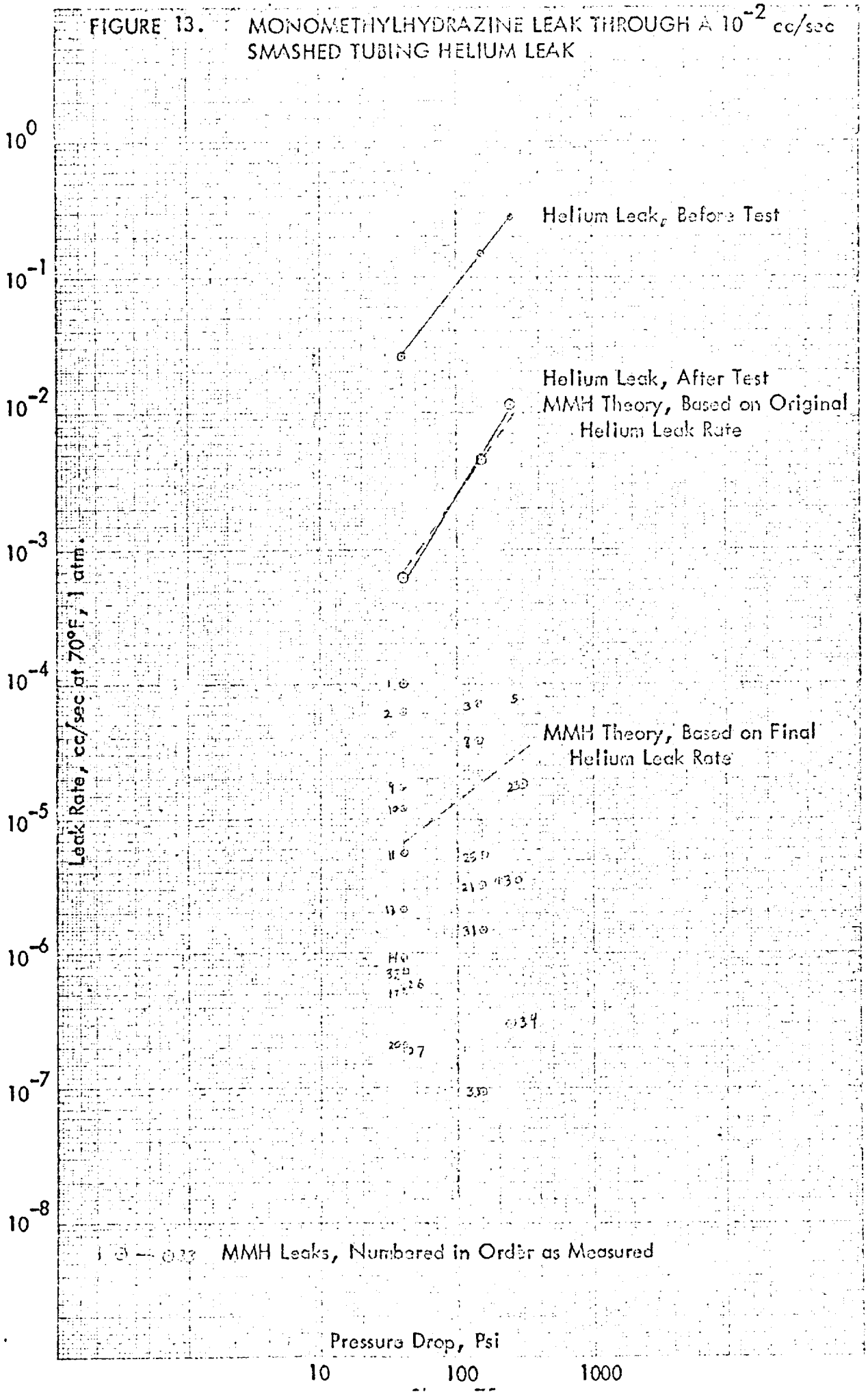

FIGURE 14. MONOMETHYLHYDRAZINE LEAK THROUGH NOMINAL 5×10^{-3} cc/sec HELIUM LEAK

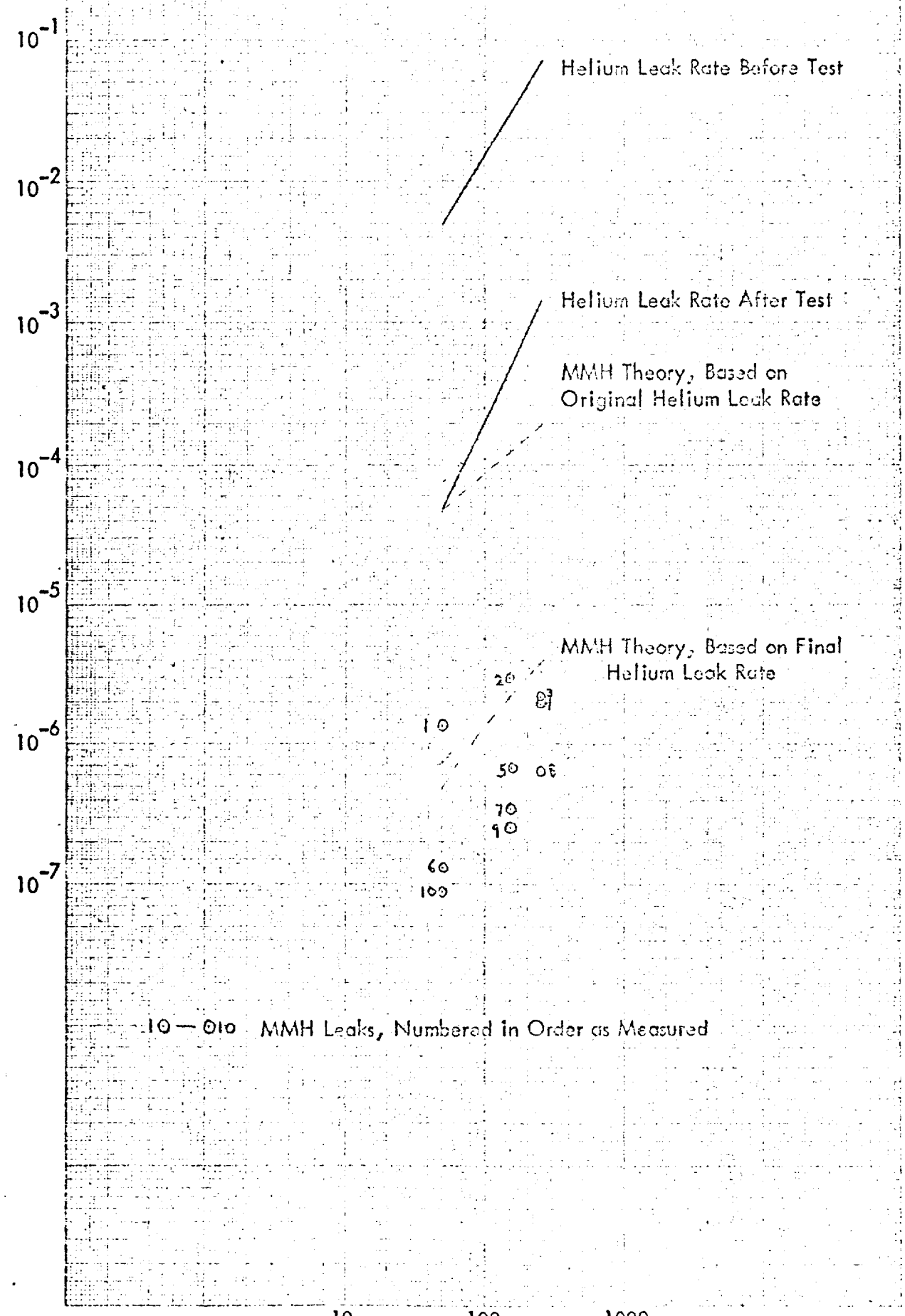

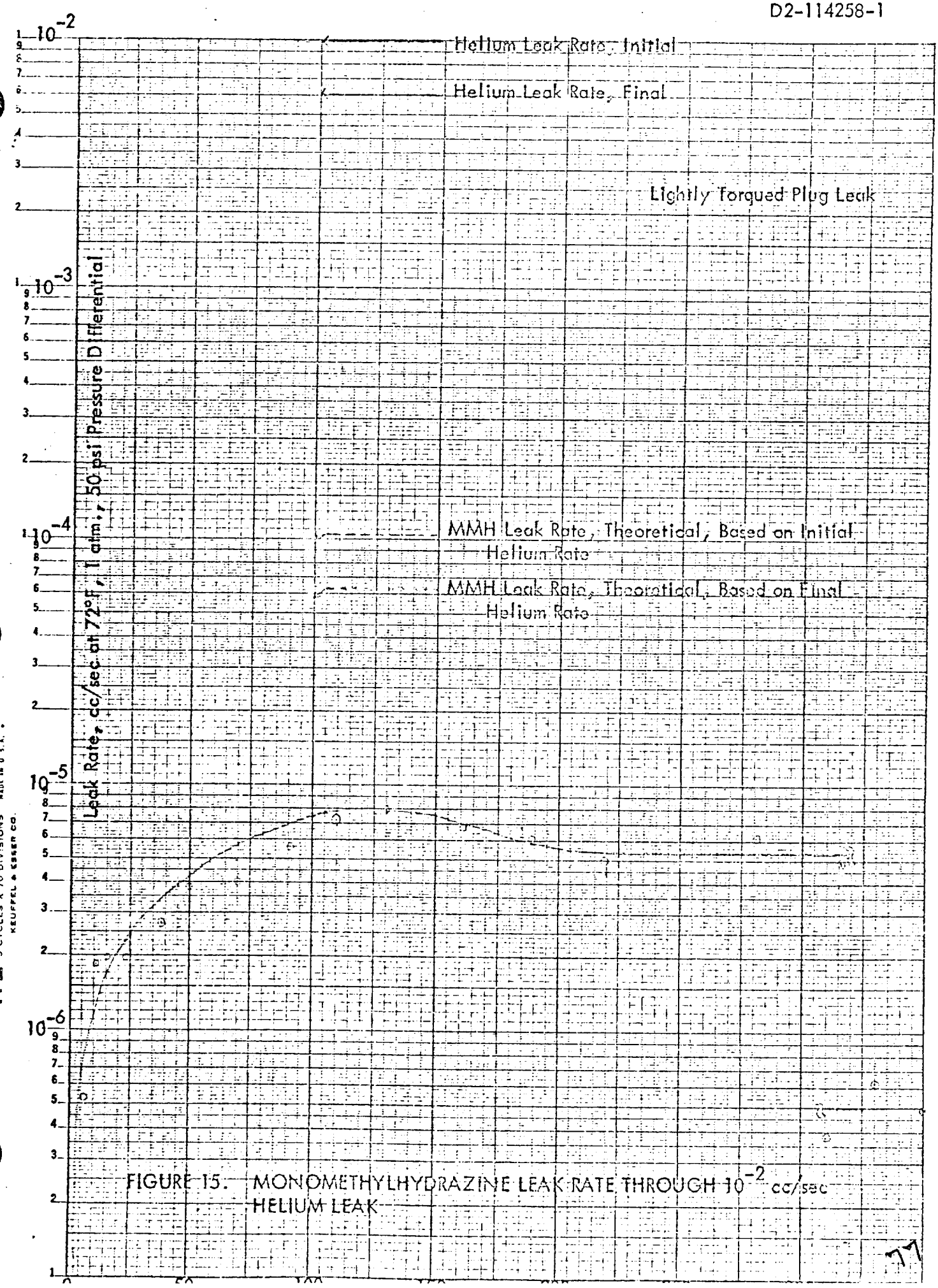

FIGURE 15. MONOMETHYLHYDRAZINE LEAK RATE THROUGH 10^{-2} cc/sec HELIUM LEAK

FIGURE 16. MONOMETHYLHYDRAZINE LEAK THROUGH A 10^{-3} cc/sec HELIUM AN PLUG LEAK

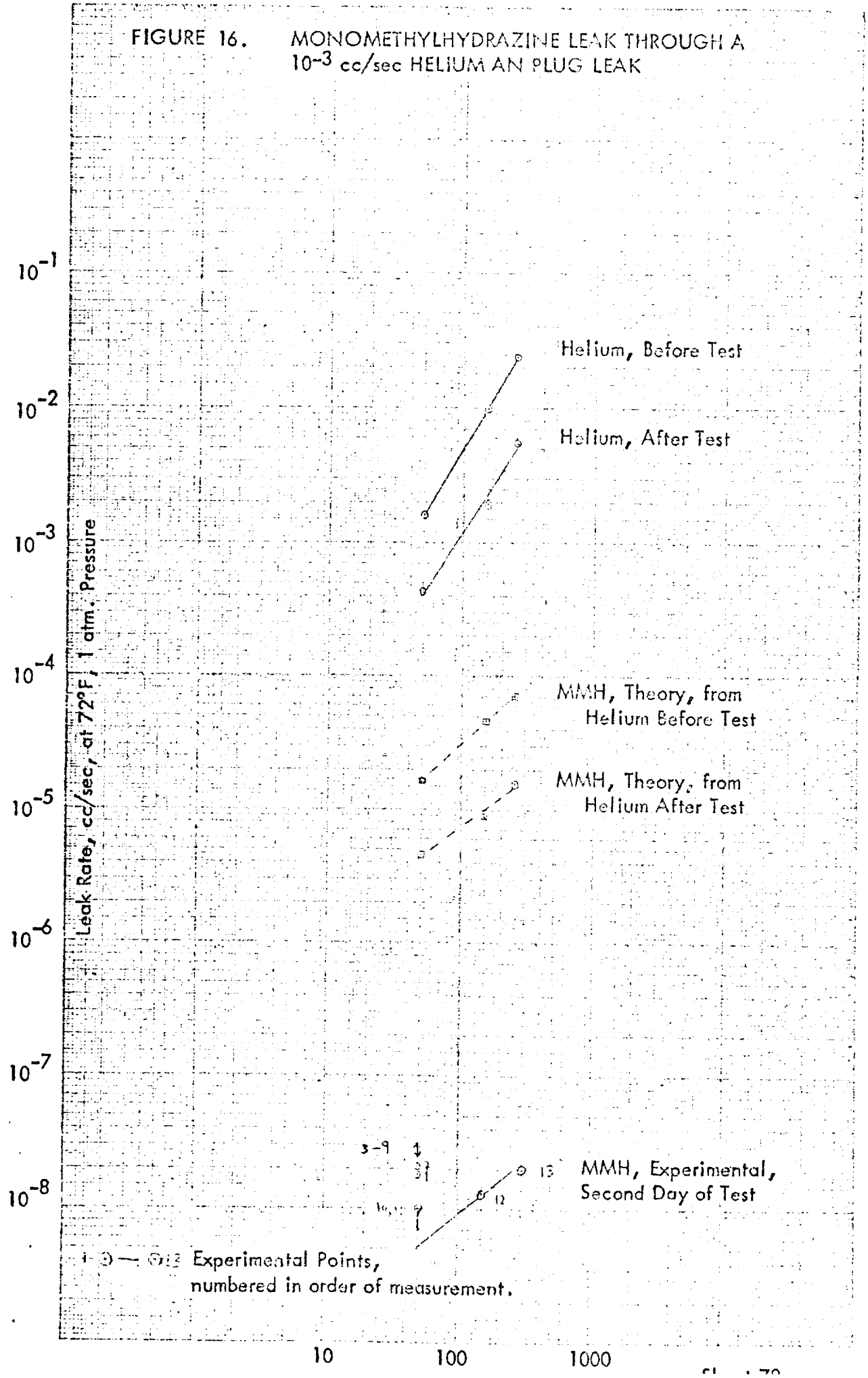

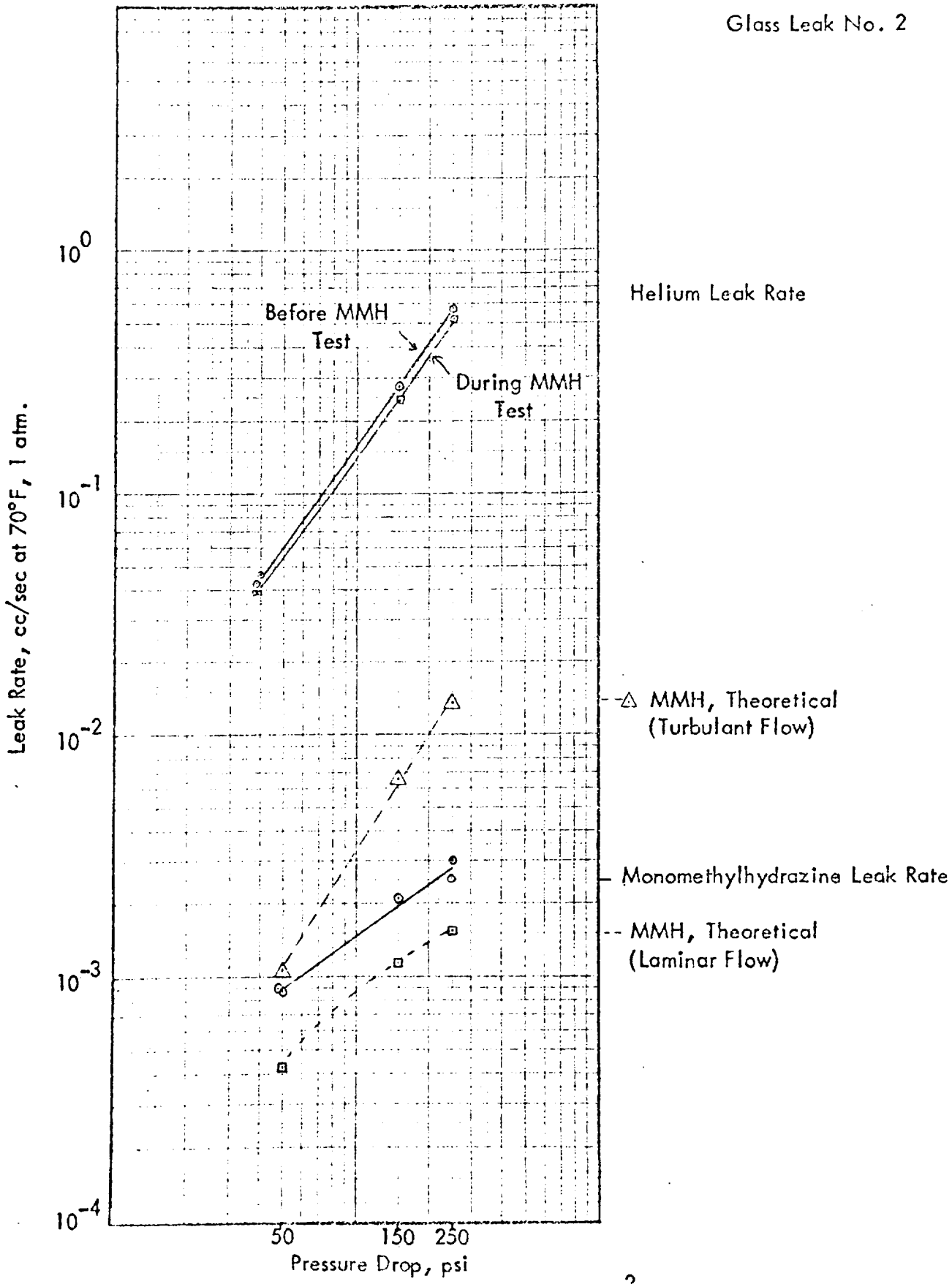

Figure 17. Monomethylhydrazine Leak Rate Through a 10^{-2} cc/sec Helium Leak

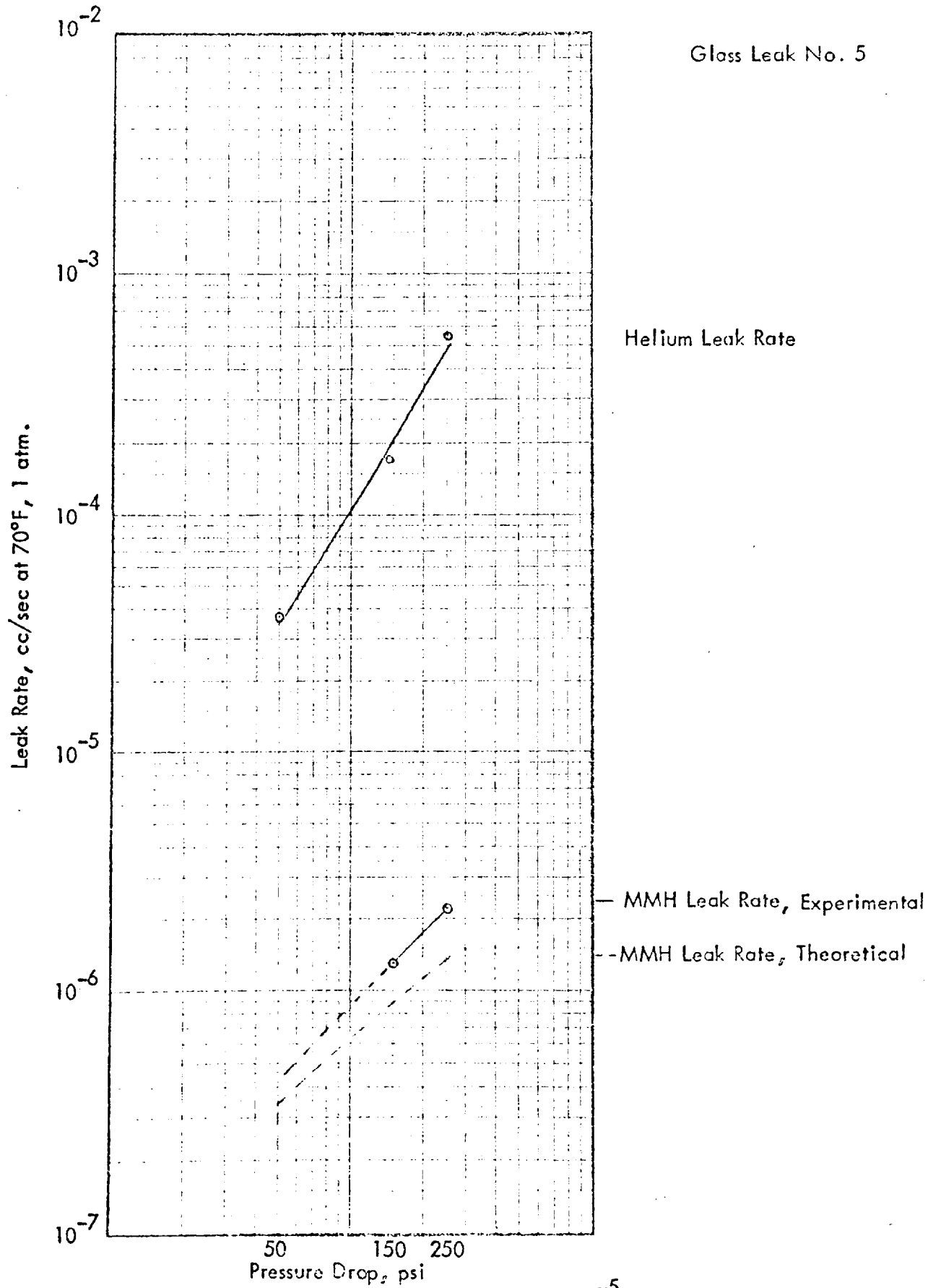

Figure 18. Monomethylhydrazine Leak Rate Through 10^{-5} cc/sec Helium Leak

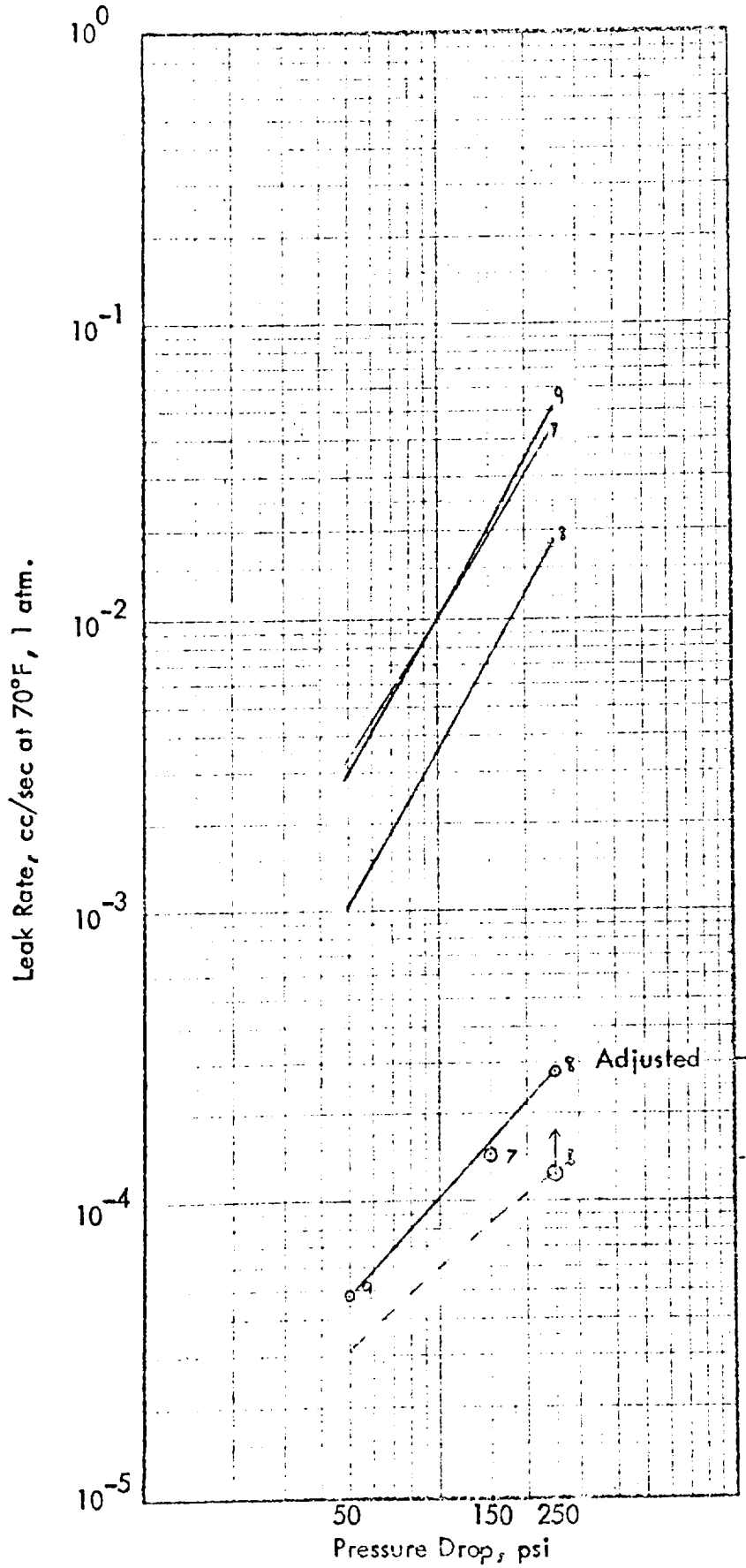

7, 8 and 9 refer to three different glass leaks.

Helium Leak Rates

MMH Leak Rates

MMH, Theoretical, based on helium curves for 7 and 9.

Data for leak 8 adjusted by moving upwards until helium curves for 8 and 9 coincide.

Figure 19. Monomethylhydrazine Leak Rates Through 10^{-3} cc/sec Helium Leaks

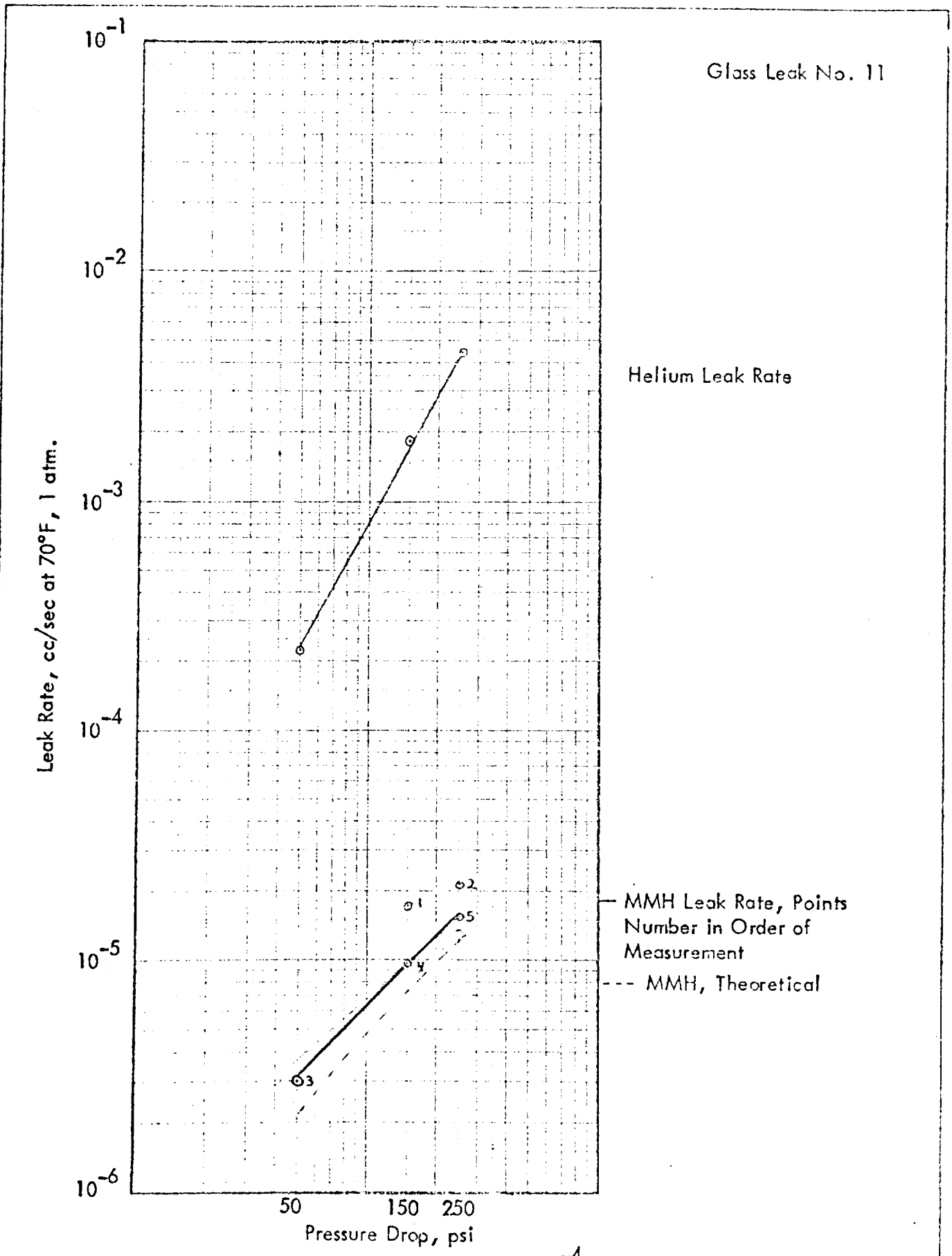

Figure 20. Monomethylhydrazine Leak Rate Through 10^{-4} cc/sec Helium Leak

FIGURE 21. AEROZINE-50 LEAK RATE THROUGH 10^{-3} cc/sec HELIUM LEAK

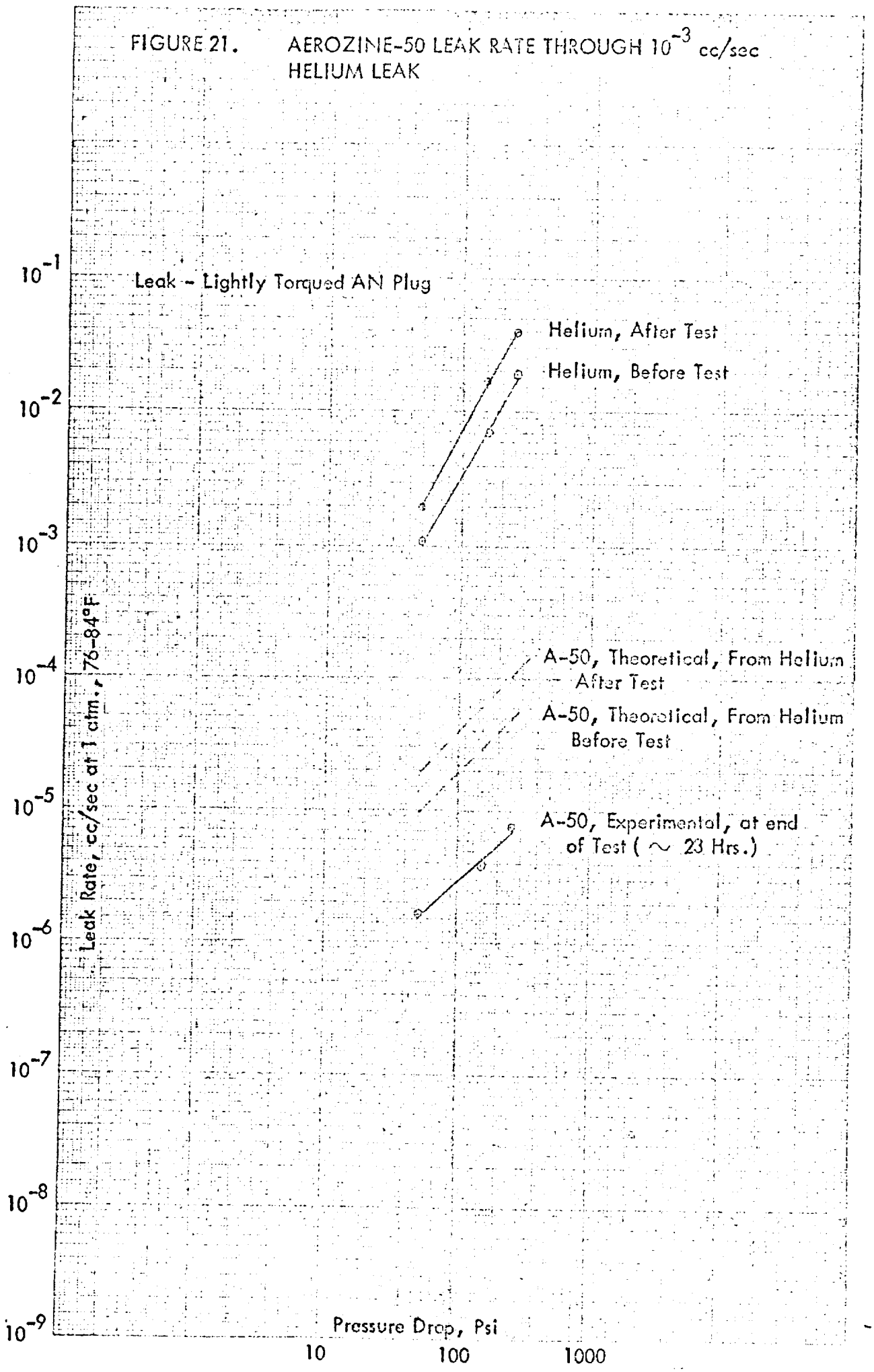

FIGURE 22. LEAK RATES OF AEROZINE-50 THROUGH A 5×10^{-3} cc/sec HELIUM LEAK

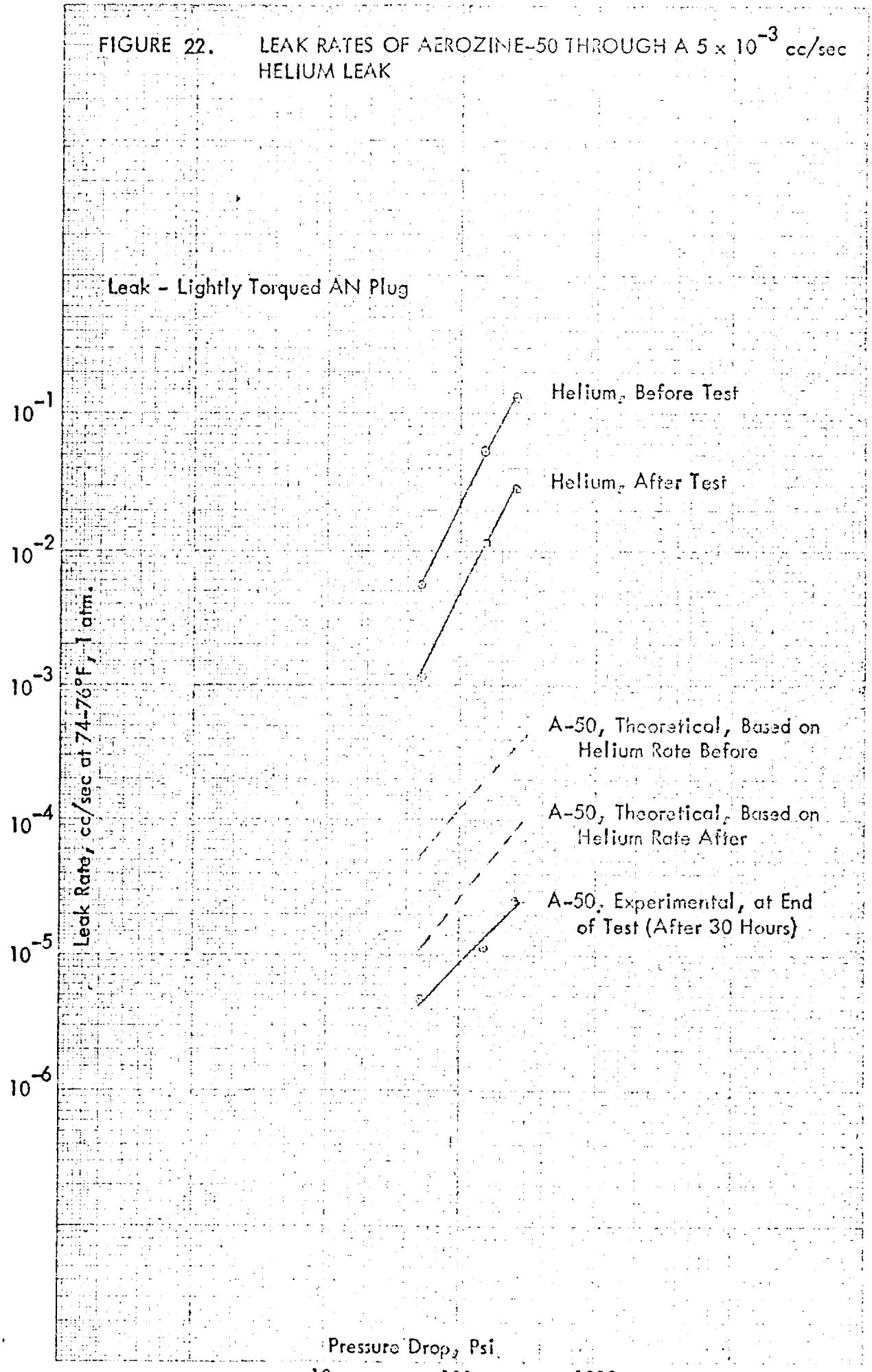

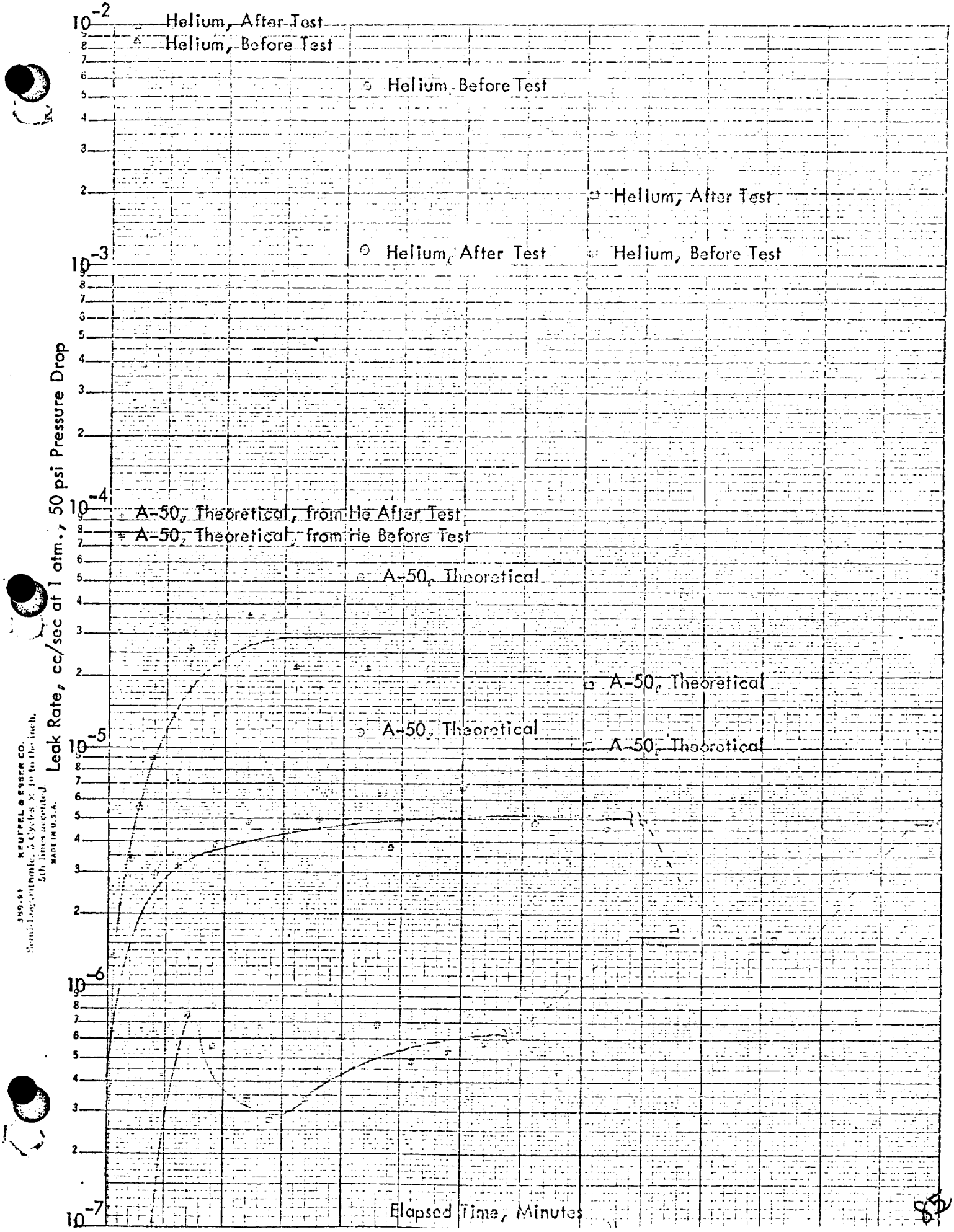
Helium, After Test
Helium, Before Test
Helium, Before Test
Helium, After Test
Helium, After Test
Helium, Before Test
A-50, Theoretical, from He After Test
A-50, Theoretical, from He Before Test
A-50, Theoretical
A-50, Theoretical
A-50, Theoretical
A-50, Theoretical
Leak Rate, cc/sec at 1 atm., 50 psi Pressure Drop
Elapsed Time, Minutes
10^-2
10^-3
10^-4
10^-5
10^-6
10^-7

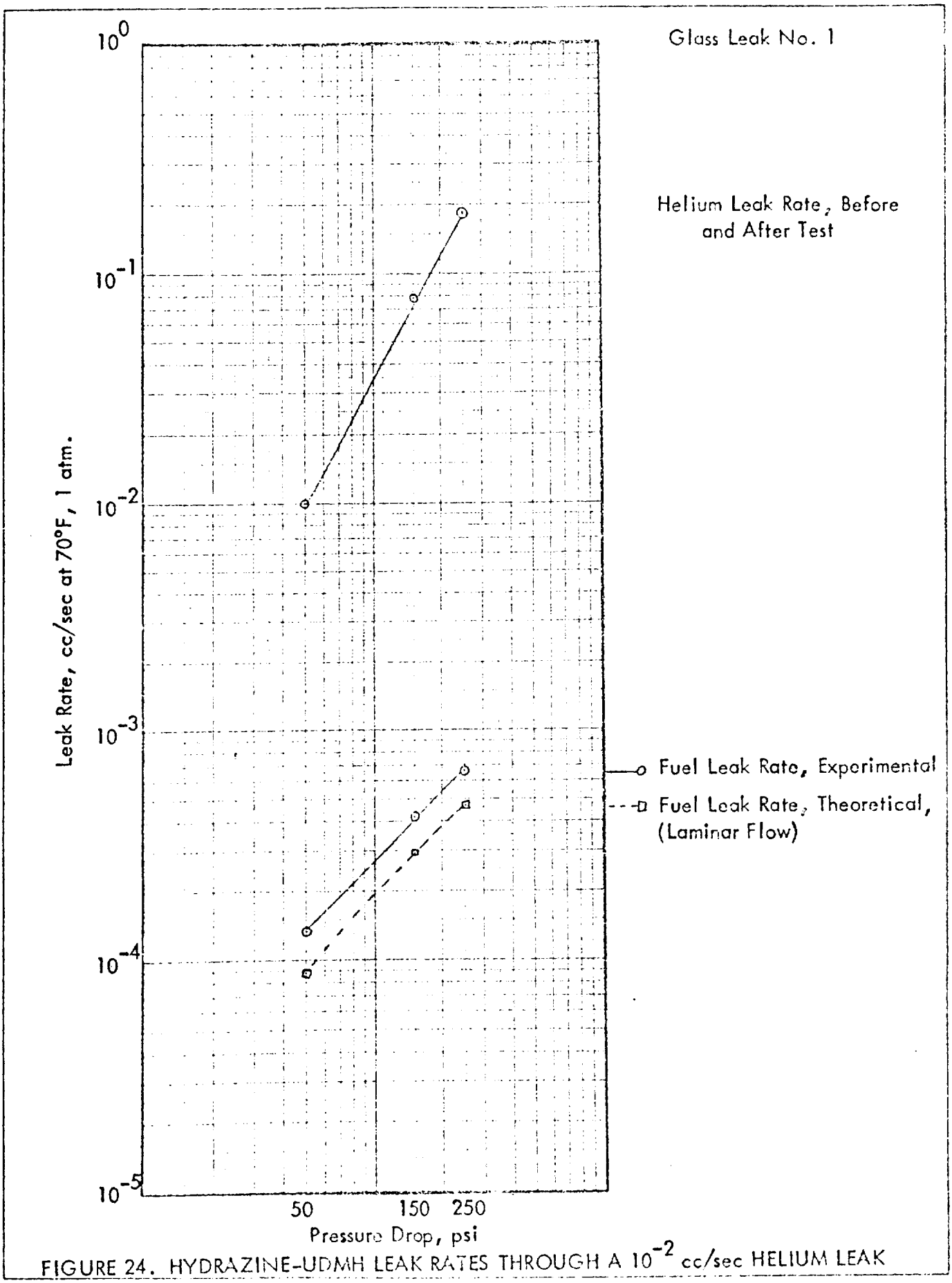

FIGURE 24. HYDRAZINE-UDMH LEAK RATES THROUGH A 10^{-2} cc/sec HELIUM LEAK

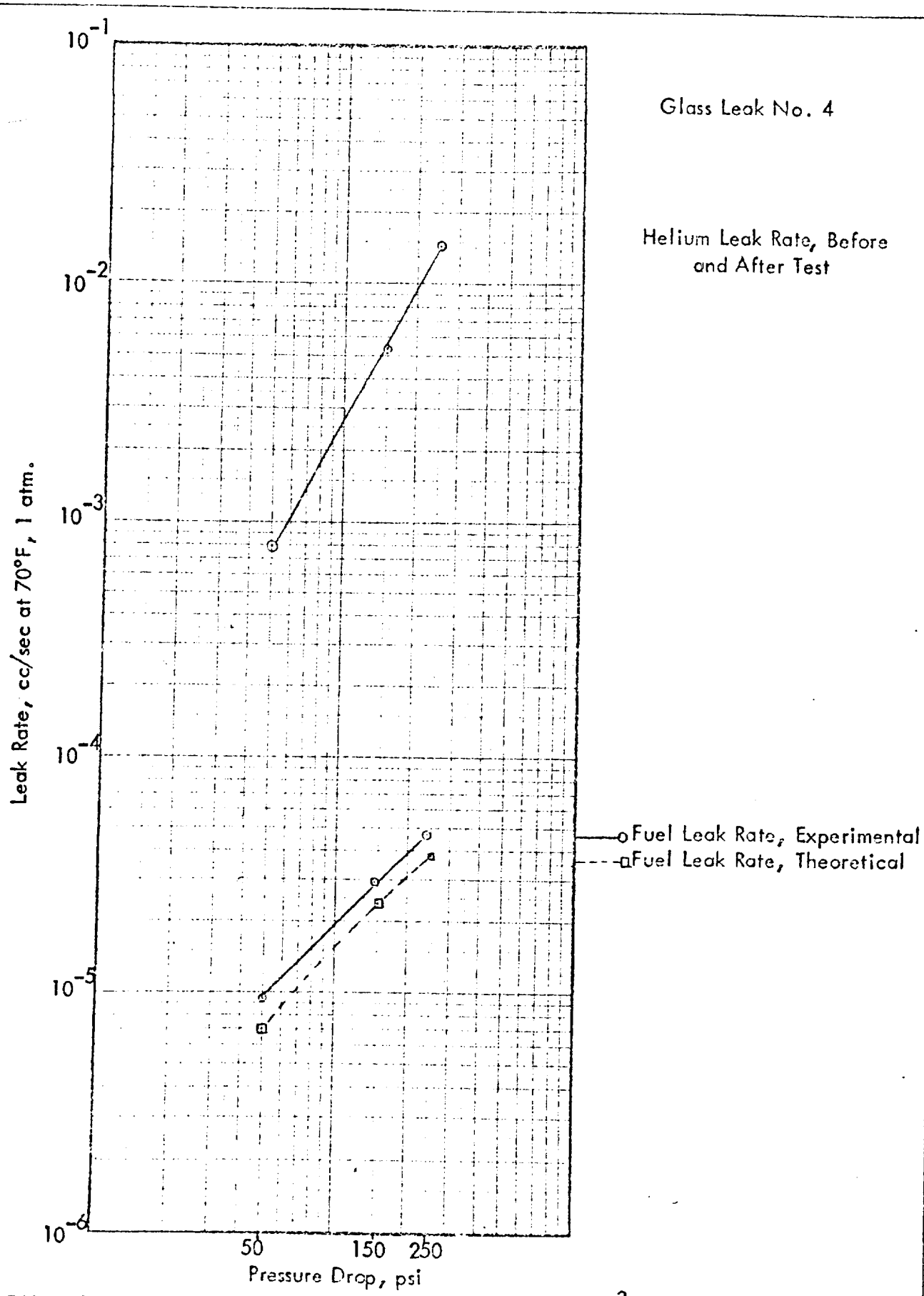

FIGURE 25. HYDRAZINE-UDMH LEAK RATE THROUGH A 10^{-3} cc/sec HELIUM LEAK

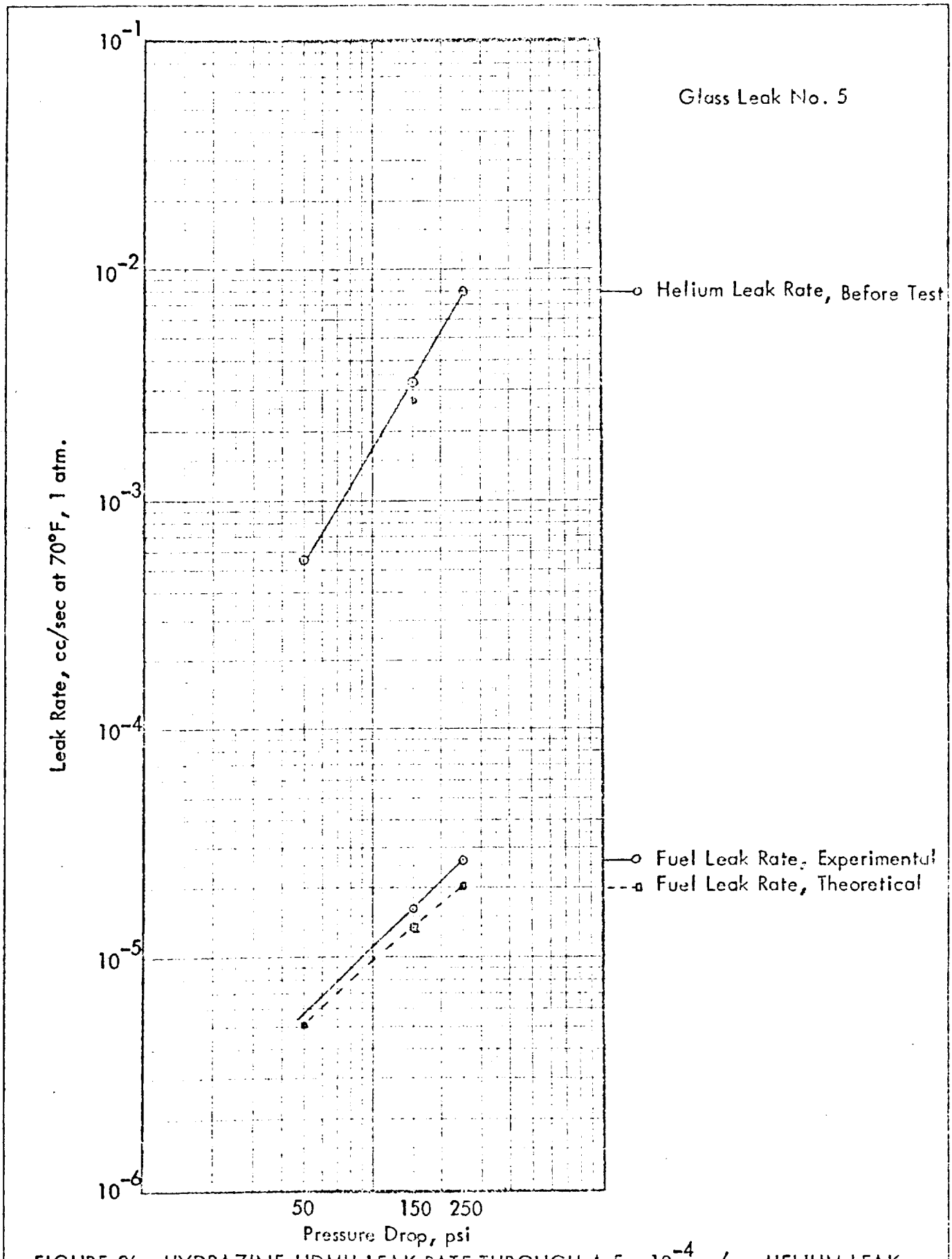

FIGURE 26. HYDRAZINE-UDMH LEAK RATE THROUGH A 5×10^{-4} cc/sec HELIUM LEAK

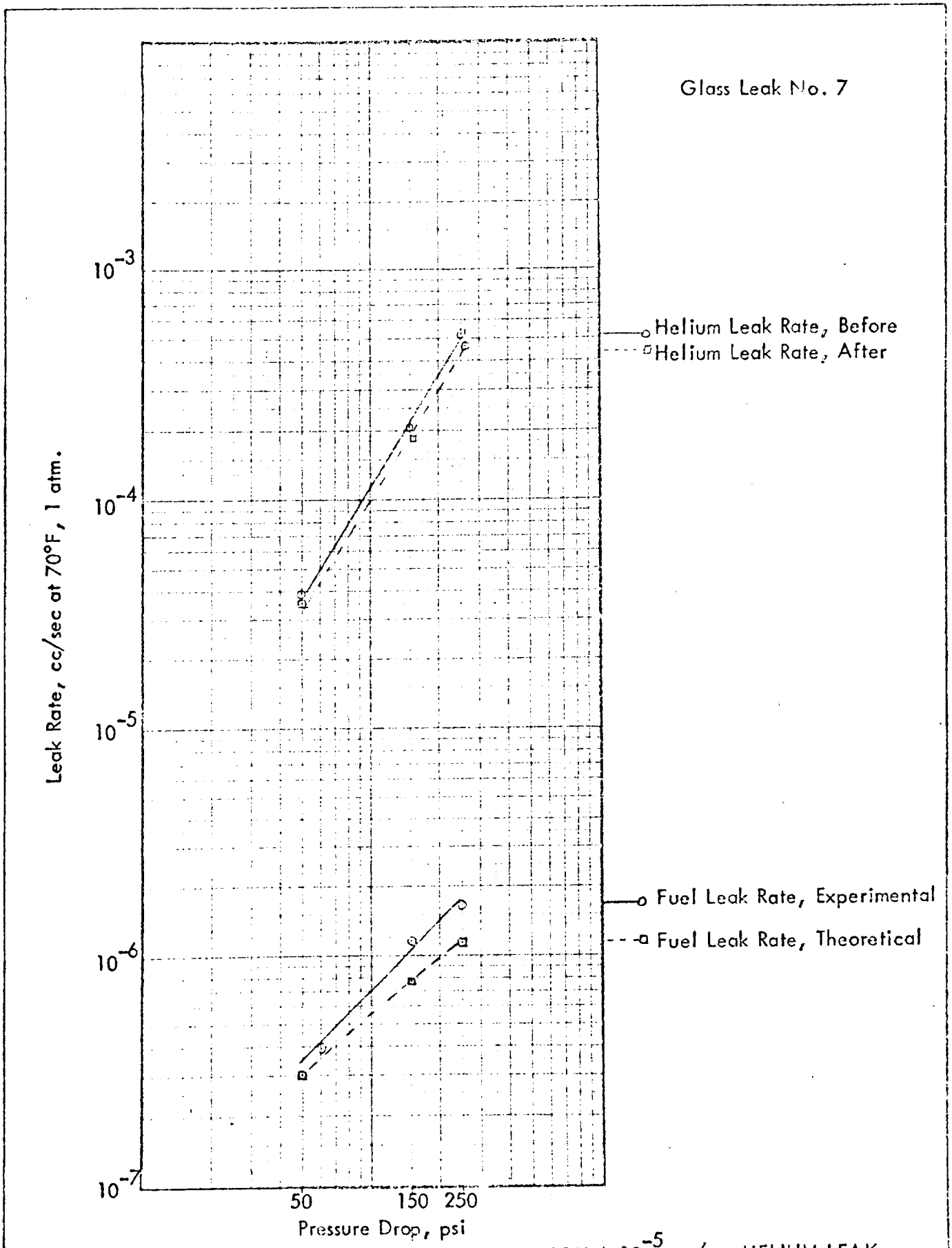

FIGURE 27. HYDRAZINE-UDMH LEAK RATE THROUGH A 10^{-5} cc/sec HELIUM LEAK

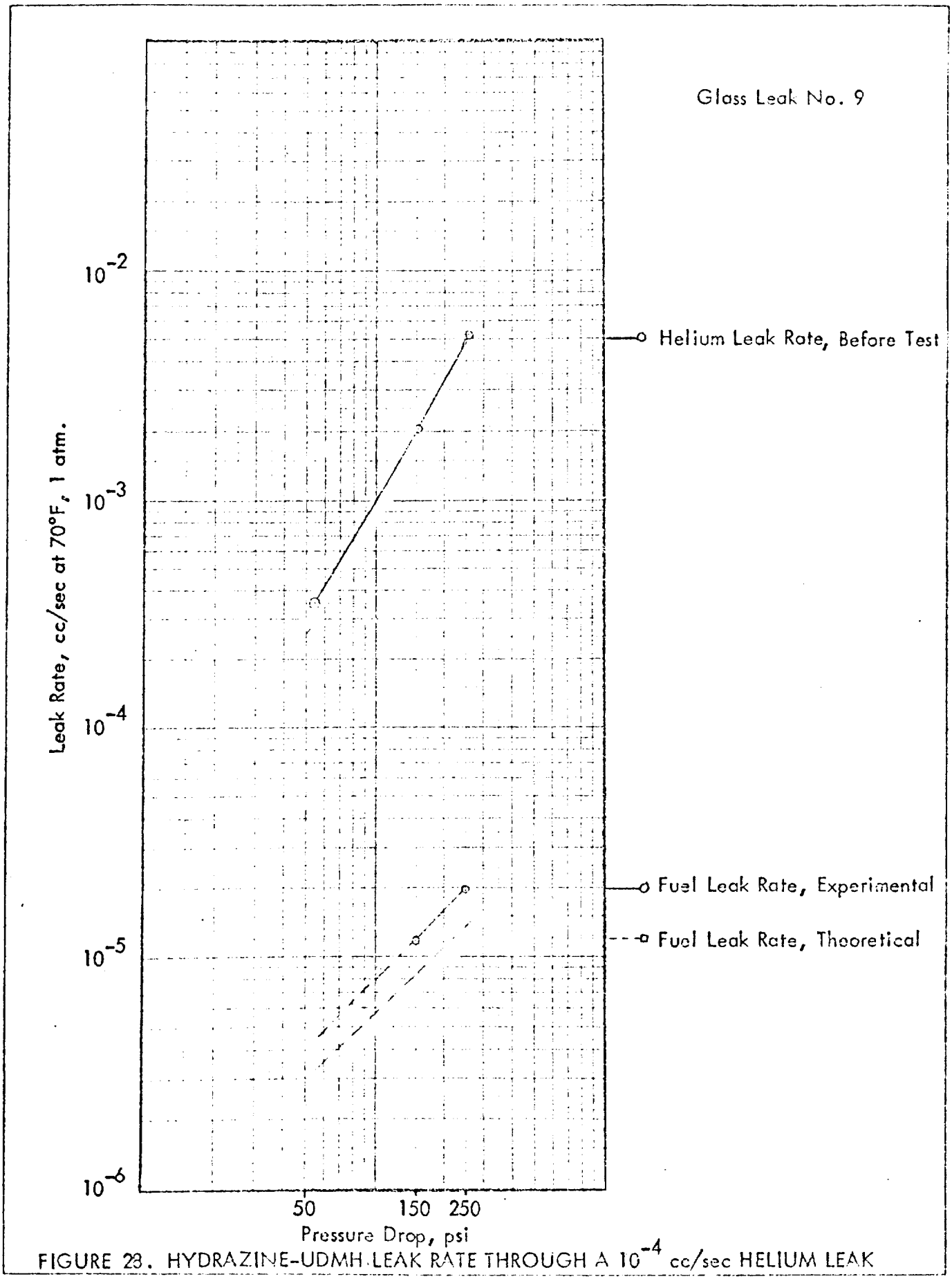

FIGURE 28. HYDRAZINE-UDMH LEAK RATE THROUGH A 10^{-4} cc/sec HELIUM LEAK

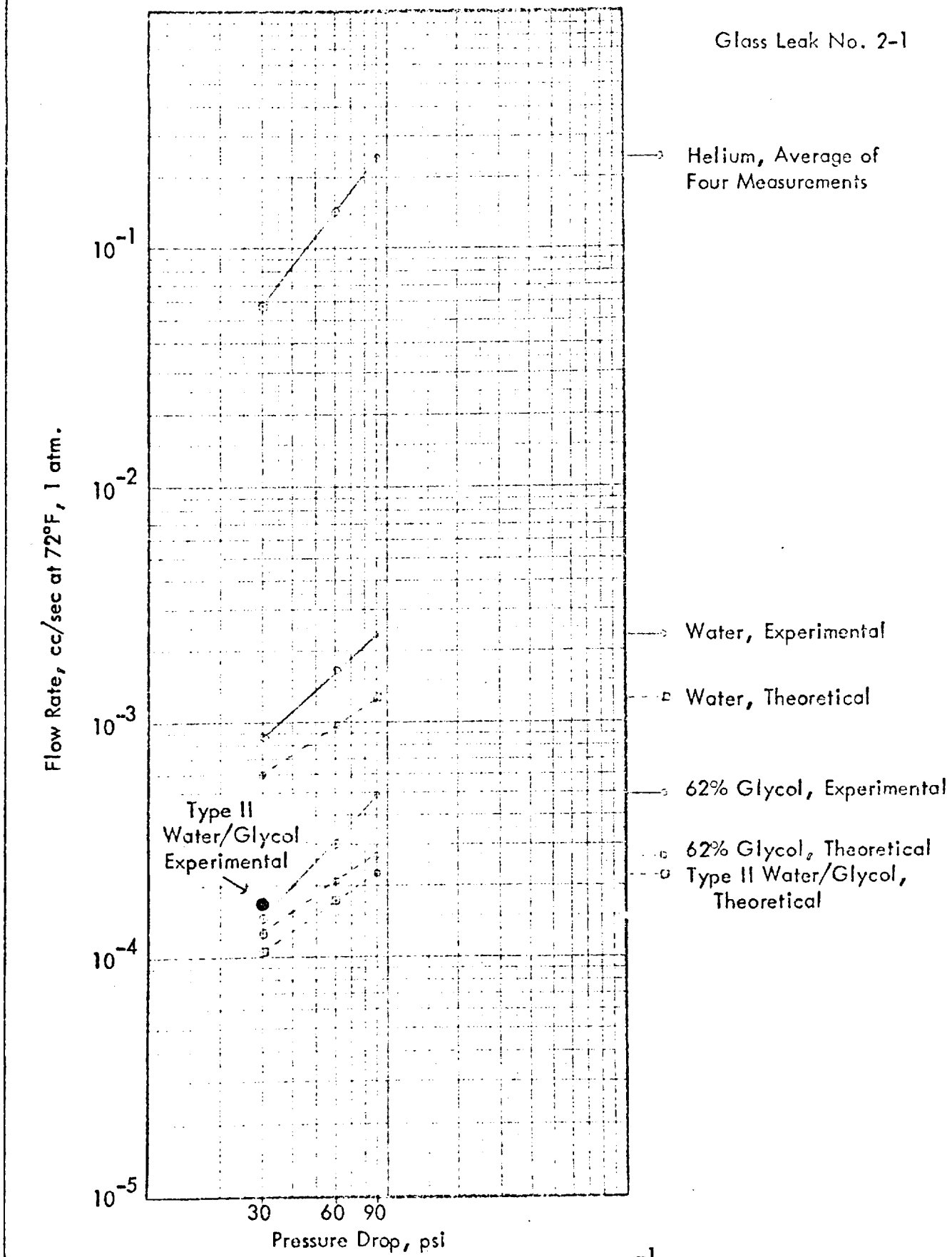

FIGURE 29. FLUID LEAK RATES THROUGH NOMINAL 10^{-1} cc/sec HELIUM LEAK

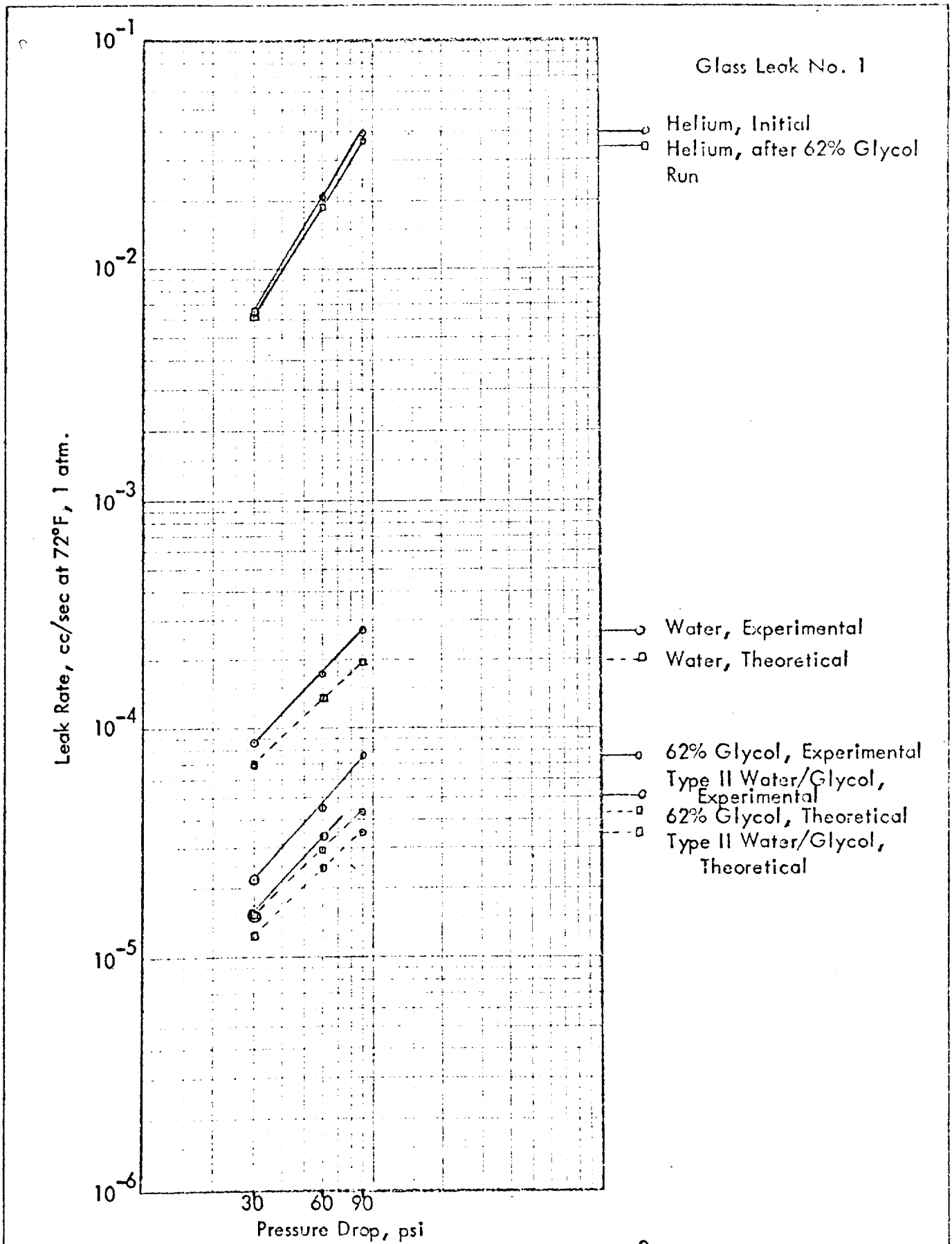

FIGURE 30. FLUID LEAK RATES THROUGH A NOMINAL 10^{-2} cc/sec HELIUM LEAK

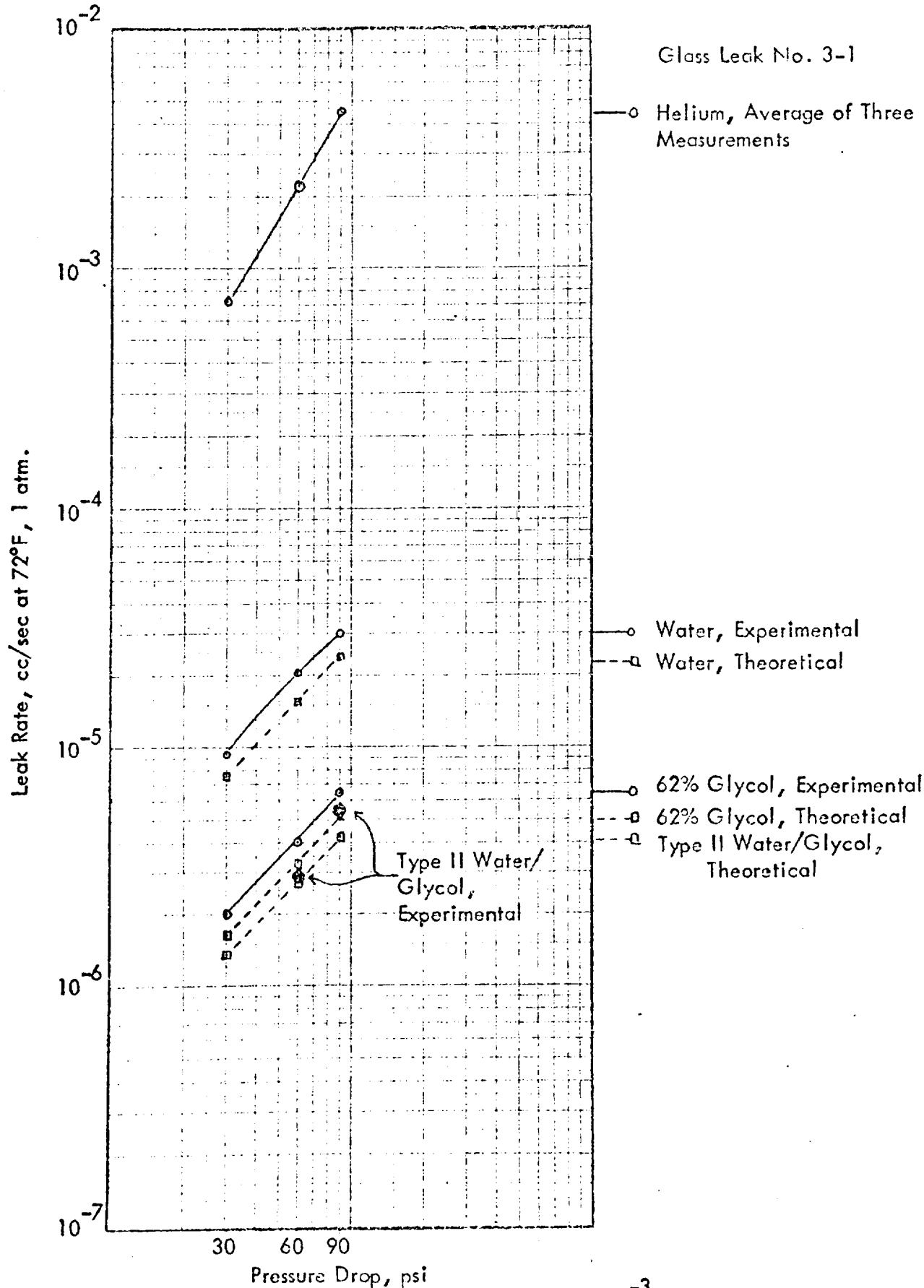

FIGURE 31. FLUID LEAK RATES THROUGH A NOMINAL 10^{-3} cc/sec HELIUM LEAK

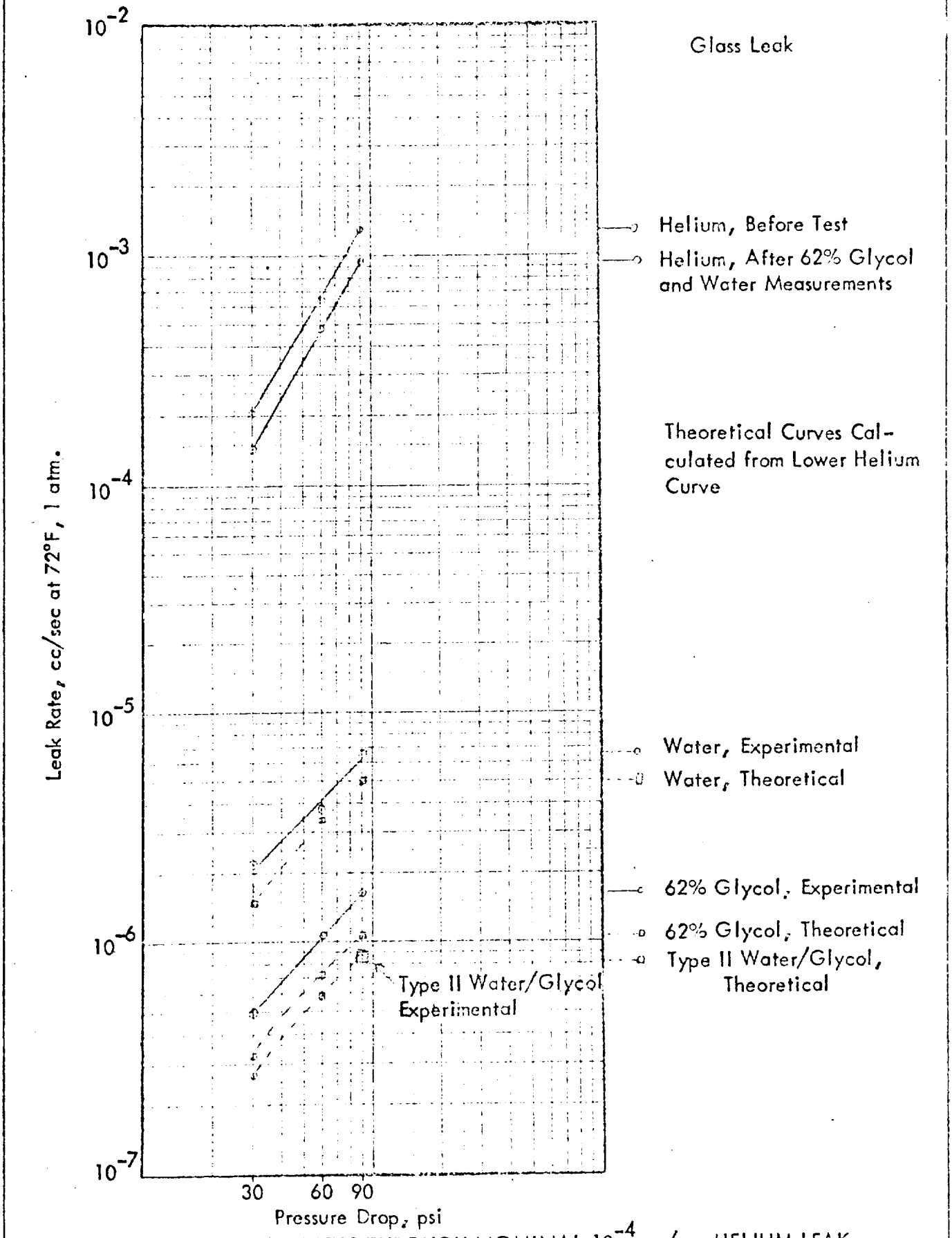

FIGURE 32. FLUID LEAK RATES THROUGH NOMINAL 10^{-4} cc/sec HELIUM LEAK

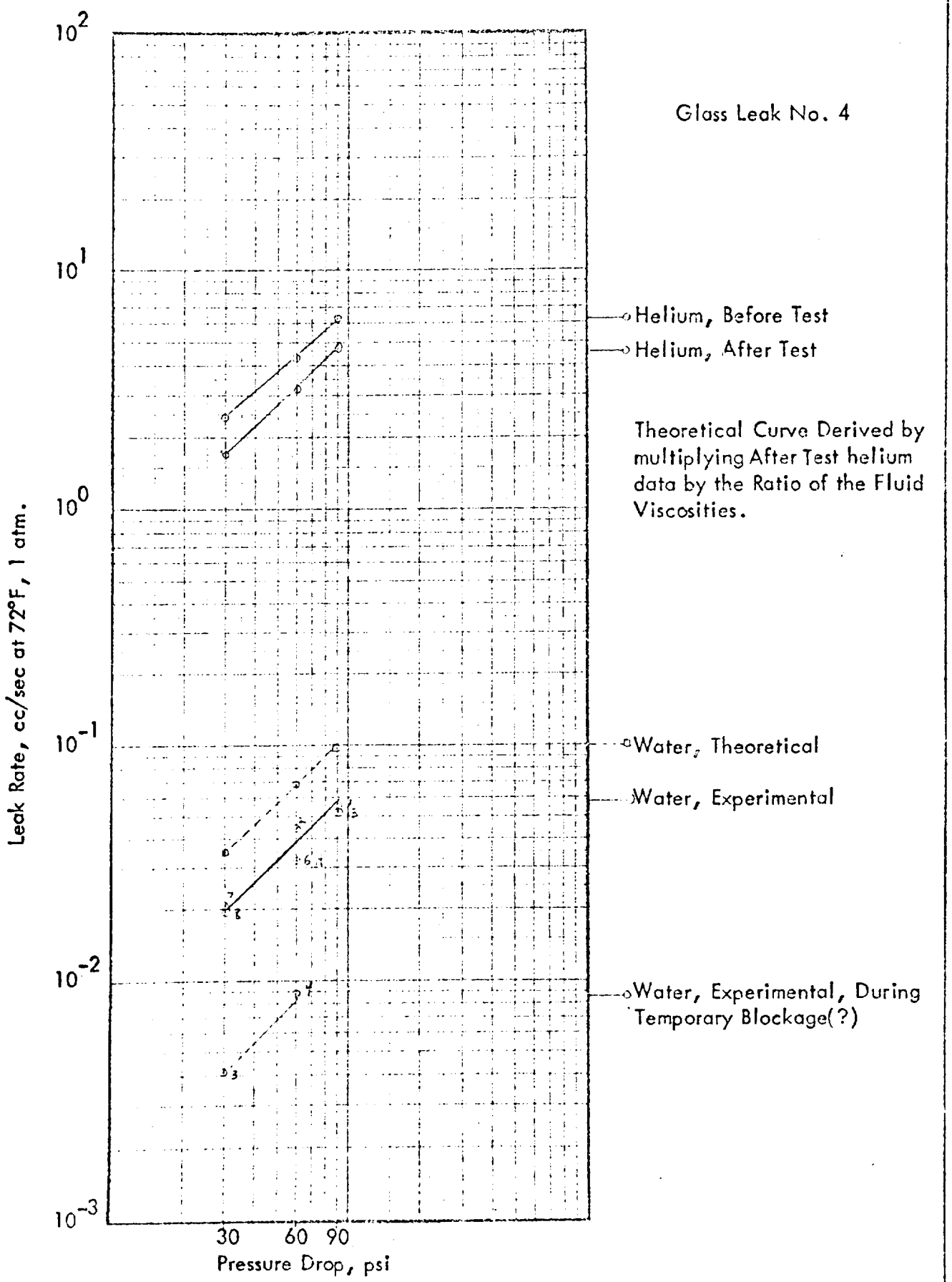

Figure 33. WATER LEAK RATES THROUGH A 1 cc/sec HELIUM LEAK

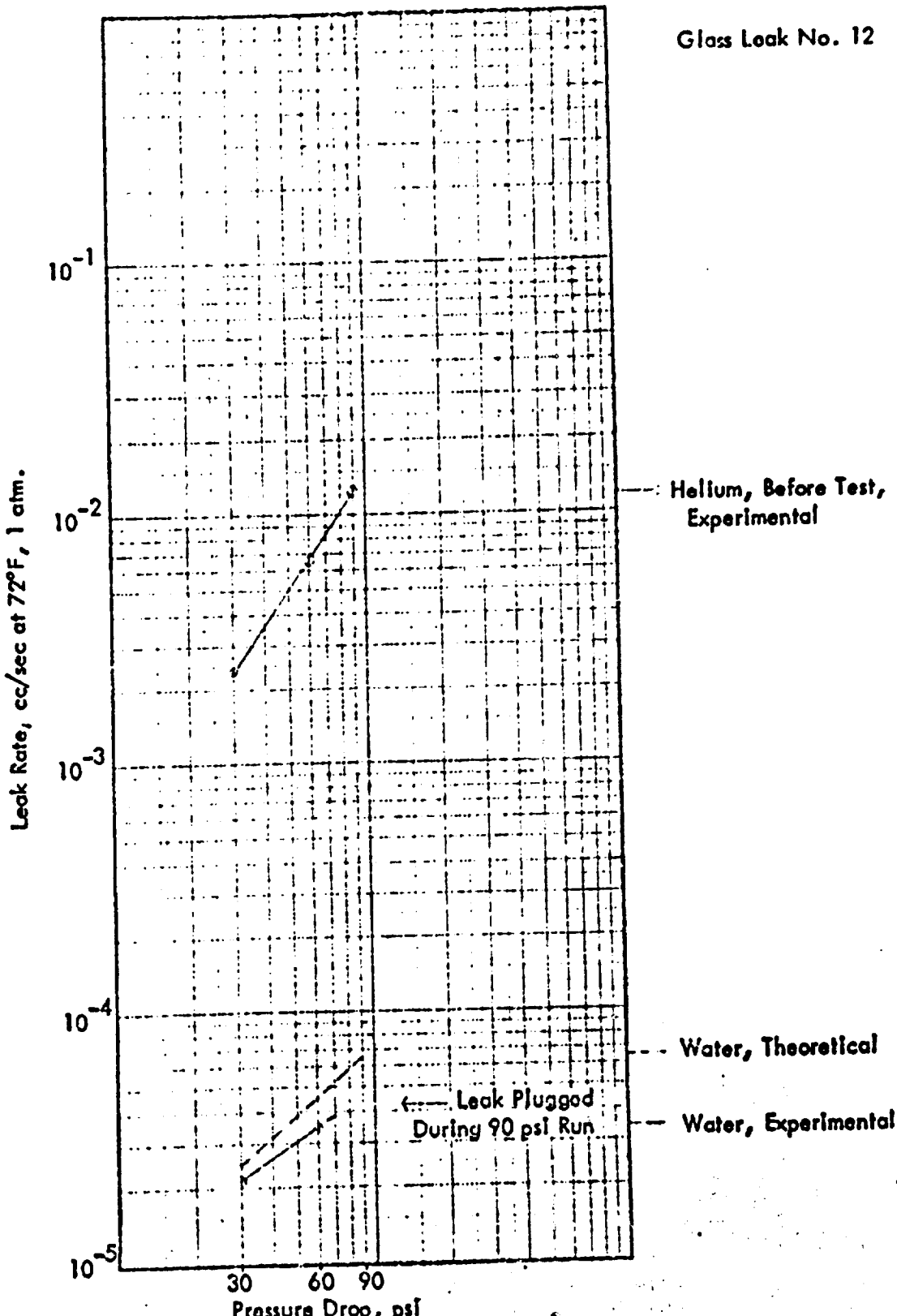

FIGURE 34. WATER LEAK RATE THROUGH A 10^{-3} cc/sec HELIUM LEAK

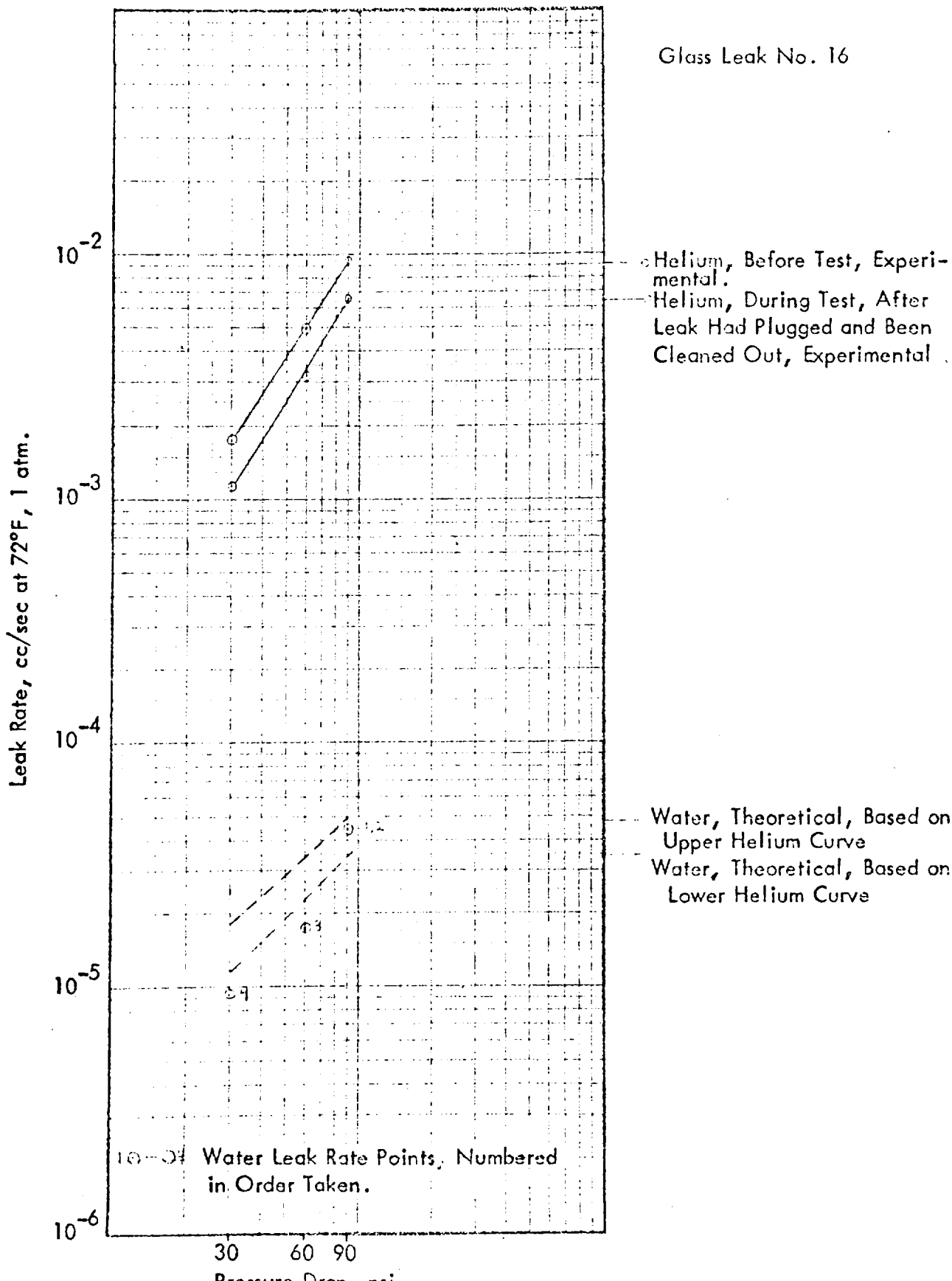

FIGURE 35. WATER LEAK RATES THROUGH A 10^{-3} cc/sec HELIUM LEAK

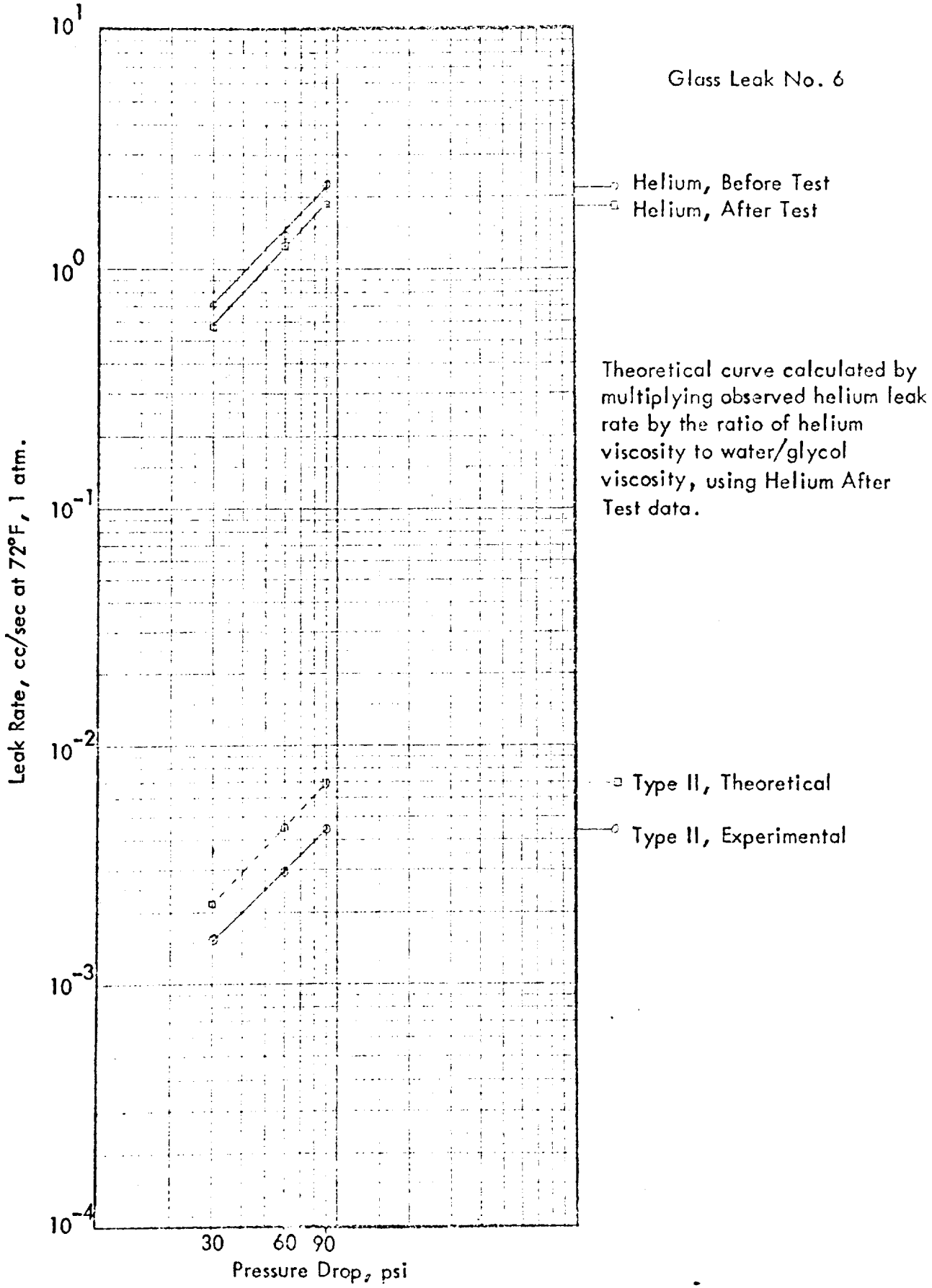

FIGURE 36. TYPE II WATER/GLYCOL LEAK RATE THROUGH A 1 cc/sec HELIUM LEAK

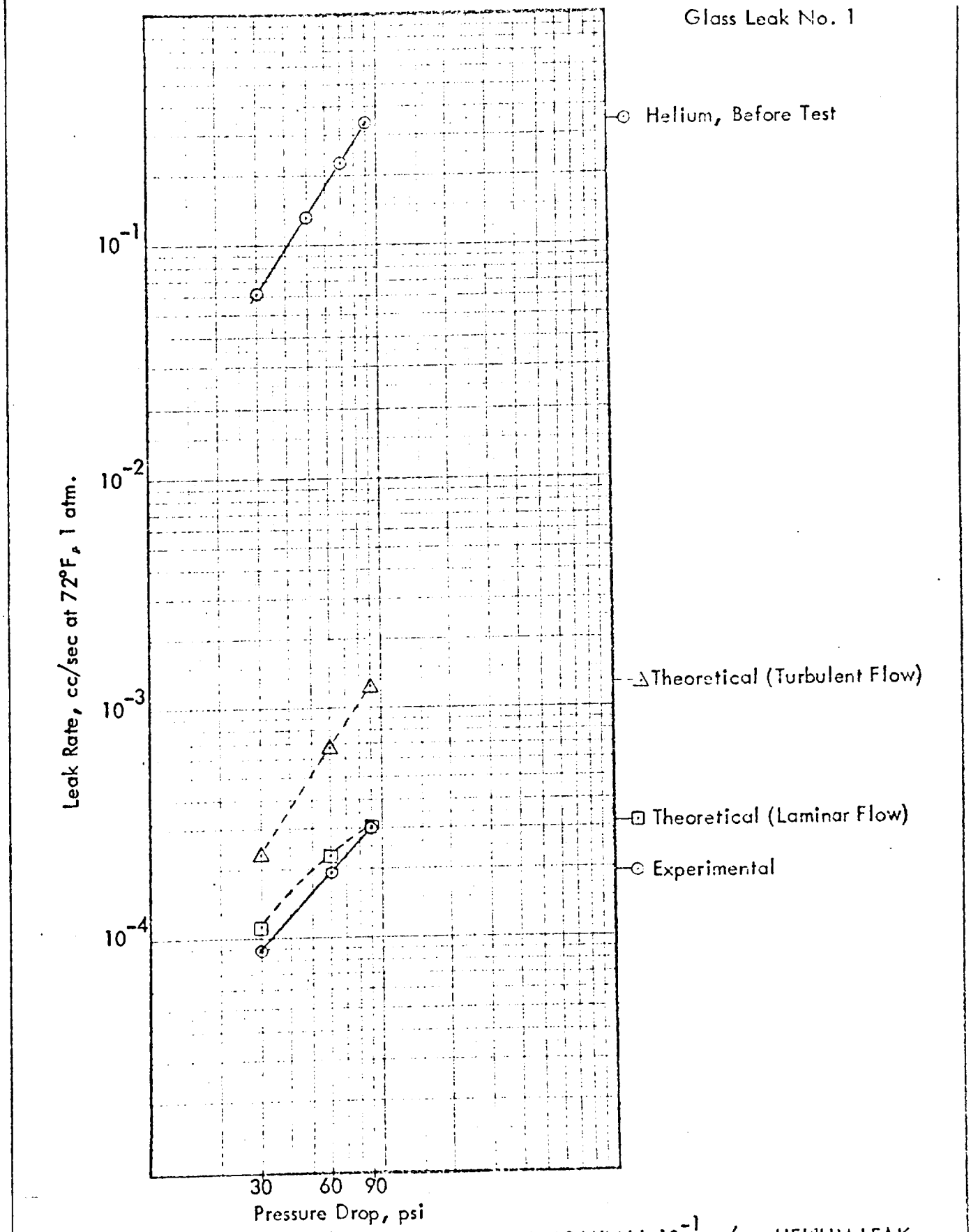

FIGURE 37. TYPE II WATER/GLYCOL THROUGH NOMINAL 10^{-1} cc/sec HELIUM LEAK

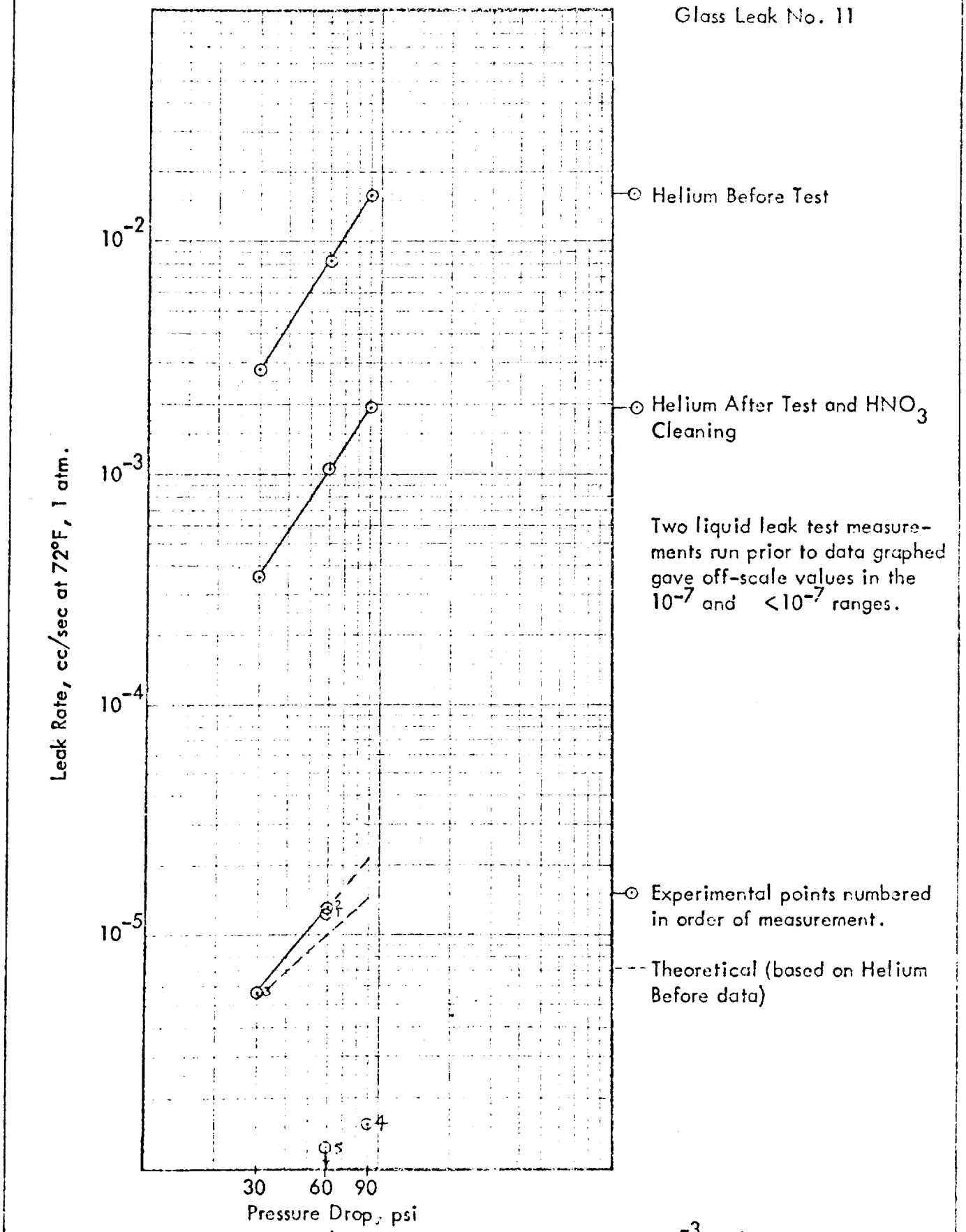

FIGURE 38. TYPE II WATER/GLYCOL LEAK RATE THROUGH 10^{-3} cc/sec HELIUM LEAK

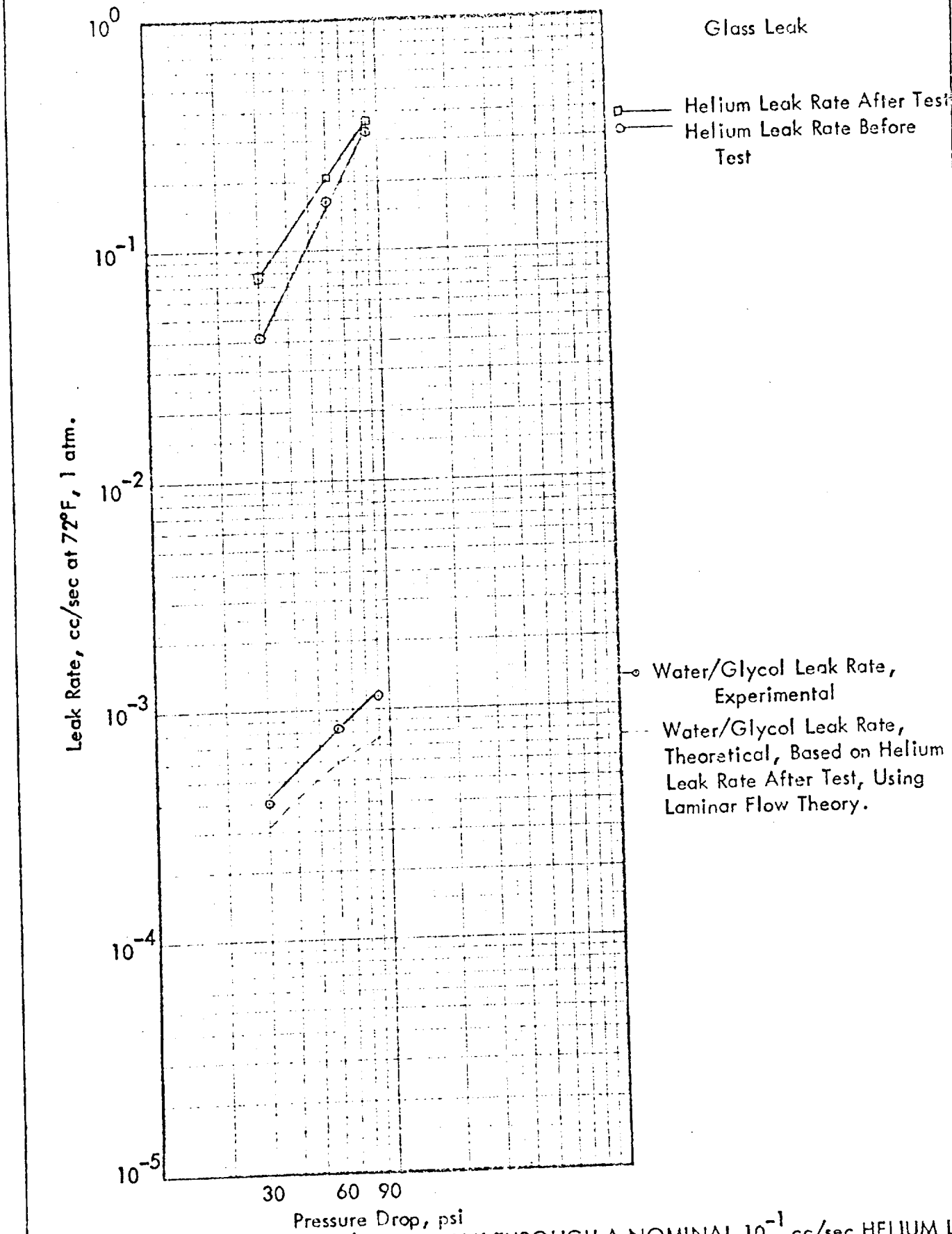

FIGURE 39. 35% GLYCOL/WATER LEAK THROUGH A NOMINAL 10^{-1} cc/sec HELIUM LEAK

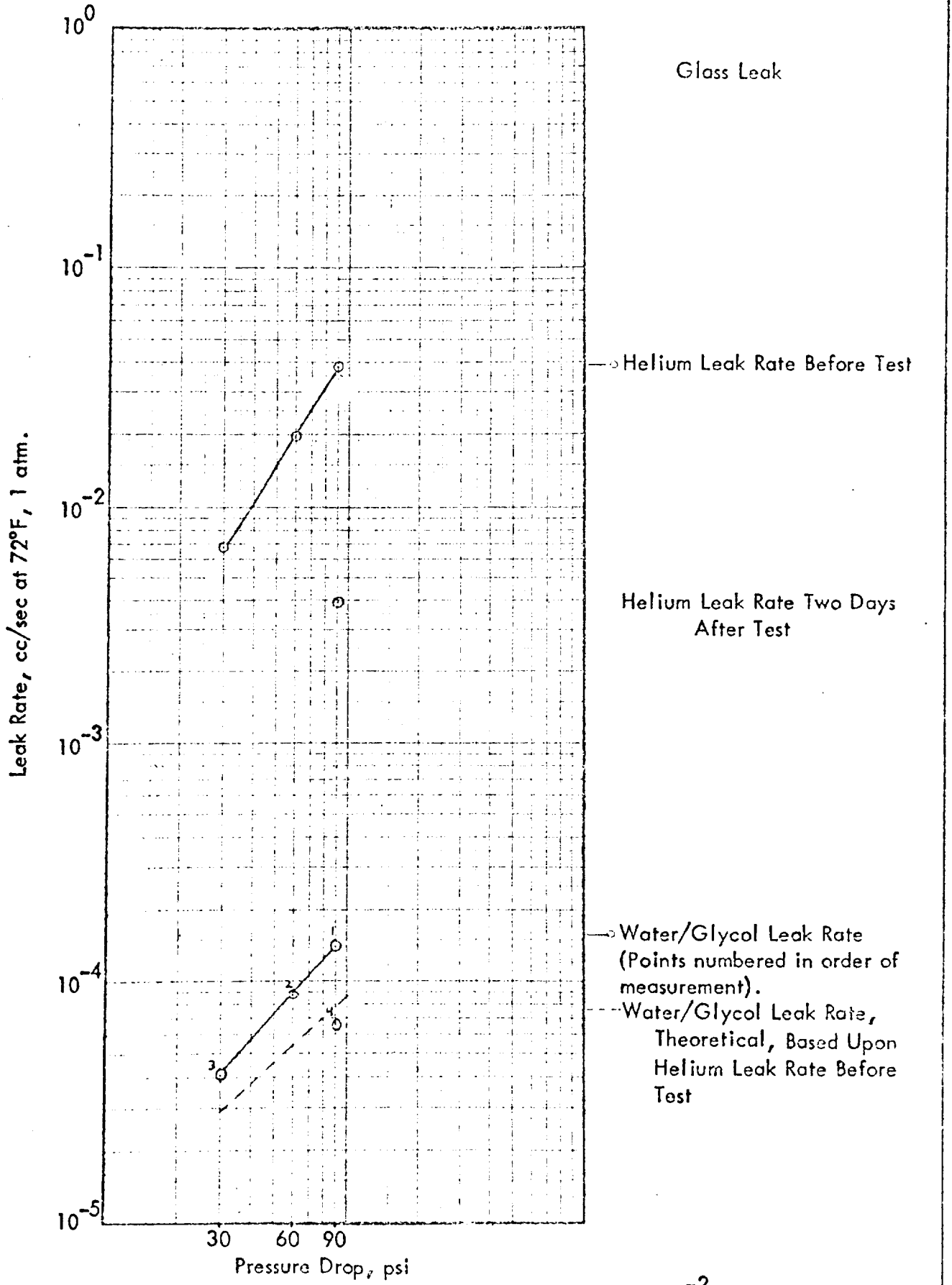

FIGURE 40. 35% GLYCOL/WATER LEAK THROUGH A NOMINAL 10^{-2} cc/sec HELIUM LEAK

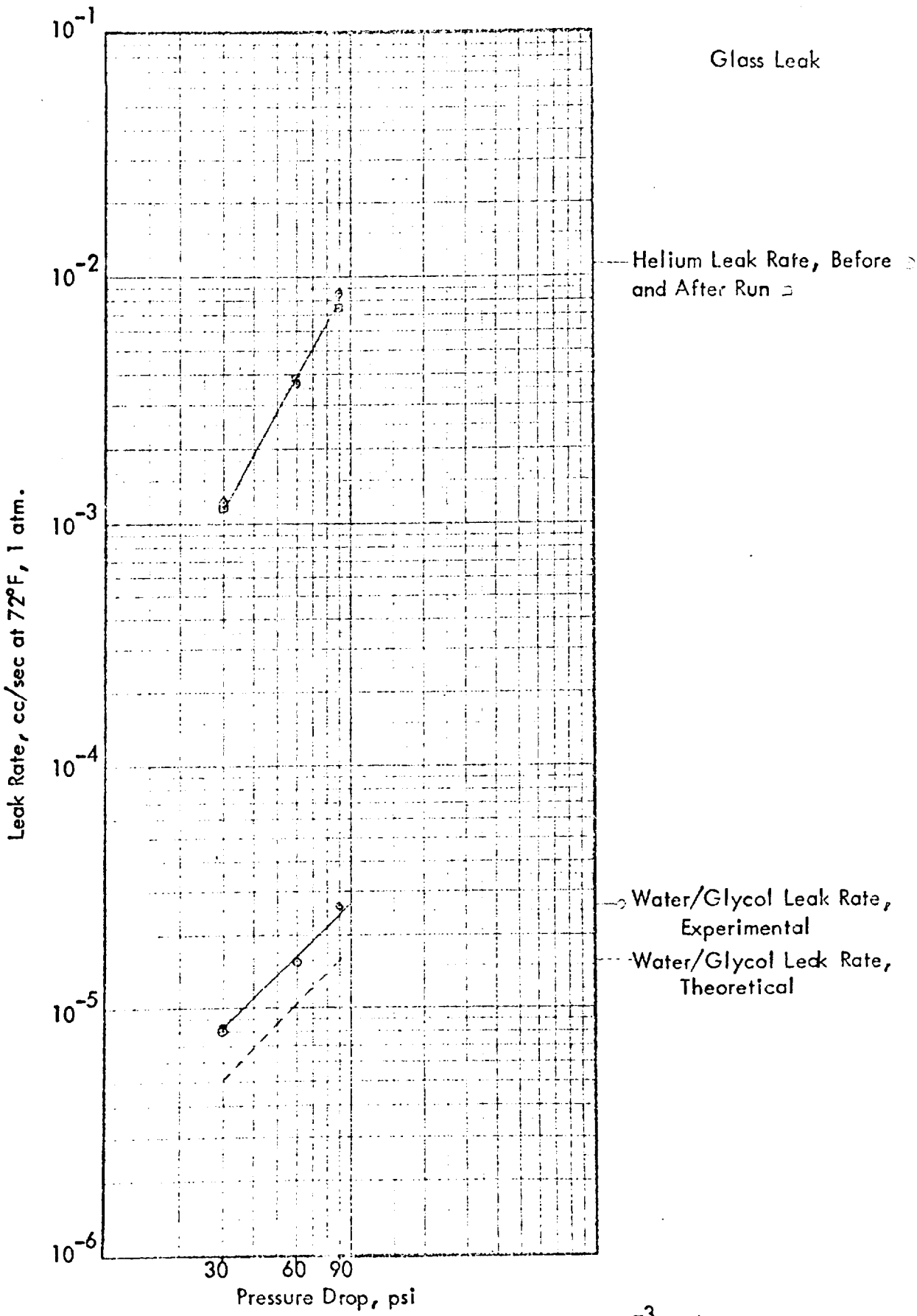

FIGURE 41. 35% GLYCOL/WATER LEAK THROUGH A 10^{-3} cc/sec HELIUM LEAK

FIGURE 42. CORRELATION OF HELIUM GAS LEAK RATE WITH LEAK RATES OF OXYGEN, NITROGEN AND HYDROGEN GAS

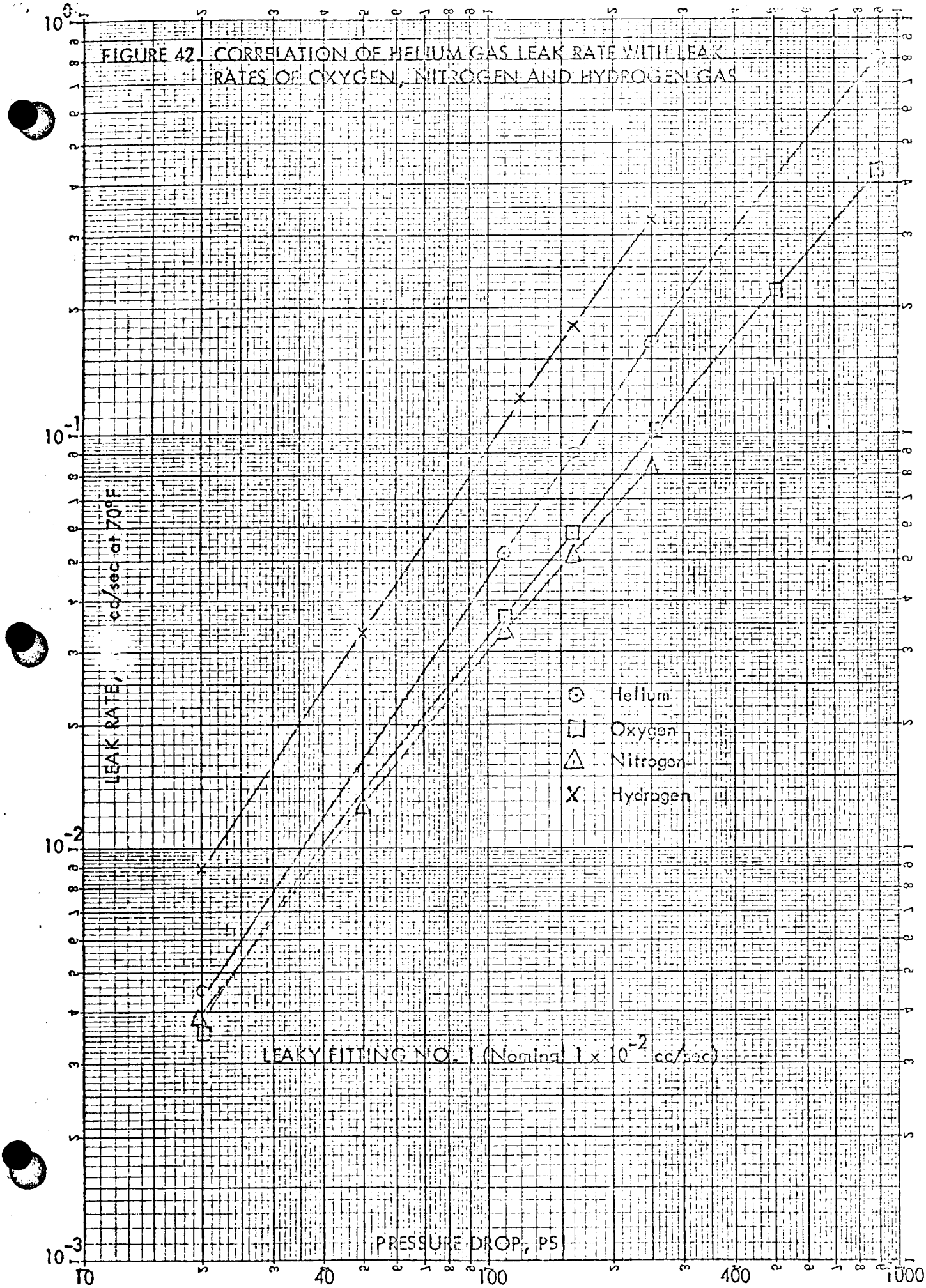

FIGURE 43. CORRELATION OF HELIUM GAS LEAK RATE WITH LEAK RATES OF HYDROGEN, OXYGEN, AND NITROGEN

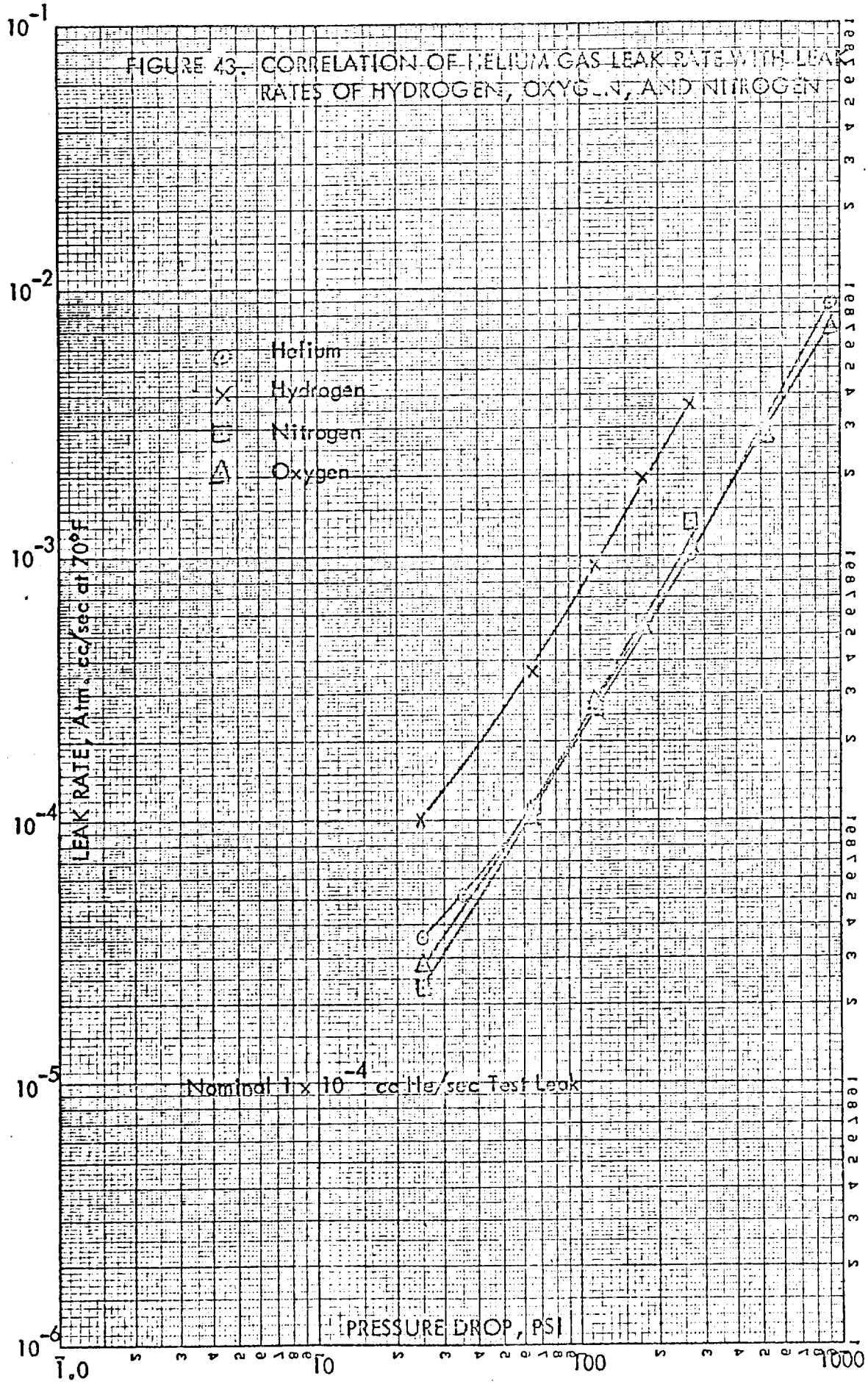

FIGURE 44. CORRELATION OF HELIUM GAS LEAK RATES WITH LEAK RATES OF HYDROGEN, OXYGEN, AND NITROGEN

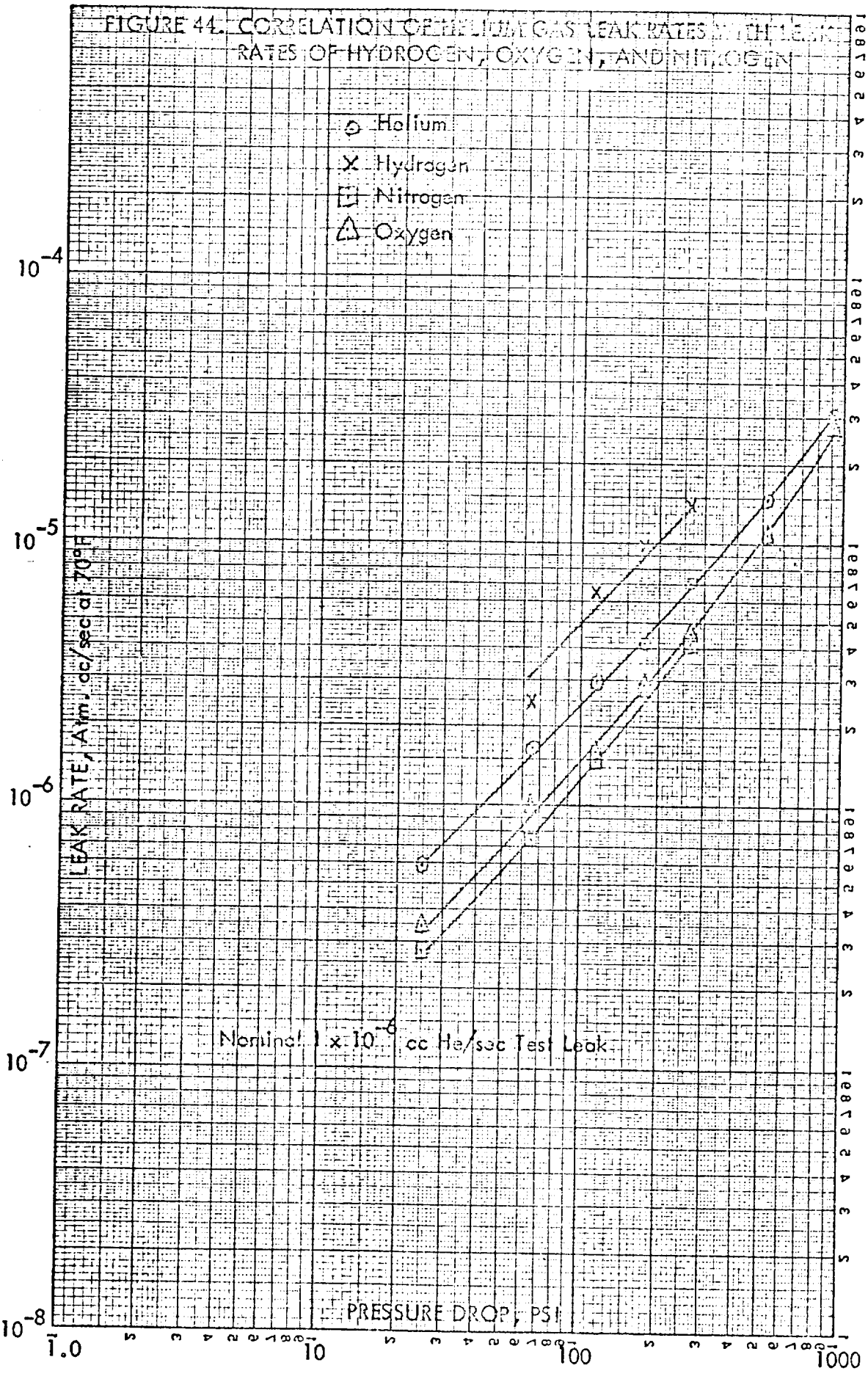

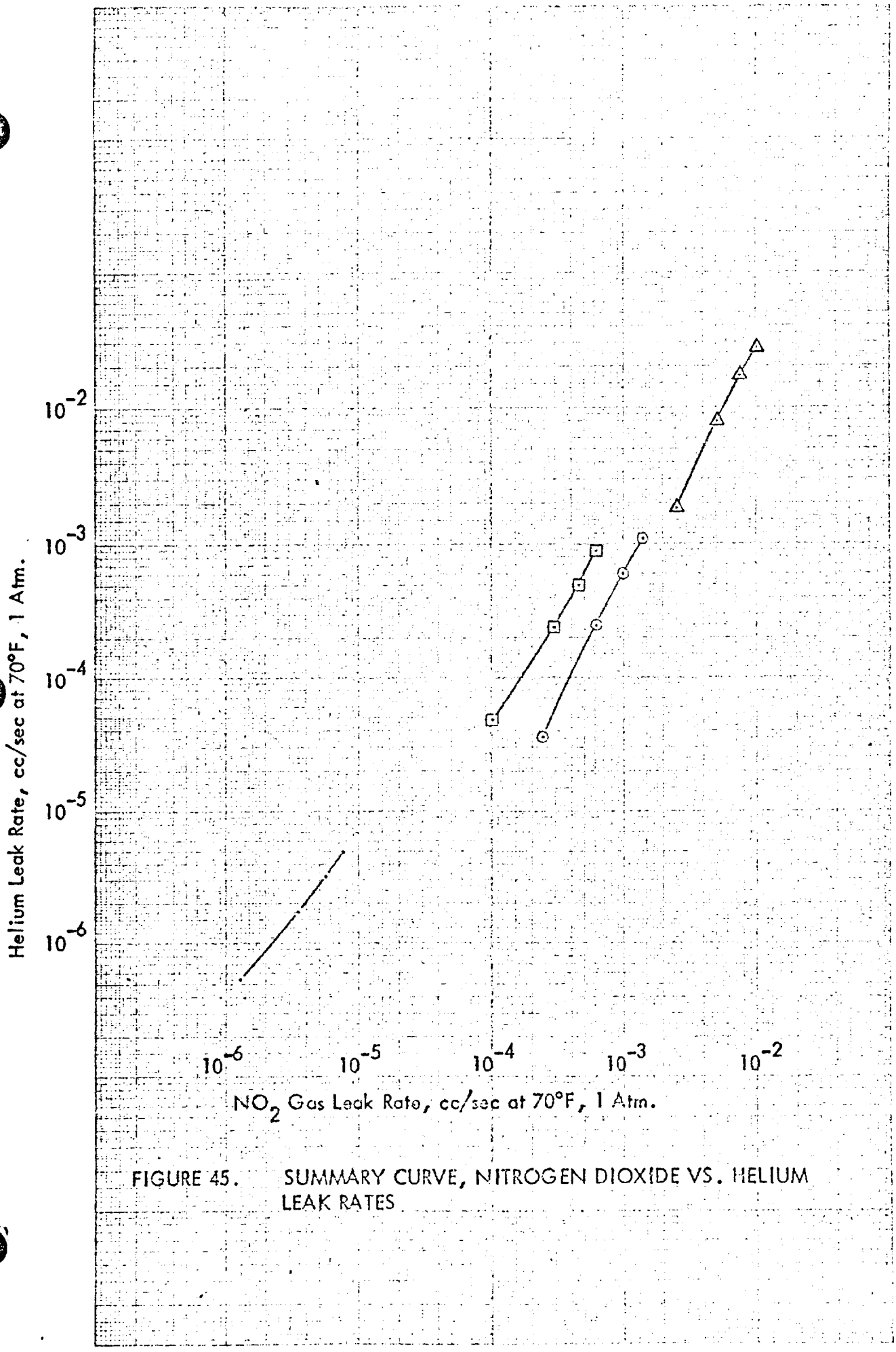

FIGURE 45. SUMMARY CURVE, NITROGEN DIOXIDE VS. HELIUM LEAK RATES

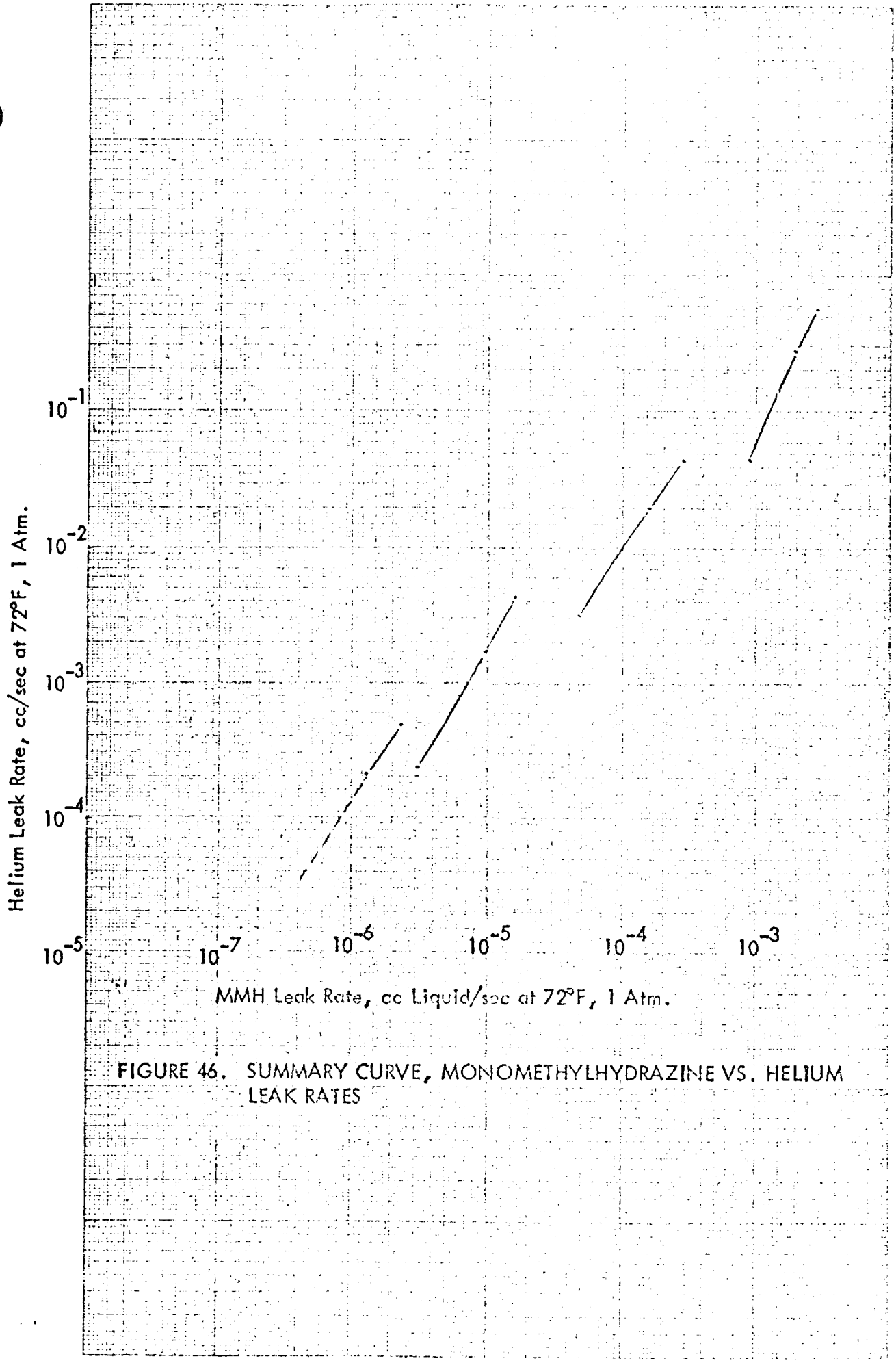

FIGURE 46. SUMMARY CURVE, MONOMETHYLHYDRAZINE VS. HELIUM LEAK RATES

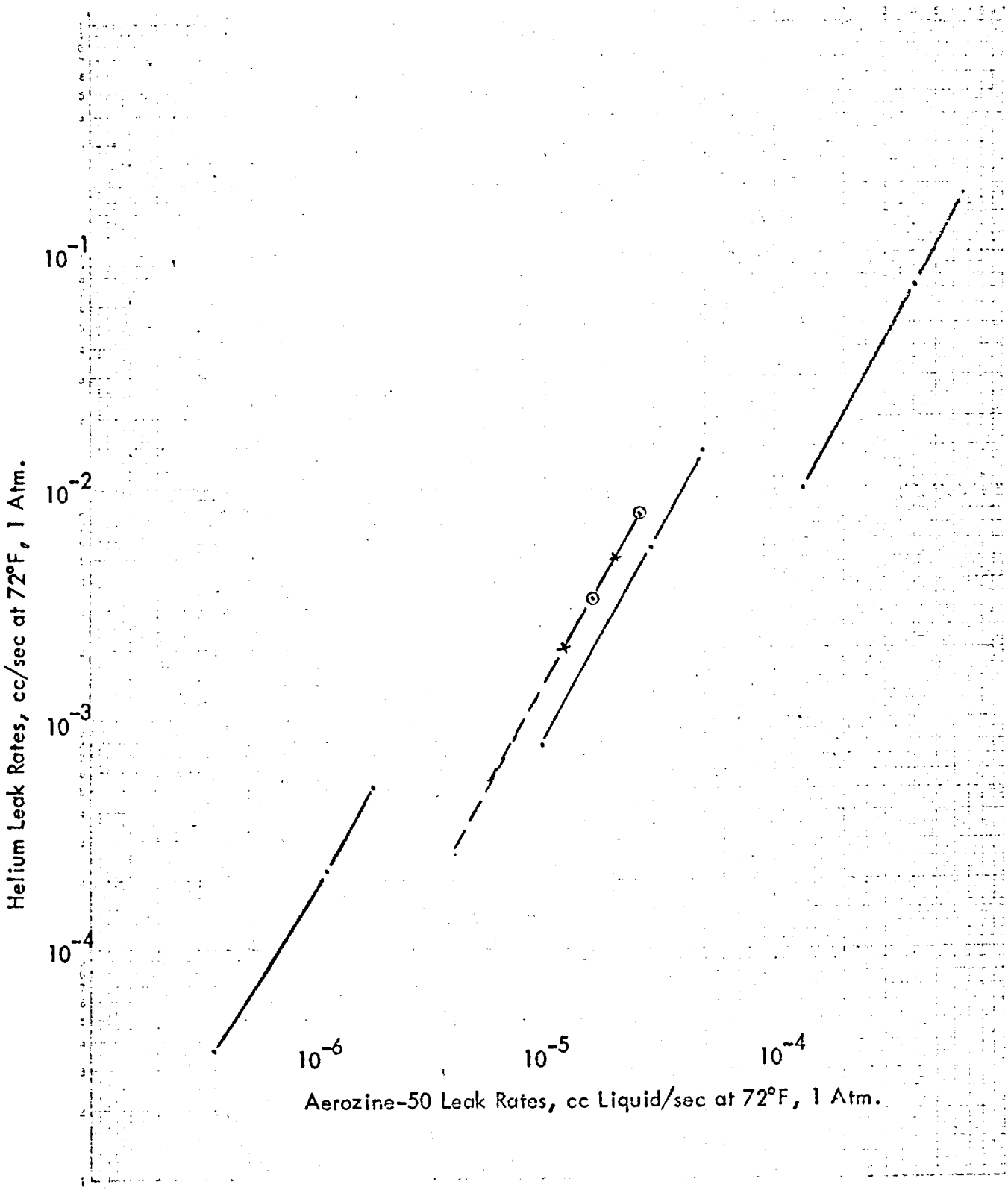

FIGURE 47. SUMMARY CURVE, AEROZINE-50 VS. HELIUM LEAK RATES

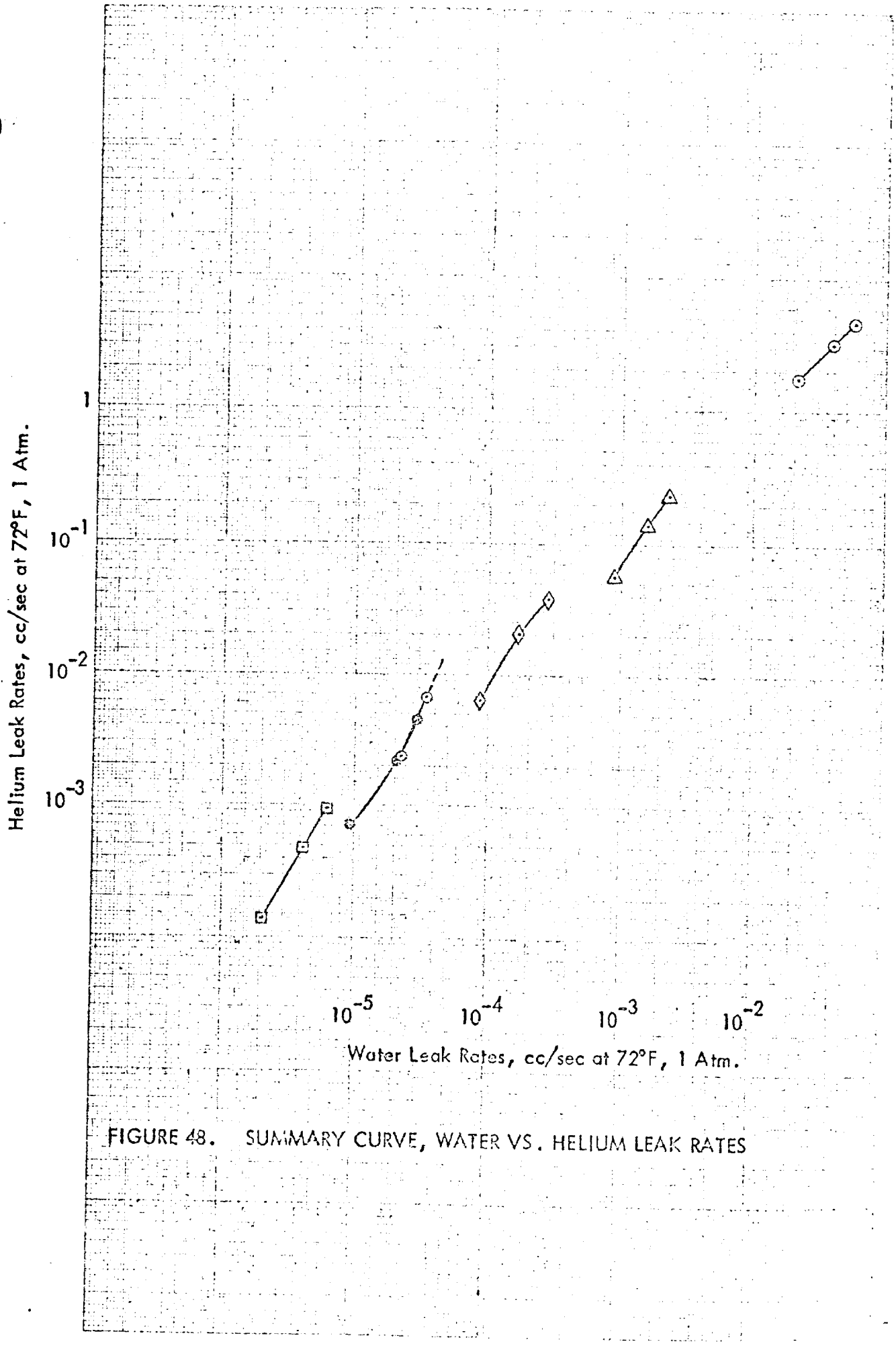

FIGURE 48. SUMMARY CURVE, WATER VS. HELIUM LEAK RATES

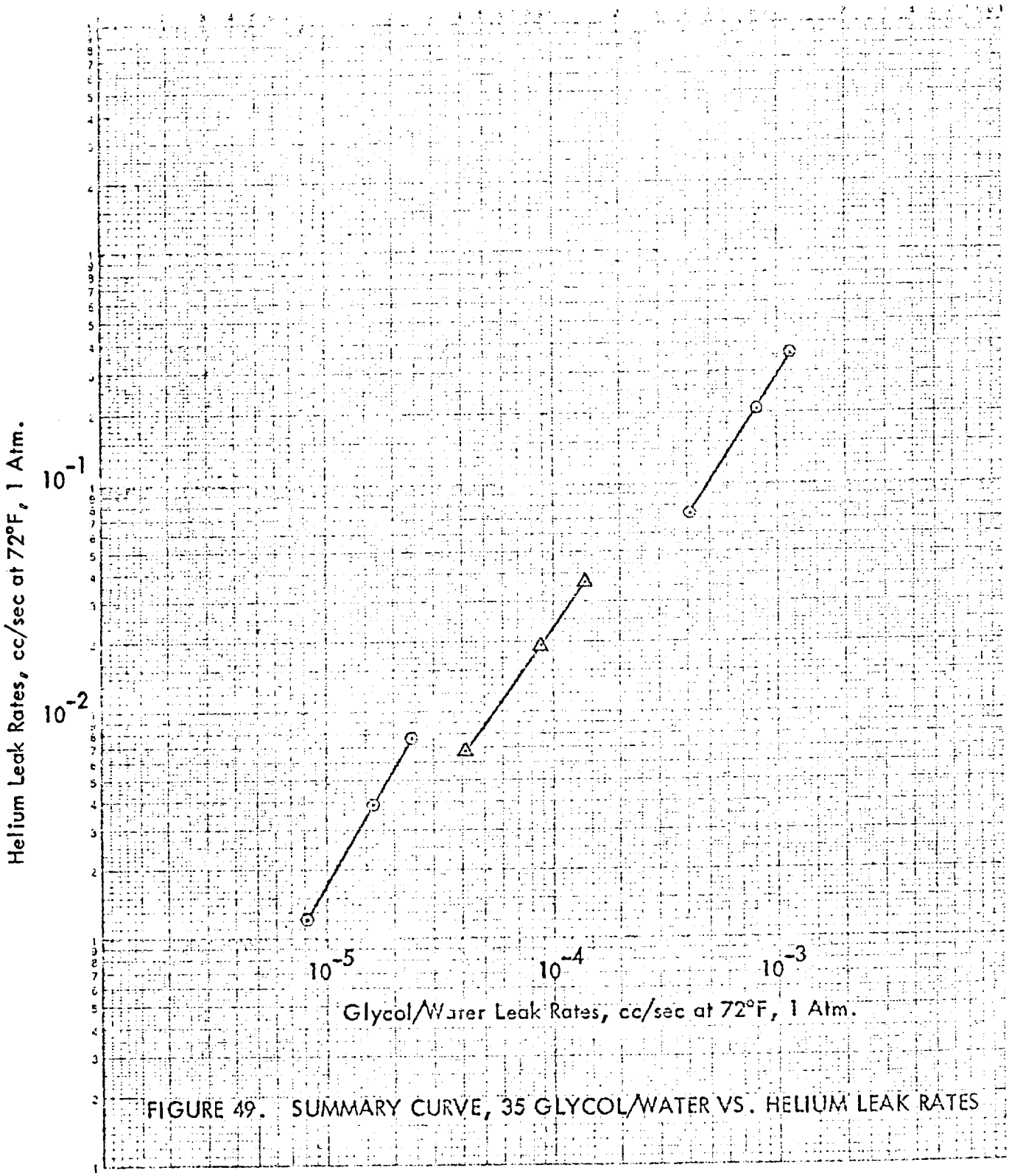

FIGURE 49. SUMMARY CURVE, 35 GLYCOL/WATER VS. HELIUM LEAK RATES

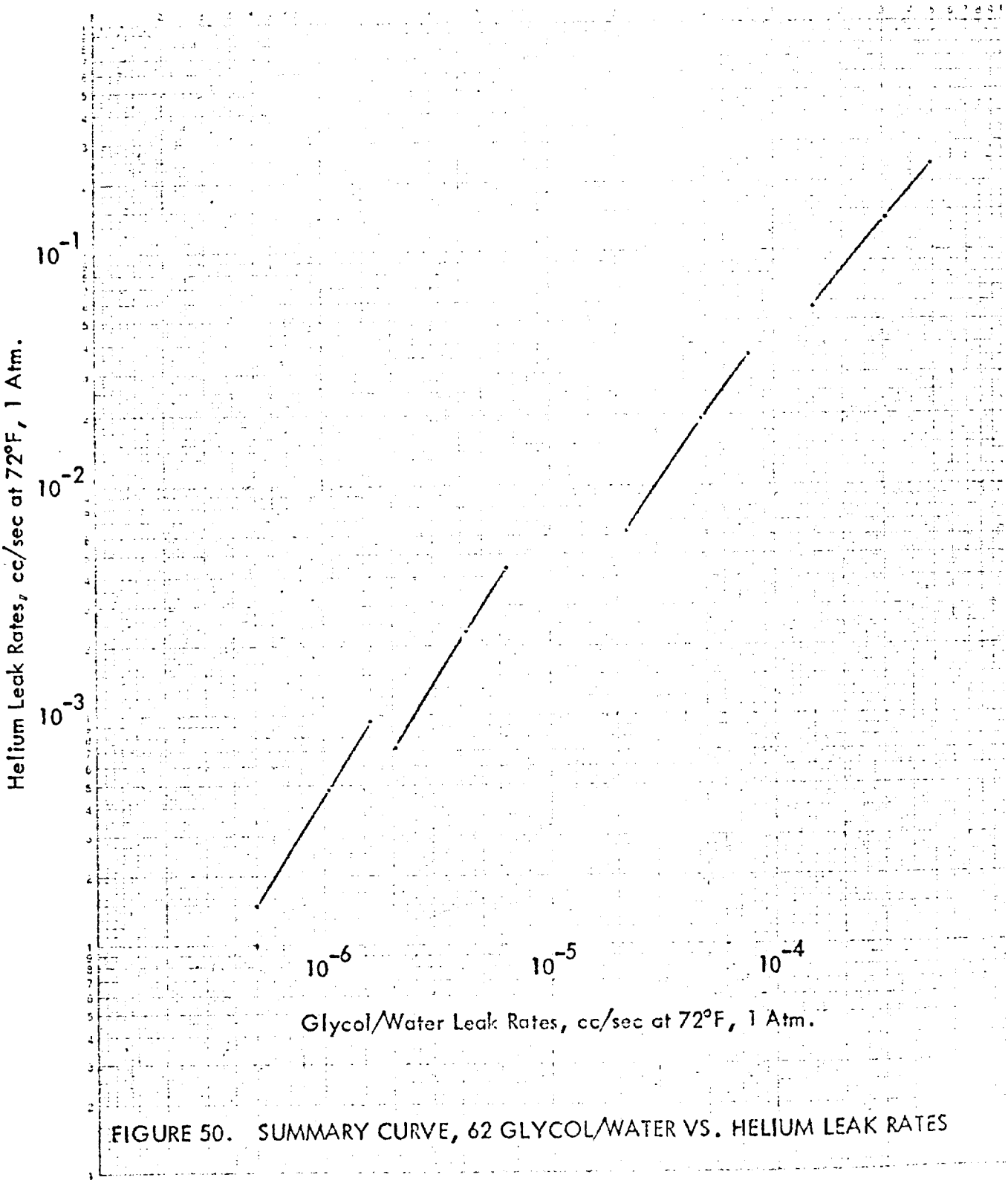

FIGURE 50. SUMMARY CURVE, 62 GLYCOL/WATER VS. HELIUM LEAK RATES

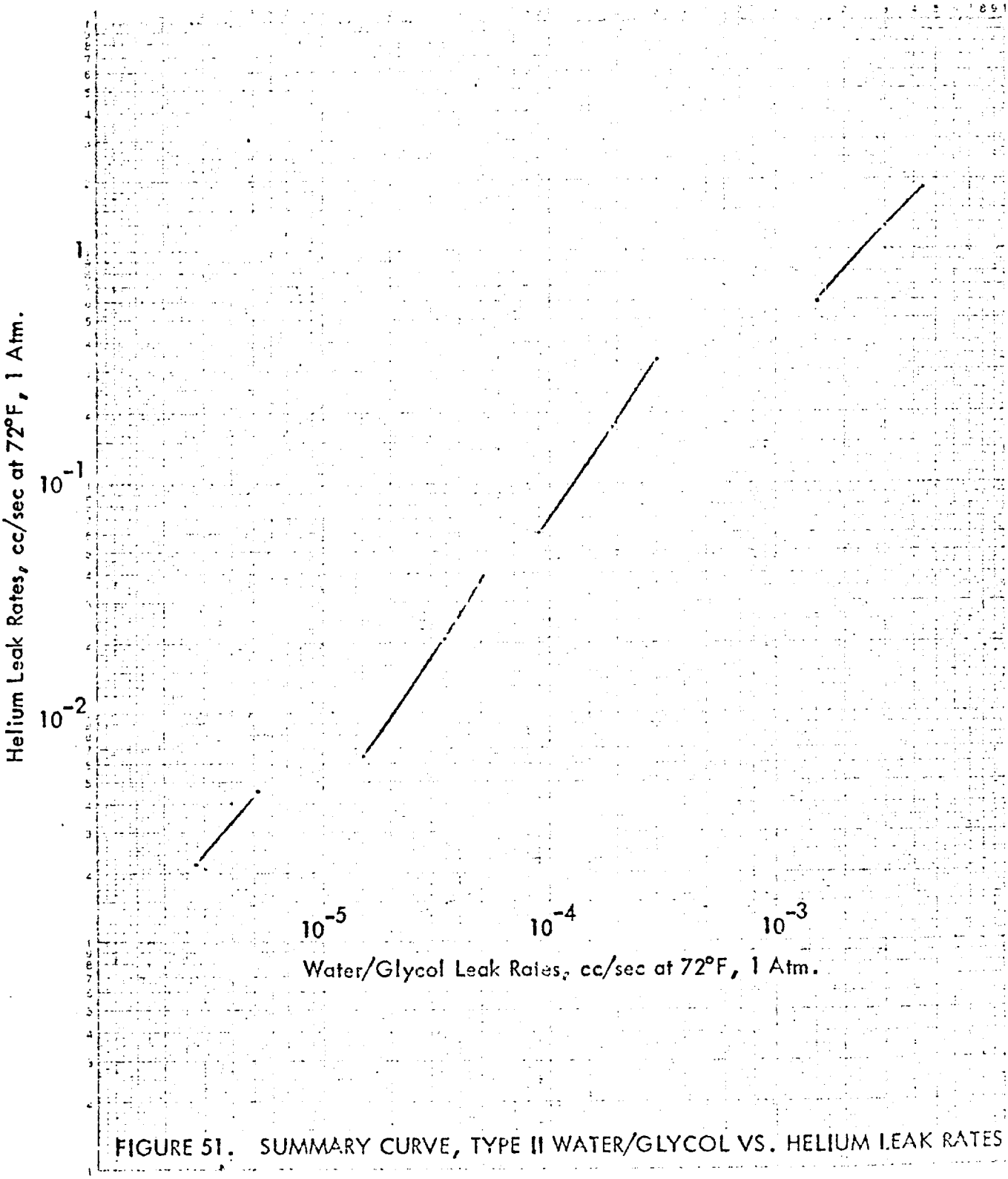

FIGURE 51. SUMMARY CURVE, TYPE II WATER/GLYCOL VS. HELIUM LEAK RATES

TABLE 11
APOLLO TIE LEAK TEST DATA

Dates: 3/5/68-3/15/63

Leak Description: Nominal 10^{-2} cc/sec helium leak, surfaces polished but not mated, plug scribed.

Fluid: Nitrogen Tetroxide

Comments: Helium leak rate measured volumetrically before test, with leak tester after test

Test Description	Date	Pressure, psig	Volume, cc	Time, sec	Leak Rate, cc/sec
Helium Leak Rate Before Test	3/5/68	35	10.0	461.	2.17×10^{-2}
		150	10.0	43.5	2.30×10^{-1}
		250	20.0	40.5	4.94×10^{-1}
		350	20.0	24.7	8.1×10^{-1}
		90	10.0	95.5	1.05×10^{-1}
		50	5.0	125.4	3.97×10^{-2}

	Date	System Pressure, psig	Elapsed Time, Hr.	NO_2 Flow ugm/min.	NO_2 Flow (Real Gas) cc/sec	NO_2 Avg. Flow cc/sec
Nitrogen Tetroxide Leak	3/6/68	350	0.5	34.0	1.67×10^{-4}	
			1.0	13.9	6.73×10^{-5}	
			3.0	0.76	3.71×10^{-6}	
			4.0	0.68	3.34×10^{-6}	
			5.0	0.60	2.94×10^{-6}	
			5.5	0.55	2.70×10^{-6}	
	3/7/68		22.5	0.63	3.09×10^{-6}	
			23.0	0.66	3.21×10^{-6}	
			23.5	0.65	3.17×10^{-6}	
			24.0	0.66	3.21×10^{-6}	
		250	0.5	0.42	2.06×10^{-6}	
			1.0	0.46	2.24×10^{-6}	
			1.5	0.47	2.30×10^{-6}	
			2.5	0.47	2.30×10^{-6}	2.30×10^{-6}
			3.0	0.47	2.30×10^{-6}	

TABLE 11 (Continued)

Date	System Pressure, psig	Elapsed Time, Hr.	NO_2 Flow[2] µgm/min.	NO_2 Flow (Real Gas) cc/sec	Avg. NO_2 Flow cc/sec
3/7/68	150	1.0	0.37	1.81×10^{-6}	
		2.0	0.40	1.96×10^{-6}	
		2.5	0.49	2.42×10^{-6}	
	350	0.5	1.27	6.22×10^{-6}	
3/8/68		16.5	1.89	9.25×10^{-6}	
		17.0	1.95	9.53×10^{-6}	
		17.5	2.06	1.01×10^{-5}	
		18.0	2.07	1.01×10^{-5}	
		18.5	2.10	1.03×10^{-5}	
		19.5	2.19	1.07×10^{-5}	
		21.5	2.26	1.11×10^{-5}	
	Leak Subjected to Sharp Knocking				
		23.0	6.69	3.23×10^{-5}	
		23.9	6.75	3.30×10^{-5}	
3/11/68		89.0	272	1.33×10^{-3}	
		89.5	287	1.41×10^{-3}	
		90.0	287	1.41×10^{-3}	
		91.5	311	1.52×10^{-3}	
	Leak Knocked, Pressure Raised				
	565	1.5	521	2.55×10^{-3}	
	352	1.0	342	1.68×10^{-3}	
		3.0	368	1.80×10^{-3}	
3/12/68		20.8	418	2.04×10^{-3}	
		21.5	420	2.05×10^{-3}	
		22.0	431	2.10×10^{-3}	
	Heat Leak, Pressurized to 600 psig, brown fumes noted.				
	350	0.17	1770	8.68×10^{-3}	
		0.75	1284	6.30×10^{-3}	
		2.0	1200	5.90×10^{-3}	
3/13/68		19.0	1110	5.44×10^{-3}	
		19.5	1110	5.44×10^{-3}	
		20.0	1110	5.44×10^{-3}	
	250	1.0	920	4.51×10^{-3}	
		2.0	920	4.51×10^{-3}	
	Heat leak again under pressure.				
	350	3.0	1770	8.68×10^{-3}	
		3.5	1676	8.21×10^{-3}	
	Heat and knock again.				

TABLE II (Continued)

Date	System Pressure, psig	Elapsed Time, Hr.	NO_2 Flow[2] µgm/min.	NO_2 Flow (Real Gas) cc/sec	Avg. NO_2 Flow cc/sec
3/14/68	350	0.5	2110	1.03×10^{-2}	1.02×10^{-2}
		1.0	2090	1.02×10^{-2}	
		2.0	2070	1.01×10^{-2}	
		3.0	2050	1.00×10^{-2}	
	247	1.5	1510	7.40×10^{-3}	7.40×10^{-3}
		1.8	1510	7.40×10^{-3}	
	150	0.5	1020	5.00×10^{-3}	5.0×10^{-3}
		1.0	1020	5.0×10^{-3}	
	52	0.8	490	2.40×10^{-3}	2.33×10^{-3}
		1.3	456	2.24×10^{-3}	
		1.8	483	2.36×10^{-3}	

	Pressure, psig	Pressure Diff. psi	Difference In CEC Reading Div	Leak Rate, cc/sec
Helium Rate After Run (5.70×10^{-6} std = 21 div.)	35	50	5,700	1.54×10^{-3}
	80	95	14,500	3.93×10^{-3}
	150	165	32,500	8.81×10^{-3}
	250	265	68,000	1.85×10^{-2}

TABLE 12
APOLLO TIE LEAK TEST DATA

Dates: 2/8/66-2/16/68

Leak Description: Nominal 10^{-2} cc/sec helium leak, scribed plug.

Fluid: Nitrogen Tetroxide

Comments: This leak rapidly plugged completely during the N_2O_4 testing. Instrument response varied as indicated below during Helium tests.

Test Description	Date	Pressure psig	Pressure Diff. psi	Difference In CEC Reading, Div.	Leak Rate, cc/sec
Helium Rate Before Run (Standard = 2100 to 1800 div. for a variable capillary standard leak set at 1×10^{-2} cc/sec of helium).	2/8/68	35	50	1,100	6.11×10^{-3}
		135	150	5,000	2.79×10^{-2}
		235	250	11,700	6.50×10^{-2}
		335	350	20,200	1.12×10^{-1}

		System Pressure, psig	Elapsed Time, Min.	NO_2 Flow µgm/min	NO_2 Flow (Real Gas) cc/sec
Nitrogen Tetroxide Leak	2/16/68	50	2	150.0	7.4×10^{-4}
			15	20.5	1.0×10^{-4}
			35	9.6	4.7×10^{-5}
			60	4.3	2.1×10^{-5}
			90	1.6	7.9×10^{-6}
		350	2	3.5	1.7×10^{-5}
			50	1.6	7.9×10^{-6}
		550	100	1.1	5.4×10^{-6}

TABLE 13

APOLLO TIE LEAK TEST DATA

Dates: 2/23/68-3/4/68

Leak Description: Nominal 10^{-2} cc/sec helium leak, scribed plug, mated surfaces.

Fluid: Nitrogen Tetroxide

Comments: Data for N_2O_4 taken on 3/1/68 was used to plot leakage graph. During measurement of the helium leak rate after test at 50 psi the needle of the CEC leak detector rapidly moved to a new higher value. This was attributed to dislodgement of a partially blocking particle.

Test Description	Date	Pressure, psig	Pressure Diff. psi	Difference In CEC Reading, Div.	Leak Rate, cc/sec
Helium Rate Before Test (A 1×10^{-2} standard leak gave 2400 to 2500 divisions)	2/23/68	35	50	1,050	4.2×10^{-3}
		135	150	7,400	2.96×10^{-2}
		235	250	17,100	7.13×10^{-2}
		335	350	31,100	1.3×10^{-1}
Helium Rate After Test (Std = 8,500 for a 7.8×10^{-6} leak)	3/4/68	35	50	41,500	3.81×10^{-5}
		Leak rate increased four-fold while on detector.			
(Std = 110 div. for 7.8×10^{-6} leak)		35	50	2,290	1.62×10^{-4}
		135	150	15,640	1.11×10^{-3}
		235	250	37,140	2.63×10^{-3}
		335	350	65,890	4.66×10^{-3}

		System Pressure, psig	Elapsed Time, Min.	NO_2 Flow µgm/min	NO_2 Flow (Real Gas) cc/sec	Avg. NO_2 Flow cc/sec
Nitrogen Tetroxide Leak	2/26/8	50	80	546	2.67×10^{-3}	
			130	339	1.65 "	
			275	319	1.56 "	
			330	325	1.59 "	
			390	319	1.56 "	
	2/27/8		1385	100	4.90×10^{-4}	
			1415	95	4.65 "	
			1470	78	3.82 "	
			1560	55.5	2.72 "	
			1680	31.6	1.55 "	
			1830	26.8	1.31 "	

TABLE 13 (Continued)

Date	System Pressure, psig	Elapsed Time, Min.	NO_2 Flow µgm/min	NO_2 Flow (Real Gas) cc/sec	Avg. NO_2 Flow cc/sec
2/28/8	50	2880	22.3	1.09×10^{-4}	1.10×10^{-4}
		2940	22.6	1.11 "	
		3000	22.6	1.11 "	
	150	10	61.0	2.99×10^{-4}	
		30	63.8	3.13 "	3.13×10^{-4}
		60	63.8	3.13 "	
		120	63.8	3.13 "	
	250	5	106.0	5.20 "	
		20	96.0	4.70 "	
		60	119.0	5.81 "	
		120	120.4	5.89 "	
2/29/8		1110	123.2	6.05 "	5.94×10^{-4}
		1140	123.2	6.05 "	
		1170	118.1	5.80 "	
		1200	123.8	6.06 "	
2/29/8	350	10	196	9.59×10^{-4}	
		120	205	1.01×10^{-3}	
		240	222	1.09×10^{-3}	
3/1/68	350	1320	275	1.35×10^{-3}	1.35×10^{-3}
		1350	"	1.35×10^{-3}	
		1380	"	1.35×10^{-3}	
	250	60	199	9.75×10^{-4}	9.75×10^{-4}
		120	"	9.75×10^{-4}	
		150	"	9.75×10^{-4}	
	154	30	126	6.18×10^{-4}	6.13×10^{-4}
		60	121	5.92 "	
		90	126	6.18 "	
		120	126	6.18 "	
	55	30	48.5	2.37×10^{-4}	2.35×10^{-4}
		60	47.2	2.32 "	
		90	48.5	2.37 "	
		120	47.9	2.35 "	

TABLE 14

APOLLO TIE LEAK TEST DATA

Dates: 2/2/68 - 2/12/68

Leak Description: Nominal 10^{-4} cc/sec helium leak, scribed plug leak.

Fluid: Nitrogen Tetroxide

Comments: Following the test the plug was found to be coated with a brown oily residue, whose IR spectrum indicated Kel-F contamination. Note, nevertheless, that the helium leak rate was increased slightly during the test.

Test Description	Date	Pressure, psig	Pressure Difference, psi	Difference In CEC Reading, Div.	Leak Rate, cc-atm/sec
Helium Rate Before Test(1.75×10^{-4} Standard Leak = 730 CEC Div.)	2/2/68	35	50	770	1.85×10^{-4}
		135	150	9,770	2.34×10^{-3}
		235	250	25,770	6.18×10^{-3}
		335	350	49,770	1.19×10^{-2}
Helium Rate After Test (Same Standard Leak = 600 Div. to 510 Div.)	2/12/68	34	49	930	2.13×10^{-4}
		135	150	9,370	3.09×10^{-3}
		236	251	22,710	7.36×10^{-3}
		336	351	40,450	1.29×10^{-2}

		System Pressure, psig	Elapsed Time at Press. Min.	NO_2 Flow gm/min.	NO_2 Flow (Real Gas) cc/sec	Avg. NO_2 Flow (Real Gas) cc/sec
Nitrogen Tetroxide Leak	2/6/68	50	50	8.95	4.48×10^{-5}	
			65	9.82	4.82 "	
			120	14.48	7.09 "	
			158	17.40	8.51 "	
			205	19.36	9.48 "	
			262	20.00	9.79 "	
			322	21.00	1.03×10^{-4} "	1.07×10^{-4}
			382	21.96	1.07 "	
			442	22.62	1.10 "	

TABLE 14 (Continued)

Date	System Pressure, psig	Elapsed Time at Press. Min.	NO_2 Flow µgm/min.	NO_2 Flow (Real Gas) cc/sec	Avg. NO_2 Flow (Real Gas) cc/sec
2/7/68	150	945	36.50	1.78×10^{-4}	1.78×10^{-4}
		1025	36.50	1.78×10^{-4}	
		1065	36.50	1.78×10^{-4}	
	250	15	62.20	3.10×10^{-4}	3.40×10^{-4}
		45	67.4	3.30 "	
		105	71.6	3.50 "	
2/8/68		1090	92.0	4.50 "	4.50×10^{-4}
		1165	92 0	4.50 "	
	350	3	109.8	5.36×10^{-4}	
		19	122.8	5.96 "	
		34	131.5	6.45 "	
		58	136.3	6.69 "	
		137	137.5	6.72 "	6.72×10^{-4}
		200	137.5	6.72 "	
		1165	137.5	6.72 "	

TABLE 15

APOLLO TIE LEAK TEST DATA

Dates: 3/18/68 - 3/20/68

Leak Description: Nominal 5×10^{-5} cc/sec Helium Leak, Crushed Tube

Fluid: Nitrogen Tetroxide

Comments: This leak, the last NO_2 leak, performed faultlessly during NO_2 testing but plugged absolutely during preparation for the final helium test, so no post-test helium leak data was obtained.

Test Description	Date	Pressure, psig	Pressure Diff. (psi)	Difference In CEC Reading, (Divisions)	Leak Rate cc/sec
Helium Before Test 5.70×10^{-6} std = 330 div.	3/18/68	35	50	2,370	4.95×10^{-5}
		135	150	13,170	2.31×10^{-4}
		235	250	27,670	4.93×10^{-4}
		335	350	47,670	8.63×10^{-4}

		System Pressure, psig	Elapsed Time, min.	NO_2 Flow (μgm/min)	NO_2 Flow (cc gas/sec)
Nitrogen Tetroxide Leak	3/20/68	55	2	23.2	1.13×10^{-4}
			20	23.2	1.13×10^{-4}
			40	23.2	1.13×10^{-4}
		156	60	58.2	2.85×10^{-4}
			80	60.5	2.95×10^{-4}
			100	60.5	2.95×10^{-4}
		251	150	92.2	4.51×10^{-4}
			170	92.2	4.51×10^{-4}
		350	225	127.5	6.23×10^{-4}
			240	"	"
		252	270	92.5	4.53×10^{-4}
		152	300	60.0	2.93×10^{-4}
		55	330	23.2	1.13×10^{-4}

TABLE 16

APOLLO TIE LEAK TEST DATA

Dates: 3/14/68 - 3/18/68

Leak Description: Nominal 5×10^{-6} cc/sec Helium Leak, Crushed Tube

Fluid: Nitrogen Tetroxide

Comments: Data of 3/18/68 used to calculate NO_2 leakage rate. This leak was fairly stable during NO_2 testing but did suffer significant blocking, as can be seen by the helium after data.

Test Description	Date	Pressure, psig	Pressure Diff. (psi)	Difference In CEC Reading, (Divisions)	Leak Rate, cc/sec
Helium Before Test 5.70×10^{-6} Std = 3250 div.	3/14/68	35	50	3,050	5.52×10^{-6}
		135	150	12,250	2.37×10^{-5}
		235	250	28,500	5.09×10^{-5}
		335	350	49,250	8.78×10^{-5}
Helium After Test 5.70×10^{-6} Std = 2950 div.	3/18/68	35	50	200	5.45×10^{-7}
		135	150	825	1.72×10^{-6}
		235	250	1,600	3.17×10^{-6}
		335	350	2,550	4.93×10^{-6}

		System Pressure, psig	Elapsed Time Hr.	Elapsed Time Min.	NO_2 Flow (µg/min.)	NO_2 Flow (cc gas/sec)
Nitrogen Tetroxide Leak	3/16/68	55		5	0.355	1.74×10^{-6}
				25	"	"
				45	"	"
	3/18/68	54	46	55	0.264	1.30×10^{-6}
			47	25	"	"
		153	48	25	0.729	3.57×10^{-6}
			48	55	0.720	3.52×10^{-6}
		254	49	35	1.092	5.36×10^{-6}
			50	5	"	"
		347	50	45	1.51	7.40×10^{-6}
			51	15	1.49	7.30×10^{-6}
		251	51	35	1.08	5.30×10^{-6}
			52	5	1.09	5.36×10^{-6}
		151	52	20	0.70	3.42×10^{-6}
			52	40	"	"
		54	53	0	0.285	1.39×10^{-6}
			53	35	0.300	1.46×10^{-6}

TABLE 18

APOLLO TIE LEAK TEST DATA

Dates: 5/14/65 - 5/15/68

Leak Description: Smashed Steel Leak, nominal 10^{-2} cc/sec Helium

Fluid: Monomethylhydrazine

Comments:

	Test Description	Pressure, psig	Volume, cc	Time, sec	Leak Rate, cc/sec
1	Helium Calibration Before Test	50	NA	NA	2.61×10^{-2}
		150	"	"	1.54×10^{-1}
		250	"	"	3.75×10^{-1}

		Elapsed Time, min.	Action	Pressure, psig	Sample No.	Leak Rate, cc/sec
2.	Monomethylhydrazine Leak Rate Test 5/14/68	0	Fill reservoir			
		1	Pressurize to	50		
		2	Sample at	54	1	1.0×10^{-4}
		3	"	54	2	6.2×10^{-5}
		4	Pressurize to	150		
		5	Sample at	145	3	7.5×10^{-5}
		6	"	145	4	8.9×10^{-5}
		7	Pressurize to	250		
		8	Sample at	250	5	7.8×10^{-5}
		9	"	250	6	8.0×10^{-5}
		10	Drop pressure to	150		
		11	Sample at	155	7	6.5×10^{-5}
		12	Sample at	155	8	3.9×10^{-5}
		13	Drop pressure to	50		
		14	Sample at	52	9	1.7×10^{-5}
		15	"	52	10	1.2×10^{-5}
		16	"	52	11	5.7×10^{-6}
		17	"	52	12	3.1×10^{-6}
		20	"	52	13	2.2×10^{-6}
		25	"	52	14	9.2×10^{-7}
		35	"	52	15	1.3×10^{-6}
		50	"	52	16	5.6×10^{-7}
		70	"	52	17	5.1×10^{-7}
		100	"	52	18	2.2×10^{-7}
		160	"	52	19	2.2×10^{-7}
		200	Sample at	52	20	2.2×10^{-7}

TABLE 13 (Continued)

	Elapsed Time, min.	Action	Pressure, psig	Sample No.	Leak Rate, cc/sec
5/14/68	225	Pressurize to	145		
	235	Sample at	145	21	3.3×10^{-6}
	245	"	145	22	2.5×10^{-6}
	255	Pressurize to	249		
	265	Sample at	249	23	1.9×10^{-5}
	285	"	249	24	2.6×10^{-5}
	292	Drop pressure to	150		
	302	Sample at	150	25	5.5×10^{-6}
	310	Drop pressure to	50		
	320	Sample at	50	26	5.6×10^{-7}
	343	"	50	27	1.9×10^{-7}
	390	Drop pressure to	15		
5/15/68	1410	Pressurize to	250		
	1415	Sample at	250	30	3.5×10^{-6}
	1420	Drop pressure to	150		
	1425	Sample at	150	31	1.5×10^{-6}
	1430	Drop pressure to	50		
	1440	Sample at	50	32	7.5×10^{-7}
	1445	Pressurize to	156		
	1455	Sample at	156	33	9.5×10^{-7}
	1460	Pressurize to	250		
	1470	Sample at	250	34	3.0×10^{-6}
	1475	Drop pressure to	150		
	1483	Sample at	150	35	1.8×10^{-6}
	1489	Drop pressure to	50		
	1500	Sample at	50	36	6.2×10^{-7}

	Pressure, psig	Volume, cc	Time, sec	Leak Rate cc/sec
3. Helium Calibration	50	NA	NA	6.2×10^{-4}
After Test	150	"	"	4.65×10^{-3}
	250	"	"	1.14×10^{-3}

TABLE 19

APOLLO TIE LEAK TEST DATA

Dates: 5/8/68 - 5/13/68

Leak Description: Smashed steel tubing leak, nominal 5×10^{-3} cc/sec Helium Leak.

Fluid: Monomethylhydrazine

Comments: Leak appeared to plug badly before initial point was measured, and continued to plug further during test.

Test Description		Pressure, psig	Volume cc	Time, sec	Leak Rate, cc/sec
1. Helium Calibrations Before Test					
	5/8/68	50	NA	NA	7.23×10^{-3}
		150			6.30×10^{-2}
		250			1.35×10^{-1}
		50			4.83×10^{-3}
		150			2.92×10^{-2}
		250			6.67×10^{-2}
	5/9/68	50			5.20×10^{-3}
		150			3.02×10^{-2}
		250			6.44×10^{-2}
		50			3.87×10^{-3}
		150			2.92×10^{-2}
		250			6.47×10^{-2}
		50			3.82×10^{-3}
		150			2.92×10^{-2}
		250			6.45×10^{-2}
	5/10/68	50			5.06×10^{-3}
		150			2.96×10^{-2}
		250			6.45×10^{-2}

TABLE 19 (Continued)

	Elapsed Time (From start of expt.) Hr.	Min.	Action	Pressure, psig	Sample No.	Leak Rate Measured of MMH cc/sec
2. Monomethyl-hydrazine Leak Rate Measurement						
5/10/68	0	0	Fill reservoir			
		20	Pressurize to	50		
		30	Sample at	50	1	1.36×10^{-6}
		40	Pressurize to	150		
		50	Sample at	149	2	3.0×10^{-6}
	1	0	Pressurize to	250		
	1	10	Sample at	245	3	2.4×10^{-6}
	1	30	Sample at	245	4	2.0×10^{-6}
	1	45	Drop pressure to	150		
	2	0	Sample at	154	5	6.7×10^{-7}
	2	30	Drop pressure to	50		
	2	40	Sample at	53	6	1.3×10^{-7}
	3	00	Pressurize to	150		
	3	20	Sample at	148	7	3.5×10^{-7}
	3	40	Pressurize to	250		
	4	00	Sample at	250	8	6.5×10^{-7}
	4	20	Drop pressure to	150		
	4	35	Sample at	154	9	2.5×10^{-7}
	4	45	Drop pressure to	50		
	5	00	Sample at	54	10	8.1×10^{-8}

	Pressure, psig	Volume, cc	Time, sec	Leak Rate, cc/sec
3. Helium Calibration After Test 5/13/68	60	NA	NA	6.00×10^{-5}
	150			4.95×10^{-4}
	250			1.45×10^{-3}

TABLE 20
APOLLO TIE LEAK TEST DATA

Dates: 6/17/68-6/18/68

Leak Description: AN Flared Fitting, with Lightly Torqued Plug, nominal 10^{-2} cc/sec Helium

Fluid: Monomethylhydrazine

Comments: During liquid leak testing the reservoir was filled with fuel, pressurized to 50 psig, and maintained there throughout the test.

Test Description	Pressure, psig	Volume, cc	Time, sec	Leak Rate, cc/sec
1. Helium Calibration Before Test	50	1.00	104.4	9.6×10^{-3}
	51	1.00	100.0	1.00×10^{-2}
	52	1.00	96.4	1.04×10^{-2}

	Elapsed Time (min) from Initial Pressurization at 50 psig	Sample No.	Leak Rate at 50 psig cc/sec
2. Monomethylhydrazine Leak Rate Test 6/17/68	2	3	$<10^{-7}$
	4	4	$<10^{-7}$
	7	5	5.3×10^{-7}
	11	6	1.85×10^{-6}
	16	7	1.98×10^{-6}
	23	8	1.98×10^{-6}
	38	9	2.76×10^{-6}
	50	10	3.80×10^{-6}
	70	11	4.00×10^{-6}
	92	12	5.6×10^{-6}
	110	13	7.2×10^{-6}
	130	14	9.95×10^{-6}
	162	15	6.7×10^{-6}
	188	16	6.1×10^{-6}
	219	17	5.0×10^{-6}
	256	18	6.1×10^{-6}
	282	19	6.1×10^{-6}
	315	20	3.95×10^{-6}
	330	21	4.5×10^{-6}
	1340	23	3.8×10^{-7}
	1360	24	6.3×10^{-7}
	1380	25	4.9×10^{-7}

TABLE 20 (Continued)

Test Description	Pressure, psig	Volume, cc	Time, sec	Leak Rate, cc/sec
3. Helium Calibration	50	1.00	167	5.99×10^{-3}
After Test	50	0.80	136	5.85×10^{-3}
	50	1.00	167	5.99×10^{-3}
	50	1.00	152	6.55×10^{-3}

TABLE 21

APOLLO TIE LEAK TEST DATA

Dates: 6/19/68-6/20/68

Leak Description: AN Flared Fitting, with Lightly Torqued Plug, nominal 10^{-3} cc/sec helium leak.

Fluid: Monomethylhydrazine

Comments: Room temperature 72°-74°F.

Test Description	Pressure, psig	Volume, cc	Time, sec	Leak Rate, cc/sec
1. Helium Calibration Before Test	50	1.00	647	1.55×10^{-3}
	50	1.00	641	1.56×10^{-3}
	150	1.00	100.3	1.00×10^{-2}
	250	1.00	41.3	2.42×10^{-2}
	250	0.60	24.9	2.42×10^{-2}
	150	0.60	60.4	9.95×10^{-3}
	50	0.60	323	1.86×10^{-3}
	50	0.60	342	1.75×10^{-3}
	50	0.60	339	1.77×10^{-3}

2. Monomethylhydrazine Leak Test	Elapsed Time, min.	Action	Pressure, psig	Sample No.	Leak Rate, cc/sec
6/19/68	0	Pressurize to	50		
	5	Sample at	50	1	1.36×10^{-8}
	7	"	50	2	2.14×10^{-8}
	27	"	50	3	2.56×10^{-8}
	47	"	50	4	2.71×10^{-8}
	75	"	50	5	2.38×10^{-8}
	160	"	50	6	3.13×10^{-8}
	235	"	50	7	2.99×10^{-8}
	265	"	50	8	3.13×10^{-8}
	295	"	50	9	2.85×10^{-8}
6/20/68	1340	"	50	10	$< 10^{-8}$
	1370	"	50	11	$< 10^{-8}$
	1375	Pressurize to	150		
	1390	Sample at	150	12	1.33×10^{-8}
	1395	Pressurize to	250		
	1420	Sample at	250	13	2.00×10^{-8}

TABLE 21 (Continued)

Test Description	Pressure, psig	Volume, cc	Time, sec	Leak Rate, cc/sec
3. Helium Calibration After Test	50	0.60	1320	4.52×10^{-4}
	150	0.20	103	1.94×10^{-3}
	250	0.60	105	5.71×10^{-3}
	50	0.10	240	4.14×10^{-4}

TABLE 22
APOLLO TIE LEAK TEST DATA

Date: 5/22/68

Leak Description: Glass leak No. 2, 4×10^{-2} cc/sec helium.

Fluid: Monomethylhydrazine

Test Description	Pressure, psig	Volume, cc	Time, sec.	Leak Rate, cc/sec
1. Helium Calibration	48	5.0	121	4.13×10^{-2}
	150	5.0	19.5	2.57×10^{-1}
	150	25.0	88	2.82×10^{-1}
	250	25.0	42.6	5.86×10^{-1}
	250	25.0	42.6	5.86×10^{-1}
	150	25.0	89	2.86×10^{-1}
	50	5.0	105	4.71×10^{-2}
2. Monomethylhydrazine Run	50	4.0×10^{-3}	4.4	9.1×10^{-4}
	150	5.0×10^{-3}	2.4	2.1×10^{-3}
	250	7.0×10^{-3}	2.75	2.5×10^{-3}
3. Helium Calibration After Run	48	5.0	128	3.92×10^{-2}
	150	25.0	101	2.46×10^{-1}
	250	25.0	48	5.21×10^{-1}
4. Monomethylhydrazine Run, Repeat	250	6.0×10^{-3}	2.0	3.0×10^{-3}
	50	4.0×10^{-3}	4.5	8.9×10^{-4}
	150	6.0×10^{-3}	Leak Plugged	

TABLE 23
APOLLO TIE LEAK TEST DATA

Date: 5/24/68

Leak Description: Glass leak No. 5, nominal 10^{-5} cc/sec helium.

Fluid: Monomethylhydrazine

Test Description	Pressure, psig	Volume, cc	Time, sec.	Leak Rate, cc/sec
1. Helium Calibration	250	0.20	355	5.65×10^{-4}
	145	0.05	285	1.73×10^{-4}
	50	0.01	266	3.76×10^{-5}
2. Monomethylhydrazine Run	250	2.0×10^{-3}	860	2.34×10^{-6}
	150	3.0×10^{-3}	2310	1.30×10^{-6}
	50	3.0×10^{-3}	Leak Plugged	

Date: 5/27/68

Leak Description: Glass leak No. 7, nominal 10^{-3} cc/sec helium.

Fluid: Monomethylhydrazine

Test Description	Pressure, psig	Volume, cc	Time, sec.	Leak Rate, cc/sec
1. Helium Calibration	48	1.0	370	2.7×10^{-3}
	150	1.0	47.5	2.1×10^{-2}
	250	0.6	11.5	5.25×10^{-2}
	150	0.6	27.5	2.18×10^{-2}
	50	1.0	317	3.15×10^{-3}
	50	1.0	327	3.06×10^{-3}
2. Monomethylhydrazine Run	150	4.0×10^{-3}	27.7	1.44×10^{-4}
	250	4.0×10^{-3}	Leak Plugged	

TABLE 24
APOLLO TIE LEAK TEST DATA

Date: 5/27/68

Leak Description: Glass leak No. 8, nominal 10^{-3} cc/sec helium.

Fluid: Monomethylhydrazine

Test Description	Pressure, psig	Volume, cc	Time, sec.	Leak Rate, cc/sec
1. Helium Calibration	47	1.0	968	1.04×10^{-3}
	150	1.0	135	7.42×10^{-3}
	250	1.0	54	1.85×10^{-2}
	150	1.0	134	7.45×10^{-3}
	50	0.6	575	1.04×10^{-3}
2. Monomethylhydrazine Run	250	4.0×10^{-3}	32	1.25×10^{-4}
	150	4.0×10^{-3}	Leak Plugged	

Date: 5/27/68

Leak Description: Leak no. 9, nominal 10^{-3} cc/sec helium.

Fluid: Monomethylhydrazine

Test Description	Pressure, psig	Volume, cc	Time, sec.	Leak Rate, cc/sec
1 Helium Calibration	50	1.0	329	3.02×10^{-3}
	150	1.0	53.6	1.87×10^{-2}
	250	1.0	24	4.18×10^{-2}
	150	1.0	51.3	1.94×10^{-2}
	50	1.0	298	3.35×10^{-3}
2. Monomethylhydrazine Run	50	2.0×10^{-3}	41.3	4.84×10^{-5}
	250	2.0×10^{-3}	Leak Plugged	

TABLE 25

APOLLO TIE LEAK TEST DATA

Date: 5/29/68

Leak Description: Glass leak No. 11, nominal 10^{-4} cc/sec helium.

Fluid: Monomethylhydrazine

Test Description	Pressure, psig	Volume, cc	Time, sec.	Leak Rate, cc/sec
1. Helium Calibration	50	0.10	482	2.08×10^{-4} (Air?)*
	150	0.10	52.6	1.90×10^{-3}
	250	1.0	222	4.50×10^{-3}
	150	0.10	53.0	1.89×10^{-3}
	50	0.10	428	2.33×10^{-4}
2. Monomethylhydrazine Run	150	3.0×10^{-3}	169	1.77×10^{-5}
	250	3.0×10^{-3}	142	2.11×10^{-5}
3. Helium, Recalibration	250	1.0	247	4.03×10^{-3}
	150	0.1	59	1.70×10^{-3}
	50	0.1	434	2.30×10^{-4}
4. Monomethylhydrazine Run	50	3.0×10^{-3}	990	3.03×10^{-6}
	150	3.0×10^{-3}	315	9.55×10^{-6}
5. Helium Recalibration	250	1.0	231	4.34×10^{-3}
6. Monomethylhydrazine	250	3.0×10^{-3}	Missed time reading.	
	250	3.0×10^{-3}	196	1.53×10^{-5}

*Probably low because air not swept from leak prior to run.

TABLE 2A

APOLLO TIE LEAK TEST DATA

Date: 5/22/68

Leak Description: Glass Leak No. 1, nominal 10^{-2} cc/sec helium.

Fluid: Monomethylhydrazine

Test Description	Pressure, psig	Volume, cc	Time, sec.	Leak Rate, cc/sec
1. Helium Calibration	50	2.0	196	1.02×10^{-2}
	50	2.0	195	1.02×10^{-2}
	150	2.0	31.2	6.39×10^{-2}
	150	2.0	31.2	6.39×10^{-2}
	250	5.0	28.6	1.69×10^{-1}
	250	5.0	28.6	1.69×10^{-1}
	150	5.0	68.3	7.3×10^{-2}
	150	5.0	68.0	7.3×10^{-2}
	50	5.0	462	1.07×10^{-2}
2. Monomethylhydrazine Run	52	5.0×10^{-3}	34	1.47×10^{-4}
	156	5.0×10^{-3}	Leak Plugged	

Date: 5/22/68

Leak Description: Glass Leak No. 3, nominal 10^{-3} cc/sec helium.

Fluid: Monomethylhydrazine

Test Description	Pressure, psig	Volume, cc	Time, sec.	Leak Rate, cc/sec
1. Helium Calibration	50	1.0	456	2.2×10^{-3}
	150	2.0	104	1.92×10^{-2}
	250	2.0	44	4.55×10^{-2}
	150	2.0	104	1.92×10^{-2}
	50	1.0	364	2.75×10^{-3}
2. Monomethylhydrazine Run	50	4.0×10^{-3}	115	3.47×10^{-5}
	150	4.0×10^{-3}	Leak Plugged	

TABLE 27

APOLLO TIE LEAK TEST DATA

Dates: 5/23-5/28/68

Leak Description: Glass Leak No.	Helium Flow Rate at 50 psig
4	2.49×10^{-4}
6	5.8×10^{-4}
10	5.8×10^{-4}

Comments: The above leaks all plugged during the attempt to measure an initial monomethylhydrazine flow rate.

TABLE 29

APOLLO TIE LEAK TEST DATA

Dates: 6/24/68 - 6/25/68

Leak Description: AN Flared Fitting, with Lightly Torqued Plug, nominal 10^{-3} cc/sec Helium Leak

Fluid: Aerozine-50

Comments: Room temperature varied between 75 and 84°F during test.

Test Description	Pressure, psig	Volume, cc	Time, sec	Leak Rate, cc/sec
1. Helium Calibration Before Test	50	0.40	387	1.03×10^{-3}
	150	0.60	86	6.99×10^{-3}
	250	0.60	31.5	1.90×10^{-2}
	150	0.60	81.3	7.39×10^{-3}
	50	0.60	509	1.18×10^{-3}
	50	0.60	523	1.14×10^{-3}

2. Fuel Leak Rate Test	Elapsed Time, min.	Action	Pressure psig	Sample No.	Leak Rate, cc/sec
6/24/68	0	Fill & pressurize to	50		
	10	Faint odor, sample at	50	2	2.21×10^{-9}
	18	Sample at	50	3	4.35×10^{-9}
	42	Faint odor, sample at	50	4	7.01×10^{-9}
	69	Odor stronger, sample at	"	5	7.50×10^{-7}
	90	Sample at	"	6	5.55×10^{-7}
	120	"	"	7	3.60×10^{-7}
	140	Odor weaker, sample at	"	8	2.74×10^{-7}
	170	Sample at	"	9	3.40×10^{-7}
	200	"	"	10	6.08×10^{-7}
	230	"	"	11	6.89×10^{-7}
	260	"	"	12	4.85×10^{-7}
	290	"	"	13	5.35×10^{-7}
	320	Sample at	50	14	5.72×10^{-7}
	Leave filled and pressurized overnight at 50 psig.				
6/25/68	1305	Sample at	50	15	1.66×10^{-6}
	1335	Sample at	50	16	1.50×10^{-6}
	1350	"	50	17	1.75×10^{-6}

TABLE 29 (Continued)

	Elapsed Time, min.	Action	Pressure, psig	Sample No.	Leak Rate, cc/sec
	1370	Sample at	150	18	1.58×10^{-6}
	1390	Sample at	150	19	2.72×10^{-6}
	1425	"	250	20	8.00×10^{-6}
	1455	"	250	21	7.75×10^{-6}
	1500	"	150	22	3.70×10^{-6}
	1530	"	150	23	4.16×10^{-6}

	Pressure, psig	Volume, cc	Time, sec	Leak Rate, cc/sec
3. Helium Calibration After Test	250	5.00	127	3.93×10^{-2}
	150	5.00	301	1.65×10^{-2}
	50	0.60	302	1.98×10^{-3}

TABLE 30

APOLLO TIE LEAK TEST DATA

Dates: 6/26/68 - 6/27/68

Leak Description: AN Flared Fitting, with Lightly Torqued Plug, nominal 5×10^{-3} cc/sec Helium Leak

Fluid: Aerozine-50

Laboratory Temperature: 74-76°F

Test Description	Pressure, psig	Volume, cc	Time, sec	Leak Rate, cc/sec
1. Helium Calibration Before Test				
6/26/68	50	0.60	106	5.65×10^{-3}
	150	5.00	95	5.25×10^{-2}
	250	5.00	38.5	1.30×10^{-1}
	250	5.00	38.5	1.30×10^{-1}
	150	5.00	95	5.25×10^{-2}
	50	1.00	176	5.68×10^{-3}

2. Fuel Leak Rate Test	Elapsed Time, min.	Action	Pressure, psig	Sample No.	Leak Rate, cc/sec
6/26/68	0	Fill & pressurize to	50		
	0	Sample at	50	1	3.82×10^{-7}
	20	"	50	2	3.43×10^{-6}
	40	"	50	3	2.82×10^{-6}
	60	"	50	4	3.16×10^{-6}
	90	"	50	5	3.38×10^{-6}
	120	"	50	6	4.77×10^{-6}
	150	"	50	7	4.05×10^{-6}
	180	"	50	8	4.91×10^{-6}
	240	"	50	9	3.75×10^{-6}
	300	"	50	10	6.69×10^{-6}
	360	"	50	11	4.77×10^{-6}
	420	"	50	12	4.60×10^{-6}
6/27/68	1520	"	50	13	1.59×10^{-6}
	1540	"	50	14	1.44×10^{-6}
	1590	"	150	15	4.04×10^{-6}
	1600	"	150	16	3.97×10^{-6}
	1700	"	250	17	2.56×10^{-5}
	1710	"	250	18	2.60×10^{-5}
	1740	"	150	19	1.18×10^{-5}

TABLE 30 (Continued)

Elapsed Time, min.	Action	Pressure, psig	Sample No.	Leak Rate, cc/sec
1750	Sample at	150	20	1.14×10^{-5}
1780	"	50	21	4.93×10^{-6}
1790	Sample at	50	22	4.77×10^{-6}

	Pressure, psig	Volume, cc	Time, sec	Leak Rate, cc/sec
3. Helium Calibration After Test	250	5.00	178	2.81×10^{-2}
	150	5.00	428	1.17×10^{-2}
	50	0.60	514	1.17×10^{-3}

APOLLO TIE LEAK TEST DATA

Date: 6/21/68

Leak Description: AN Flared Fitting, with Lightly Torqued Plug, nominal 10^{-2} cc/sec Helium Leak

Fluid: Aerozine-50

Comments: Room temperature = 72°F.

Test Description	Pressure, psig	Volume, cc	Time, sec	Leak Rate, cc/sec
1. Helium Calibration Before Test	50	0.60	71	8.45×10^{-3}
	150	5.00	56.5	8.85×10^{-2}
	250	5.00	21.9	2.28×10^{-1}
	250	5.00	21.8	2.29×10^{-1}
	150	5.00	54.0	9.25×10^{-2}
	50	0.60	66.0	9.10×10^{-3}
	50	0.60	68.5	8.75×10^{-3}

2. Fuel Leak Rate Test	Elapsed Time, min	Action	Pressure, psig	Sample No.	Leak Rate, cc/sec
	0	Fill & pressurize to	50	1	$< 4 \times 10^{-8}$
	6	Faint odor, sample at	50	2	1.31×10^{-6}
	18	Strong odor, "	50	3	2.89×10^{-6}
	27	Sample at	50	4	5.65×10^{-6}
	38	"	50	5	9.00×10^{-5}
	55	"	50	6	1.37×10^{-5}
	70	"	50	7	2.60×10^{-5}
	95	"	50	8	1.99×10^{-5}
	120	"	50	9	3.59×10^{-5}
	160	"	50	10	2.19×10^{-5}
	220	"	50	11	2.13×10^{-5}
	250	Raise pressure to	150, leak drips fluid.		

3. Helium Calibration After Test	Pressure, psig	Volume, cc	Time, sec	Leak Rate, cc/sec
	50	0.6	60.0	1.00×10^{-2}
	150	5.0	58.1	8.60×10^{-2}
	250	5.0	235	2.12×10^{-1}

TABLE 32

APOLLO TIE LEAK TEST DATA

Date: 6/3/68

Leak Description: Glass Leak No. 1, nominal 10^{-2} cc/sec Helium

Fluid: Hydrazine-UDMH 50%-50%

Test Description	Pressure, psig	Volume, cc	Time, sec.	Leak Rate cc/sec
1. Helium Calibration Before Run	250	5.0	27.1	1.85×10^{-1}
	250	5.0	26.9	1.86×10^{-1}
	250	5.0	27.1	1.84×10^{-2}
	150	5.0	63.7	7.86×10^{-2}
	150	5.0	63.6	7.88×10^{-2}
	50	2.0	194.5	1.03×10^{-2}
	50	2.0	193.8	1.03×10^{-2}
	150	5.0	63.5	7.88×10^{-1}
	250	5.0	26.9	$1.86 \times 10^{}$
2. Fuel Run	50	5.0×10^{-3}	37.5	1.33×10^{-4}
	150	7.0×10^{-3}	16.6	4.22×10^{-4}
	250	7.0×10^{-3}	10.5	$6.67 \times 10^{}$
3. Helium Leak Rate After Run	250	5.0	27.6	1.81×10^{-1}
	250	5.0	27.5	1.82×10^{-2}
	155	5.0	63.0	7.94×10^{-2}
	150	5.0	65.0	7.70×10^{-3}
	50	2.0	202.4	$9.87 \times 10^{}$
4. Fuel Run	250	7.0×10^{-3}	12.9	5.42×10^{-4}

Leak may be plugging - discard point.

TABLE 33
APOLLO TIE LEAK TEST DATA

Date: 6/3/68

Leak Description: Glass Leak No. 4, nominal 10^{-3} cc/sec Helium Leak

Fluid: Hydrazine-UDMH

Test Description	Pressure, psig	Volume, cc	Time, sec.	Leak Rate, cc/sec
1. Helium Calibration Before Run	250	1.0	68.5	1.46×10^{-2}
	150	1.0	184.0	5.44×10^{-3}
	50	0.4	493.0	8.12×10^{-4}
2. Fuel Run	240	6.0×10^{-3}	128.0	4.68×10^{-5}
	146	6.0×10^{-3}	203.0	2.96×10^{-5}
	50	6.0×10^{-3}	635.0	9.45×10^{-6}
3. Helium Leak Rate After Run	250	1.0	69.5	1.44×10^{-2}
	150	1.0	188.0	5.32×10^{-3}
	50	0.2	255.0	7.85×10^{-4}

Date: 6/4/68

Leak Description: Glass Leak No. 5, nominal 5×10^{-4} cc/sec Helium Leak

Fluid: Hydrazine-UDMH

Test Description	Pressure, psig	Volume, cc	Time, sec.	Leak Rate, cc/sec
1. Helium Calibration Before Run	250	1.0	126.2	7.93×10^{-3}
	150	1.0	361.0(?)	2.77×10^{-3}
	250	1.0	124.0	8.06×10^{-3}
	150	0.6	184.0	3.26×10^{-3}
	50	0.2	366.0	5.47×10^{-4}
2. Fuel Run	250	4.0×10^{-3}	151.0	2.65×10^{-5}
	150	4.0×10^{-3}	250.0	1.60×10^{-5}
	50	4.0×10^{-3}	Leak Plugged	

TABLE 34
APOLLO TIE LEAK TEST DATA

Date: 6/6/68

Leak Description: Glass Leak No. 7, nominal 10^{-5} cc/sec Helium Leak

Fluid: Hydrazine-UDMH

Test Description	Pressure, psig	Volume, cc	Time, sec	Leak Rate, cc/sec
1. Helium Calibration Before Run	250	0.20	380.0	5.26×10^{-4}
	150	0.10	490.0	2.04×10^{-4}
	50	0.09	2352.0	3.83×10^{-5}
2. Fuel Run	250	2.0×10^{-3}	1200.0	1.67×10^{-6}
	150	4.0×10^{-3}	3420.0	1.17×10^{-6}
	60	2.0×10^{-3}	5110.0	3.93×10^{-7}
3. Helium Calibration After Run	260	0.10	214.0	4.67×10^{-4}
	155	0.50	273.0	1.83×10^{-4}
	50	0.01	284.0	3.52×10^{-5}

Date: 6/10/68

Leak Description: Glass Leak No. 9, nominal 10^{-4} cc/sec Helium Leak

Fluid: Hydrazine-UDMH

Test Description	Pressure, psig	Volume, cc	Time, sec.	Leak Rate, cc/sec
1. Helium Calibration Before Test	255	1.0	191.0	5.24×10^{-3}
	155	1.0	487.0	2.06×10^{-3}
	55	0.80	2261.0	3.54×10^{-4}
2. Fuel Leak Rate	250	5.0×10^{-3}	253.0	1.97×10^{-5}
	150	4.0×10^{-3}	341.0	1.18×10^{-5}
	50	4.0×10^{-3}	Leak Plugged	

TABLE 35

APOLLO TIE LEAK TEST DATA

Dates: 5/3/68-6/10/68

Leak Description	Glass Leak No.	Helium Flow Rate at 50 psig, cc/sec	Hydrazine-UDMH Flow Rate, cc/sec
	2	7.95×10^{-4}	9.8×10^{-6} (50 psig)
	3	3.11×10^{-4}	-
	6	2.31×10^{-5}	1.01×10^{-6} (250 psig)
	8	4.17×10^{-4} (at 60 psig)	-

Comments: All of these leaks plugged during hydrazine-UDMH testing, numbers 3 and 8 during the first measurement, and numbers 2 and 6 during the second measurement.

TABLE 37
APOLLO TIE LEAK TEST DATA

Date: 5/10/68-5/13/68, 5/21/68

Leak Number 2-1

Description: Glass capillary, nominal 10^{-1} cc/sec helium leak.

Fluids: 62% Glycol/Water, filtered through 0.45 micron filter. Also Type II Water/Glycol and Distilled Water, so filtered.

	Test Description	Pressure, psig	Volume, cc	Time, sec	Flow Rate, cc/sec
1.	Helium Calibration Prior to Run	30	5.00	73	6.85×10^{-2}
		60	10.00	79.5	1.26×10^{-1}
		90	10.00	41.5	2.41×10^{-1}
		30	6.00	90	6.66×10^{-2}
		60	10.00	63.5	1.57×10^{-1}
2.	62% Glycol/Water	60	5.0×10^{-3}	14.9	3.36×10^{-4}
		90	10.0×10^{-3}	20.3	4.94×10^{-4}
		30	5.0×10^{-3}	33.5	1.49×10^{-4}
		60	10.0×10^{-3}	36.6	2.73×10^{-4}
3.	Helium Calibration After Run	60	2.00	14.8	1.35×10^{-1}
		30	2.00	36.3	5.52×10^{-2}
		90	10.00	38.8	2.58×10^{-1}
4.	Helium Recalibration, One Week Later	30	6.0	140	4.28×10^{-2}
		60	10.0	102	9.80×10^{-2}
		90	10.0	54.5	1.83×10^{-1}
5.	Rinse Leak with Distilled Water, Recalibrate with Helium	90	8.0	38.5	2.08×10^{-1}
		60	5.0	33.0	1.52×10^{-1}
		30	1.0	19.5	5.12×10^{-2}

TABLE 37, Continued

Leak Number 2-1 Continued:

Test Description	Pressure, psig	Volume, cc	Time, sec.	Flow Rate, cc/sec
6. Distilled Water	30	2.0×10^{-2}	22.5	8.9×10^{-4}
	60	2.0×10^{-2}	12.2	1.64×10^{-3}
	90	3.0×10^{-2}	13.0	2.31×10^{-3}
7. Recalibrate with Helium	90	5.0	21	2.38×10^{-1}
	60	5.0	33	1.52×10^{-1}
	30	2.0	34.5	5.80×10^{-2}
8. Water-Glycol Type II	30	1.0×10^{-2}	59.5	1.68×10^{-4}
9. Helium	30	2.0	40.8	4.93×10^{-2}
10. Water-Glycol Type II	60	1.0×10^{-2}	Leak Plugged	
11. Helium, After Cleaning Leak	60	1.6	22.5	7.1×10^{-2}
	60	2.0	25.7	7.8×10^{-2}

TABLE 33

APOLLO TIE LEAK TEST DATA

Date: 5/14/68

Leak Number: 1

Description: Glass capillary, nominal 10^{-2} cc/sec helium leak.

Fluids: 62% Glycol-Water, Type II Water-Glycol; Distilled Water

Test Description	Pressure, psig	Volume, cc	Time, sec	Flow Rate, cc/sec
1. Helium Calibration Before Run	30	1.00	155	6.46×10^{-3}
	60	1.00	48	2.08×10^{-2}
	90	2.00	52.2	3.91×10^{-2}
2. 62% Glycol-Water	60	5.0×10^{-3}	111	4.53×10^{-5}
	30	2.0×10^{-3}	95	2.12×10^{-5}
	90	5.0×10^{-3}	66	7.57×10^{-5}
3. Helium Calibration After 62% Water-Glycol Run	90	2.00	54	3.71×10^{-2}
	60	1.00	53	1.89×10^{-2}
	30	0.60	96.6	6.21×10^{-3}
4. Distilled Water	30	10.0×10^{-3}	111.3	9.05×10^{-5}
	90	10.0×10^{-3}	36.2	2.76×10^{-4}
	60	10.0×10^{-3}	58 0	1.73×10^{-4}
	30	5.0×10^{-3}	60.0	8.34×10^{-5}
5. Type II Water-Glycol	30	5.0×10^{-3}	327.5	1.53×10^{-5}
	60	5.0×10^{-3}	147.8	3.39×10^{-5}
	90	Leak plugged, ending test.		

TABLE 39
APOLLO TIE LEAK TEST DATA

Date: 5/14/68, 5/22/68

Leak Number: 3-1

Description: Glass capillary, nominal 10^{-3} cc/sec helium leak.

Fluid: 62% Glycol/Water, filtered th rough 0.45 micron filter. Also Type II Water/Glycol and Distilled Water filtered through 0.45 micron filter.

Test Description	Pressure, psig	Volume, cc	Time, sec	Flow Rate, cc/sec
1. Helium Calibration Before Run	90	1.00	203	4.93×10^{-3}
	59	0.60	258	2.32×10^{-3}
	29	0.20	267	7.49×10^{-4}
2. 62% Glycol-Water	30	2.0×10^{-3}	961	2.08×10^{-6}
	60	1.0×10^{-3}	249	4.02×10^{-6}
	90	1.0×10^{-3}	155	6.46×10^{-6}
	30	0.5×10^{-3}	262	1.91×10^{-6}
3. Helium Calibration After Run	30	0.20	275	7.27×10^{-4}
	60	0.80	343	2.34×10^{-3}
	90	1.00	225	4.44×10^{-3}
4. Helium Calibration, One Week Later	30	0.6	1053	5.70×10^{-4}
	60	0.4	256	1.56×10^{-3}
	90	0.8	259	3.09×10^{-3}
5. Distilled Water	90	2.0×10^{-3}	72	2.77×10^{-5}
	60	1.0×10^{-3}	49.2	2.03×10^{-5}
	30	1.0×10^{-3}	109.5	9.13×10^{-6}
	90	2.0×10^{-3}	66.7	3.00×10^{-5}
	60	1.0×10^{-3}	48.8	2.05×10^{-5}
	30	1.0×10^{-3}	105.7	9.46×10^{-6}
6. Helium Calibration, Following Water Run	90	0.4	553	7.23×10^{-4}
	60	0.6	283	2.12×10^{-3}
	90	1.0	237	4.23×10^{-3}
7. Type II Water-Glycol	90	1.0×10^{-3}	138	5.31×10^{-6}
	60	1.0×10^{-3}	352	2.84×10^{-6}
	30	1.0×10^{-3}	Leak Plugged	

THE BOEING COMPANY

TABLE 40
APOLLO TIE LEAK TEST DATA

Dates: 5/23/68-5/24/68

Leak Description: Glass Capillary, nominal 10^{-4} cc/sec Helium

Fluids: Type II water-glycol, 62% glycol-water, and distilled water, all filtered through a 0.45 micron filter.

Comments: Helium calibration carried out by water displacement in a 50 microliter Hamilton syringe.

Test Description		Pressure, psig	Volume, cc x 10^{-3}	Time, sec.	Flow Rate cc/sec.
1. Helium Calibration, Before Run		30	20.0	101	1.97×10^{-4}
		60	30.0	45.5	6.59×10^{-4}
		90	30.0	23.0	1.31×10^{-3}
		90	30.0	23.2	1.29×10^{-3}
		60	20.0	31.7	6.32×10^{-4}
		30	20.0	94.5	2.12×10^{-4}
2. Distilled Water Run -	Water	90	2.0	236	8.50×10^{-6}
	Helium	90	30.0	31.4	9.56×10^{-4}
	Water	60	1.0	Stopwatch Failed	
	Helium	60	30.0	80.5	3.73×10^{-4}
	Helium	90	30.0	32.7	9.17×10^{-4}
	Water	60	1.0	255	3.93×10^{-6}
	Helium	60	30.0	61.0	4.92×10^{-4}
	Helium	90	35.0	35.2	9.95×10^{-4}
	Water	30	1.0	420	2.38×10^{-6}
	Helium	30	30.0	186	1.62×10^{-4}
	Helium	60	30.0	58.5	5.14×10^{-4}
	Helium	90	30.0	30.4	9.88×10^{-4}
	Water	90	2.0	298	6.71×10^{-6}
	Helium	90	30.0	30	1.0×10^{-3}
3. 62% Glycol-Water					
	W/G	90	1.0	613	1.63×10^{-6}
	He	90	30.0	31.8	9.45×10^{-3}
	W/G	60	1.0	930	1.07×10^{-6}
	He	90	30.0	29.8	1.01×10^{-3}
	W/G	30	1.0	2018	4.96×10^{-7}
	He	30	30.0	167.3	1.79×10^{-4}
	W/G	90	1.0	615	1.63×10^{-6}

TABLE 10 (Continued)

Test Description		Pressure, psig	Volume, cc x 10^{-3}	Time, sec.	Flow Rate, cc/sec.
4. Helium Calibration, following 62% Glycol/Water		90	30.0	31.4	9.55×10^{-4}
		60	30.0	62.1	4.84×10^{-4}
		30	30.0	207	1.45×10^{-4}
5. Type II Water/Glycol	W/G	90	1.0	1137	8.81×10^{-7}
	He	90	32.0	36.5	8.76×10^{-4}
	He	60	30.0	74.4	4.03×10^{-4}
	W/G	60	1.0	Leak Plugged	

TABLE 41
APOLLO TIE LEAK TEST DATA

Date: 4/4/68

Leak Description: Glass Leak No. 4, nominal 1 cc/sec Helium Leak

Fluid: Distilled Water

Comments: Leak rate measurement by weighing expelled water.

Test Description	Pressure, psig	Wt. Collected Mg	Vol. Collected cc	Time, sec.	Leak Rate, cc/sec
1. Helium Calibration Before Test	30		25.0	10.5	2.38
	30		25.0	10.4	2.40
	60		60.0	13.8	4.35
	60		80.0	18.5	4.32
	90		80.0	12.5	6.40
	90		100	15.9	6.28
	90		100	16.0	6.25
2. Water Leak Rate	90	830	0.830	15.0	5.53×10^{-2}
	60	885	0.885	20.0	4.42×10^{-2}
(Probably plugged)	30	242	0.242	56.4	4.16×10^{-3}
	60	104	0.104	11.7	8.90×10^{-3}
	90	1103	1.103	20.2	5.46×10^{-2}
	60	1239	1.239	39.1	3.16×10^{-2}
	30	610	0.610	30.0	2.03×10^{-2}
	30	457	0.457	23.1	1.98×10^{-2}
	60	940	0.940	30.0	3.13×10^{-2}
3. Helium Calibration After Test	60		80.0	23.8	3.36
	60		80.0	24.0	3.33
	60		40.0	13.1	3.05
	60		100	32.0	3 13
	90		100	21.3	4.69
	90		100	21.1	4.73
	30		90.0	49.5	1.82
	30		100	54.7	1.83

TABLE 42

APOLLO TIE LEAK TEST DATA

Date: 4/9/68

Leak Number: 12

Description: Glass Capillary, nominal 10^{-3} cc/sec helium leak.

Fluid: Distilled Water

Test Description	Pressure, psig	Volume, cc	Time, sec	Flow Rate, cc/sec
1. Helium Calibration Before Run	90	2.00	159	1.26×10^{-2}
	60	2.00	303	6.62×10^{-3}
	30	1.00	425	2.36×10^{-3}
2. Distilled Water	30	5.0×10^{-3}	228	2.19×10^{-5}
	60	4.7×10^{-3}	136	3.46×10^{-5}
	90	7.15×10^{-3}	Leak Plugged During Test	

TABLE 13
APOLLO TIE LEAK TEST DATA

Date: 4/10/68

Leak Number: 16

Description: Glass Capillary, nominal 10^{-3} cc/sec helium leak.

Fluid: Distilled Water

Test Description	Pressure, psig	Volume, cc	Time, sec	Flow Rate, cc/sec
1. Helium Calibration Before Test	30	1.00	573	1.75×10^{-3}
	60	1.00	201	4.97×10^{-3}
	90	2.00	210	9.54×10^{-3}
2. Distilled Water	90	2.0×10^{-3}	43.8	4.56×10^{-5}
	90	2.0×10^{-3}	43.7	4.55×10^{-5}
	60	Leak Plugged During Run		
3 Cleaned out leak thoroughly.				
4. Distilled Water	60	2.0×10^{-3}	114	1.74×10^{-5}
5. Helium Calibration After Cleaning	60	0.80	250	3.2×10^{-3}
	90	1.00	153	6.60×10^{-3}
	30	0.40	352	1.14×10^{-3}
6. Distilled Water	30	2.0×10^{-3}	218	9.17×10^{-6}
	90	Leak Plugged Completely		

TABLE 44

APOLLO TIE LEAK TEST DATA

Date: 3/28/68

Leak Description: Glass Leak No. 6, nominal 1 cc/sec of Helium.

Fluid: Type II Water/Glycol, contains inhibitor.

Comments: Liquid leak rate measured by collecting and weighing expelled solution.

Test Description	Pressure psig	Weight Collected Mgm.	Volume Collected cc	Time, sec	Leak Rate, cc/sec
1. Helium Calibration Before Test	30		80.0	98.0	0.816
	60		50.0	36.0	1.39
	90		40.0	18.2	2.20
	90		80.0	35.7	2.24
2. Type II Water/Glycol Leak	90	625	0.579	120	4.82×10^{-3}
	60	542	0.503	176	2.86×10^{-3}
	30	309	0.238	295	9.7×10^{-4}
	30	337	0.312	465	6.71×10^{-4}
	30	1330	1.232	811	1.52×10^{-4}
	60	379	0.351	124	2.86×10^{-3}
	90	279	0.258	67.3	3.84×10^{-3}
	90	1249	1.158	242	4.78×10^{-3}
	30	507	0.470	309	1.52×10^{-3}
	60	985	0.912	301	3.03×10^{-3}
3. Helium Calibration After Test	60		70.0	56.2	1.24
	90		60.0	32.3	1.86
	30		60.0	104.5	0.574

TABLE 15
APOLLO TIE LEAK TEST DATA

Dates: 3/22/68-3/26/68

Leak Description: Glass Leak No. 1, Nominal 10^{-1} cc/sec of Helium

Fluid: Type II Water/Glycol, contains inhibitor.

Comments: Fluid leak rate determined by collecting expelled droplets in flasks and weighing.

Test Description	Pressure, psig	Volume, cc	Time, sec	Leak Rate, cc/sec
1. Helium Calibration Before Test	30	10.0	160	6.25×10^{-2}
	50	10.0	77.2	1.29×10^{-1}
	70	10.0	44.5	2.24×10^{-1}
	90	10.0	29.9	3.34×10^{-1}
	30	10.0	168.3	5.94×10^{-2}
	50	10.0	75.0	1.33×10^{-1}
	70	20.0	88.9	2.25×10^{-1}
	15	5.0	207.8	2.40×10^{-2}

	Pressure, psig	Flow Time, sec.	Weight Collected Mgm	Volume Collected cc	Leak Rate, cc/sec
2. Type II Water/Glycol Leak	30	2170	205	0.189	8.71×10^{-5}
	60	2634	247	0.228	8.67×10^{-5}
	90	173.2	57	0.0525	3.04×10^{-4}
	90	355	114	0.106	2.97×10^{-4}
	60	703	146	0.134	1.91×10^{-4}
	60	441	88	0.081	1.84×10^{-4}

Leak broken before helium leak rate could be rechecked.

TABLE 46
APOLLO TIE LEAK TEST DATA

Dates: 4/3/68-4/8/68

Leak Description: Glass Leak No. 11, nominal 10^{-3} cc/sec helium leak.

Fluid: Type II Water-Glycol, inhibited.

Comments: Liquid leak rate measured by washing tip of leak with distilled water before and after time period, collecting final washings in a volumetric flask, and analyzing chemically for glycol content.

Test Description	Pressure, psig	Glycol Collected Mg	Volume Collected cc	Time, sec	Leak Rate, cc/sec
1. Helium Calibration Before Run 4/3/68	90		0.40	25.6	1.56×10^{-2}
	90		1.00	60.8	1.64×10^{-2}
	60		2.0	238	8.40×10^{-3}
	30		1.0	353	2.84×10^{-3}
2. Type II Water-Glycol Leak Rate 4/3/68	30	0.17	2.5×10^{-4}	600	4.1×10^{-7}
	60	0.23	3.4×10^{-4}	600	5.7×10^{-7}
	90	0.26	3.7×10^{-4}	600	6.3×10^{-7}
		Cleaned out leak.			
4/3/68	90	<0.05		600	$<1 \times 10^{-7}$
	60	<0.05		600	$<1 \times 10^{-7}$
	30	<0.05		600	$<1 \times 10^{-7}$
		Cleaned out leak again.			
4/3/68	60	5.35	7.4×10^{-3}	600	1.23×10^{-5}
	60	5.67	7.8×10^{-3}	600	1.30×10^{-5}
	30	2.40	3.3×10^{-3}	600	5.50×10^{-6}
4/4/68	90	0.670	9.2×10^{-4}	600	1.54×10^{-6}
	60	0.065	9.0×10^{-5}	600	1.5×10^{-7}
	30	<0.05		600	$<1 \times 10^{-7}$
4/8/68		Cleaned leak with nitric acid flush.			
3. Helium Calibration After Run 4/8/68	90		2.0	1045	1.91×10^{-3}
	60		2.0	1860	1.08×10^{-3}
	30		0.6	1676	3.58×10^{-4}

TABLE 47

APOLLO TIE LEAK TEST DATA

Date: 6/13/68

Leak Description: Glass Leak, nominal 10^{-1} cc/sec Helium

Fluid: 35-percent Glycol-Water

Test Description	Pressure, psig	Volume, cc	Time, sec.	Leak Rate cc/sec
1. Helium Calibration Before Run	30	1.0	23.9	4.19×10^{-2}
	60	8.0	48.8	1.64×10^{-1}
	90	10.0	30.9	3.24×10^{-1}
2. Water/Glycol	90	5.0×10^{-3}	4.4	1.13×10^{-3}
	90	10.0×10^{-3}	8.7	1.15×10^{-3}
	60	10.0×10^{-3}	12.1	8.27×10^{-4}
	60	10.0×10^{-3}	12.1	8.27×10^{-4}
	30	10.0×10^{-3}	23.6	(Fluid left on tube wall)
	30	10.0×10^{-3}	24.8	4.04×10^{-4}
	30	10.0×10^{-3}	24.6	4.06×10^{-4}
3. Helium Calibration After Run	30	4.0	51.0	7.85×10^{-2}
	60	4.0	18.9	2.12×10^{-1}
	90	10.0	28.1	3.56×10^{-1}
	60	10.0	48.6	2.06×10^{-1}
	30	10.0	131.0	7.64×10^{-2}

TABLE 48
APOLLO TIE LEAK TEST DATA

Date: 6/11/68, 6/13/68

Leak Description: Glass Leak, nominal 10^{-2} cc/sec Helium Leak

Fluid: 35-percent Glycol-Water

Test Description	Pressure, psig	Volume, cc	Time, sec.	Leak Rate, cc/sec
1. Helium Calibration Before Run	30	1.0	147.2	6.79×10^{-3}
	60	1.0	51.8	1.93×10^{-2}
	90	1.0	26.8	3.73×10^{-2}
2. Water/Glycol Test	90	4.0×10^{-3}	28.5	1.40×10^{-4}
	60	2.0×10^{-3}	22.8	8.78×10^{-5}
	30	2.0×10^{-3}	49.7	4.03×10^{-5}
	90	4.0×10^{-3}	60.4	Partially plugged?
3. Helium Calibration After Test	Leak Completely Plugged			
4. Helium Calibration Two Days Later	90	1.0	259.0	3.86×10^{-3}

TABLE 49
APOLLO TIE LEAK TEST DATA

Date: 6/11/68

Leak Description: Glass Leak, nominal 10^{-3} cc/sec Helium

Fluid: 35-percent Glycol-Water

Test Description	Pressure, psig	Volume, cc	Time, sec	Leak Rate, cc/sec
1. Helium Calibration Prior to Run	90	1.0	117.6	8.50×10^{-3}
	60	1.0	274.	3.65×10^{-3}
	30	0.40	324.	1.23×10^{-3}
2. Water/Glycol	30	1.0×10^{-3}	123.8	8.1×10^{-6}
	60	2.0×10^{-3}	125.3	1.59×10^{-5}
	90	2.0×10^{-3}	75.5	2.65×10^{-5}
	30	1.0×10^{-3}	121 2	8.25×10^{-6}
3. Helium Calibration After Run	30	0.40	334.	1.20×10^{-3}
	60	0.80	209.	3.83×10^{-3}
	90	0.80	105.0	7.61×10^{-3}

TABLE 50
APOLLO TIE LEAK TEST DATA

SENSITIVITY DETERMINATION FOR BENDIX MASS SPECTROMETER

Date: 4/10/68

1. Setting a Standard Leak in the 10^{-4} cc/sec Helium Range

   a. Throttled CEC Leak Detector to read 380 divisions while testing a calibration standard 1.12×10^{-6} atm-cc/sec helium leak.

   b. Torqued a smashed tubing leak until it gave a reading of 39,000 divisions at 250 psig He under same instrument parameters.

   c. Smashed tubing leak rate = $\frac{39{,}000 - 380}{380} \times 1.12 \times 10^{-6} = 1.14 \times 10^{-4}$ atm-cc/sec He at 250 psig.

2. Bendix Mass Spectrometer Response for He, H_2, N_2, O_2

   Valved the above smashed tubing leak into the Bendix, with all operating parameters and throttling valves adjusted as in the 10^{-4} and 10^{-5} cc/sec leak rate measurements for the fixed gases.

Gas	Upstream Pressure, Psia	Indicated Flight Tube Pressure, Torr 10^{-9}	Instrument Reading Divisions on 10^{-11} Scale	Response at 265 psia (265 Reading - Background)
Helium	0	2.0	14	
	265	2.5	1100	1086
Hydrogen	0	2.0	285	
	265	2.8	2000	1715
Oxygen	0	2.2	170	
	265	2.5	6300	6130
Nitrogen	0	2.1	1000	
	265	3.0	8700	7700

TABLE 50 (Continued)

3. Calculation of Bendix Sensitivity Ratios for H_2, O_2 and N_2 to He.

Gas	Viscosity, cps *	Leak Rate[1] Atm-cc/sec	Instrument Response at 265 psia Div. on 10^{-11} Scale	Instrument Sensitivity Atm-cc/sec/div. on 10^{-11} scale	Sensitivity Factor, Helium to Gas
He	0.0197	1.14×10^{-4}	1086	1.05×10^{-7}	1.00[2]
H_2	0.0089	2.52×10^{-4}	1715	1.47×10^{-7}	1.40
O_2	0.0207	1.08×10^{-4}	6130	1.77×10^{-8}	0.169
N_2	0.0178	1.26×10^{-4}	7700	1.64×10^{-8}	0.156

(1) Calculated from $Q_G = Q_{He} \frac{\eta_{He}}{\eta_G}$, assuming Poiseuille flow, and using $Q_{He} = 1.14 \times 10^{-4}$ as measured above.

(2) By definition

* Reference: D. J. Santeler, et al, "Vacuum Technology and Space Simulation", NASA SP-105 (1966).

TABLE 51
APOLLO TIE LEAK TEST DATA

Dates: 3/26/68 - 3/28/68

Leak Description: Scribed plug, nominal 10^{-2} cc/sec helium leak.

Fluids: Hydrogen, Helium, Nitrogen, Oxygen (all in gaseous state).

Comments: Volumes were measured by water displacement in a 50ml burette at room temperature (70°F) and ambient pressure. The data presented is not corrected for water vapor, nor have the volumes been converted to standard temperature and pressure.

Test Description	Upstream Pressure, psig	Volume, cc	Time, sec.	Leak Rate, cc/sec
1. Helium Leak Rate	20	1.0	222	4.51×10^{-3}
	50	1.0	63.6	1.57×10^{-2}
	109.5	5.0	96	5.21×10^{-2}
	160	10.0	111	9.0×10^{-2}
	248	10.0	60.6	1.65×10^{-1}
	895	20.0	25.5	7.85×10^{-1}
	895	20.0	24.6	8.13×10^{-1}
2. Hydrogen Leak Rate	20	1.0	109.2	9.16×10^{-3}
	20	0.5	52.8	9.48×10^{-3}
	20	0.5	55.8	8.96×10^{-3}
	50	2.0	60.6	3.30×10^{-2}
	50	2.0	60.0	3.33×10^{-2}
	120	10.0	82.2	1.22×10^{-2}
	122	10.0	82.2	1.22×10^{-2}
	160	10.0	54.9	1.83×10^{-1}
	160	10.0	55.2	1.81×10^{-1}
	160	10.0	56.5	1.77×10^{-1}
	250	10.0	30.6	3.27×10^{-1}

TABLE 51 (Continued)
APOLLO TIE LEAK TEST DATA

Dates: 3/26/68 - 3/28/68 (Continued)

Test Description	Upstream Pressure, psig	Volume, cc	Time, sec.	Leak Rate, cc/sec
3. Oxygen Leak Rate	500	10.0	48.4	2.07×10^{-1}
	900	10.0	24.0	4.17×10^{-1}
	895	15.0	34.8	4.31×10^{-1}
	895	20.0	46.5	4.30×10^{-1}
	505	10.0	45 0	$2 22 \times 10^{-1}$
	255	10.0	98.4	1.02×10^{-2}
	159	5.0	85.8	5.83×10^{-2}
	159	5.0	86.4	5.79×10^{-2}
	110	2.0	54.9	3.64×10^{-2}
	110	2.0	54.6	3.66×10^{-2}
	20	0.3	84.9	3.53×10^{-3}
	20	0.3	85.8	3.50×10^{-3}
4. Nitrogen Leak Rate	160	10.0	195	5.13×10^{-2}
	160	10.0	196.8	5.09×10^{-2}
	110	5.0	150.6	3.32×10^{-2}
	50	1 0	78.6	1.27×10^{-2}
	19.4	1 0	261.0	3.83×10^{-3}
	160	10 0	195.6	5.11×10^{-2}
	250	10.0	120.6	8.3×10^{-2}

TABLE 52
APOLLO TIE LEAK TEST DATA

Date: 4/8/68

Leak Description: Smashed tubing leak, nominal 10^{-4} cc/sec helium leak.

Fluids: Hydrogen, Helium, Nitrogen, Oxygen (all in gaseous state).

Comments: A standard helium leak of 5.7×10^{-6} atm-cc/sec gave a reading of 35 divisions above background on the 10^{-11} scale of the Bendix under the conditions of this test. The sensitivity was thus 1.63×10^{-7} atm-cc/sec of helium for 1 division on this dare.

Gas	Pressure, psia	Instrument Reading Div. on 10^{-11} Scale	Apparent Leak Rate(1) atm-cc/sec	Sensitivity Factor Helium to Test Gas	Actual Leak Rate(2) atm-cc/sec
He	0	0	-	1.00	-
	35.5	320	5.22×10^{-5}		5.22×10^{-5}
	65	700	1.14×10^{-4}		1.14×10^{-4}
	115	1,400	2.28×10^{-4}		2.28×10^{-4}
	175	3,200	5.22×10^{-4}		5.22×10^{-4}
	25	220	3.59×10^{-5}		3.59×10^{-5}
	265	6,200	1.01×10^{-3}		1.01×10^{-3}
	515	18,000	2.93×10^{-3}		2.93×10^{-3}
	915	53,000	8.64×10^{-3}		8.64×10^{-3}
H_2	0	0	-	1.40	-
	265	16,000	2.61×10^{-3}		3.65×10^{-3}
	25	450	7.33×10^{-5}		1.025×10^{-4}
	65	1,600	2.61×10^{-4}		3.65×10^{-4}
	115	4,100	6.68×10^{-4}		9.35×10^{-4}
	175	8,500	1.39×10^{-3}		1.94×10^{-3}
N_2	0	600	-	0.156	-
	25	1,500	1.47×10^{-4}		2.30×10^{-5}
	65	5,000	7.17×10^{-4}		1.12×10^{-4}
	115	11,000	1.69×10^{-3}		2.64×10^{-4}
	175	23,000	3.65×10^{-3}		5.70×10^{-4}
	265	54,000	8.70×10^{-3}		1.36×10^{-3}

TABLE 52 (Continued)

Gas	Pressure, psia	Instrument Reading Division on 10^{-11} Scale	Apparent Leak Rate(1) atm-cc/sec	Sensitivity Factor Helium to Test Gas	Actual Leak Rate(2) atm-cc/sec
O_2	0	75	-	0.169	-
	265	40,000	6.52×10^{-3}		1.10×10^{-3}
	515	100,000	1.63×10^{-2}		2.75×10^{-3}
	915	260,000	4.24×10^{-2}		7.15×10^{-3}
	175	20,000	3.26×10^{-3}		5.50×10^{-4}
	115	10,000	1.63×10^{-3}		2.75×10^{-4}
	65	3,900	6.23×10^{-4}		1.05×10^{-4}
	25	1,000	1.50×10^{-4}		2.54×10^{-5}

(1) Apparent Leak Rate = (Instrument Reading - Background Reading) $\times 1.63 \times 10^{-7}$ atm-cc/sec.

(2) Actual Leak Rate = Apparent Leak Rate x Instrument Sensitivity Factor (to convert from He to Gas).

TABLE 53
APOLLO TIE LEAK TEST DATA

Date: 4/9/68 - 4/10/68

Leak Description: Smashed tubing leak, nominal 10^{-6} cc/sec of helium.

Fluids: Hydrogen, Helium, Nitrogen, Oxygen (all in gaseous state).

Comments: A standard leak of 1.12×10^{-6} atm-cc/sec of helium gave a reading of 19 divisions above background on the 10^{-11} scale of the Bendix, under these test conditions, for a sensitivity of 5.89×10^{-8} atm-cc/sec of helium for 1 division on the 10^{-11} scale. During the nitrogen run, the instrument background varied and was remeasured for each point.

Gas	Pressure, psia	Instrument Reading Div. on 10^{-11} Scale	Apparent Leak Rate(1) atm-cc/sec	Sensitivity Factor(1) He to Test Gas	Actual Leak Rate(2) Atm-cc/sec
He	0	10	-	1.00	-
	25	20	5.9×10^{-7}		5.9×10^{-7}
	65	38	1.65×10^{-6}		1.65×10^{-6}
	115	60	2.95×10^{-6}		2.95×10^{-6}
	175	81	4.19×10^{-6}		4.19×10^{-6}
	265	130	7.08×10^{-6}		7.08×10^{-6}
	515	260	1.48×10^{-5}		1.48×10^{-5}
	915	550	3.19×10^{-5}		3.19×10^{-5}
H_2	0	680	-	1.40	-
	175	800	7.1×10^{-6}		9.95×10^{-6}
	115	760	4.72×10^{-6}		6.62×10^{-6}
	65	710	1.77×10^{-6}		2.48×10^{-6}
	265	850	1.00×10^{-5}		1.40×10^{-5}

TABLE 53 (Continued)

Gas	Pressure, psia	Instrument Reading Div. on 10^{-11} Scale	Apparent Leak Rate(1) atm–cc/sec	Sensitivity Factor(1) He to Test Gas	Actual Leak Rate(2) atm–cc/sec
N_2	0	920	-	0.156	-
	175	1200	1.65 or 1.89 x 10^{-5}	(avg. = 1.77 x 10^{-5})	2.77 x 10^{-6}
	0	890			
	115	1000	6.49 x 10^{-6}		
	0	890		(avg.=9.45 x 10^{-6})	1.48 x 10^{-6}
	115	1100	1.24 x 10^{-5}		
	0	900			
	65	980	4.72 x 10^{-6}		7.37 x 10^{-7}
	0	905			
	25	935	1.77 x 10^{-6}		2.77 x 10^{-7}
	0	920			
	265	1350	2.54 x 10^{-5}	(avg. = 2.57 x 10^{-5})	
	0	910			
	265	1350	2.60 x 10^{-5}		4.01 x 10^{-6}
O_2	0	210	-	0.169	
	175	500	1.71 x 10^{-5}		2.88 x 10^{-6}
	115	370	9.44 x 10^{-6}		1.59 x 10^{-6}
	65	310	5.9 x 10^{-6}		9.94 x 10^{-7}
	25	245	2.06 x 10^{-6}		3.47 x 10^{-7}
	265	670	2.71 x 10^{-5}		4.57 x 10^{-6}
	515	1300	6.43 x 10^{-5}		1.08 x 10^{-5}
	915	3000	1.65 x 10^{-4}		2.78 x 10^{-5}

(1) Apparent Leak Rate = (Instrument Reading - Background Reading) x 5.89 x 10^{-8} atm–cc/sec.

(2) Actual Leak Rate = Apparent Leak Rate x Instrument Sensitivity Factor (to convert from He to test gas).

APPENDIX

LABORATORY DIRECTIONS FOR CHEMICAL ANALYSIS

I. NITROGEN DIOXIDE

A. Introduction

NO_2 is determined colorimetrically by the sulfanilic acid diazotization method of Saltzman.

B. Reference

B. E. Saltzman, Anal. Chem. 26: 1949 (1954).

C. Equipment

Klett-Summerson Model 900.3 photoelectric colorimeter (or equivalent) equipped with a #54 green filter and 1/2" test tube.

D. Reagents

N-1-Naphthylethylenediamine dihydrochloride (Eastman #4835): 1.000 gm/l

Absorbing Solution: Dissolve 10.0 gm sulfanilic acid (Eastman #238) with heating in 500 ml water, add 1 liter water, add 280 ml glacial acetic acid, add 40 ml N-1-Naphthylethylenediamine dihydrochloride solution and dilute to 2 liters.

E. Standards

It has been empirically determined that 0.72 gm NO_2, added as $NaNO_2$, gives a color development equivalent to 1 gm of gaseous NO_2.

(1) 1.50 gm $NaNO_2$/l

(2) 10 ml (1)/100 ml. This gives 0.139 μgm $NO_2/\mu l$.

F. Standardization

Standardization is accomplished by diluting ml quantities of Standard (2) with absorbing solution. The resultant color development is read 15-20 minutes later against an absorbing solution blank.

The calibration curve is appended. The maximum sensitivity is 1 microgram of NO_2 in 20 ml of absorbing solution.

G. Procedure

Collect sample in 20 ml absorbing solution using small fritted glass bubblers. Bubbler efficiency falls off badly if the color becomes too dark. It is wise to run series bubblers until some feel for the solution saturation color is obtained. At moderate concentrations the bubblers are 99+% efficient.

Dilute if necessary with absorbing solution

Read color development 15-20 minutes after dilution with the Klett (#54 filter, 1/2" diameter test tube cell) against an absorbing solution blank.

Obtain micrograms NO_2 from Klett reading using standard curve.

H. Calculation

$$\text{ml } NO_2 \text{ gas/sec} = \frac{(4.9 \times 10^{-6})(\mu\text{gm } NO_2 \text{ measured})(\text{dilution factor})}{(\text{minutes sampling time})}$$

NITROGEN DIOXIDE ANALYSIS CALIBRATION CURVE

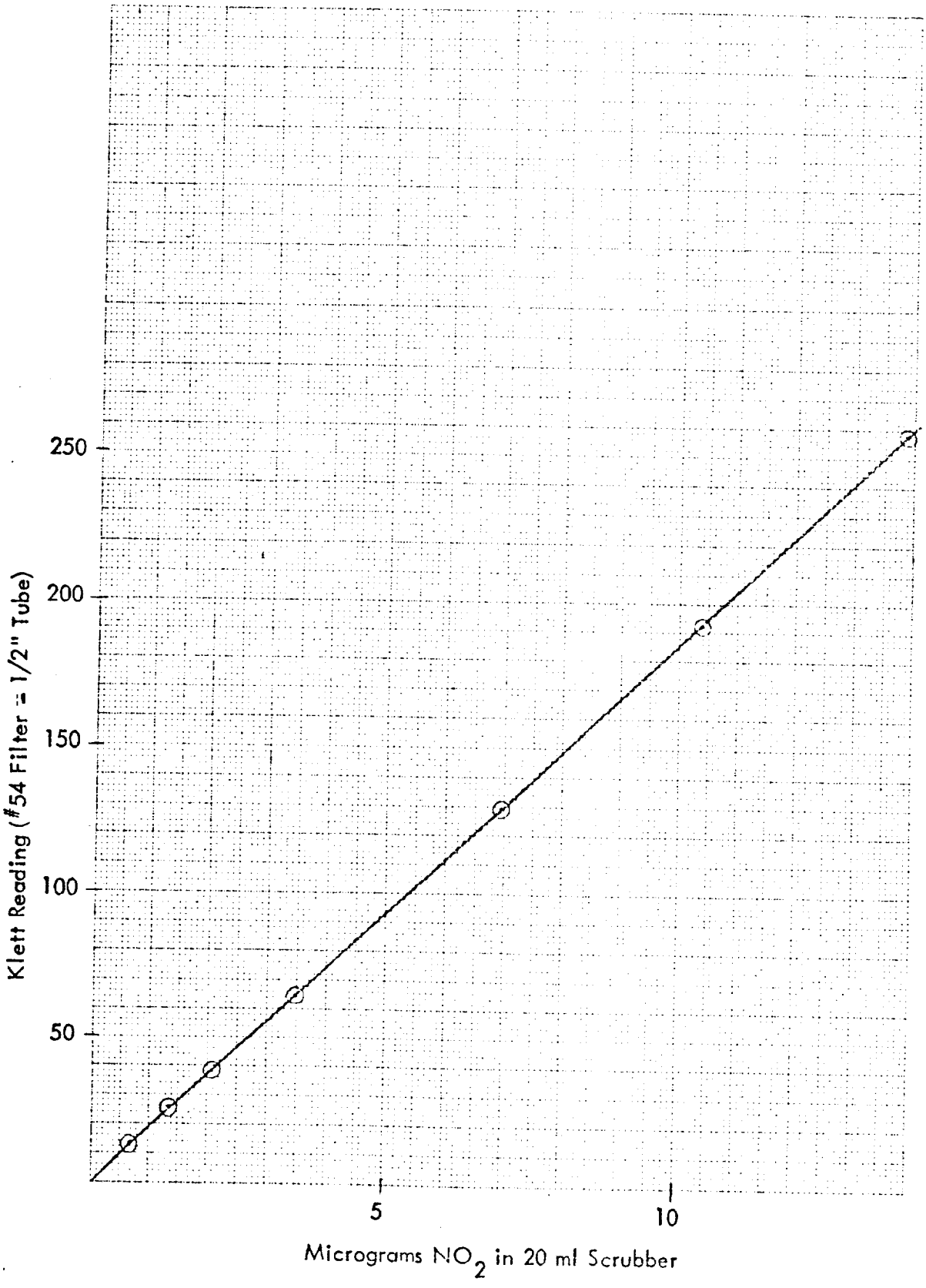

II. MONOMETHYLHYDRAZINE

A. Introduction

MMH is determined colorimetrically by its reaction with p-dimethylamino-benzaldehyde in an acid medium. The procedure is an adaptation of the Feigl spot test for hydrazine, but in this instance the reaction mechanism is not as well known and the procedure is several times less sensitive than for hydrazine.

B. Reference

F. Feigl, "Spot Tests in Inorganic Analyses, 5th Ed.", Elsevier Publishing Co., Amsterdam (1956).

C. Equipment

Klett-Summerson Model 900.3 photoelectric colorimeter (or equivalent) equipped with a #44 blue filter and 1/2" test tube.

D. Reagent

Add 2 ml concentrated hydrochloric acid to a solution of 0.40 gm p-dimethyl-aminobenzaldehyde (Eastman #95) dissolved in 20 ml ethyl alcohol (U.S.P.).

E. Standards

(1) 1 ml MMH (density 0.876) diluted to 100 ml with distilled water.

(2) 1 ml (1) diluted to 100 ml. This gives 87.6 μgm MMH/ml.

F. Standardization

To approximately 6 ml of water add Standard (2) and 2 ml Reagent and make up to 10 ml. Read at 15 minutes against a blank of 2 ml Reagent plus 8 ml water.

The calibration curve is appended. The maximum sensitivity is 5 micrograms of MMH in 20 ml of absorbing solution.

G. Procedure

Collect sample in scrubber containing 20 ml water, dilute as necessary, add 2 ml Reagent, make up to 10 ml with water, and read after 15 minutes against

a blank of 2 ml Reagent plus 8 ml water ing Klett (#44 filter and 1/2" test tube). Obtain micrograms MMH from Klett reading using standard curve.

H. Calculation

For a 20 ml sample:

$$\text{ml MMH/sec} = \frac{(3.8 \times 10^{-4})\,(\mu\text{gm MMH measured})}{(\text{min. spl. time})(\mu\text{L sample used})}$$

MONOMETHYLHYDRAZINE ANALYSIS CALIBRATION CURVE

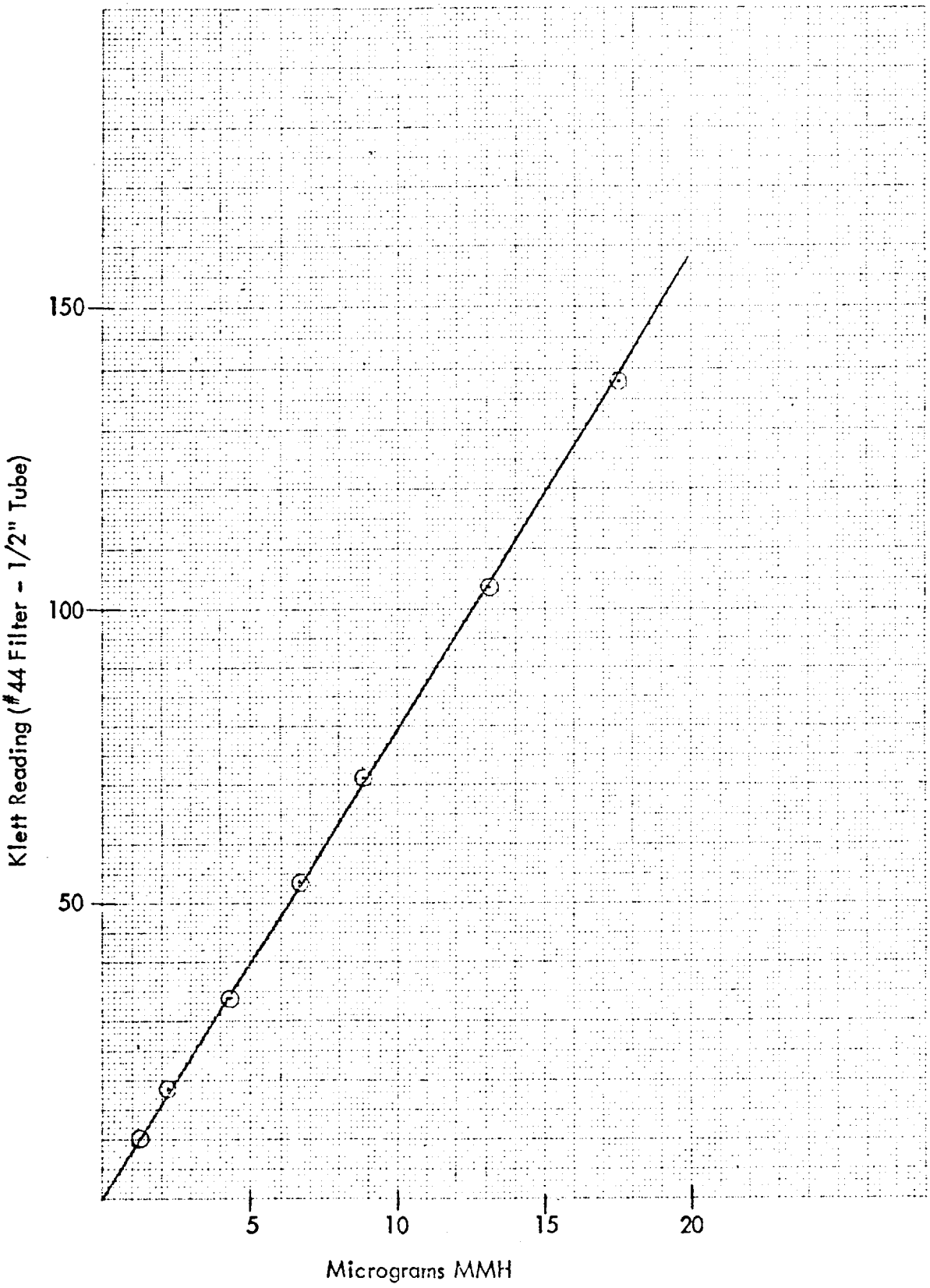

III. HYDRAZINE

A. Introduction

Hydrazine is determined colorimetrically by its reaction with p-dimethylaminobenzaldehyde in acid medium to form a deeply colored quinoidal cation. The procedure is an adaptation of the Feigl spot test.

B. Reference

F. Feigl, "Spot Tests in Inorganic Analysis, 5th Ed.", Elsevier Publishing Co., Amsterdam (1958).

C. Equipment

Klett-Summerson Model 900? photoelectric colorimeter (or equivalent) equipped with a #44 blue filter and 1/2" test tube.

D. Reagent

Add 10 ml concentrated hydrochloric acid to a solution of 2.0 gm p-dimethylaminobenzaldehyde (Eastman #95) dissolved in 100 ml ethyl alcohol (U.S.P.).

E. Standards

(1) 1 ml N_2H_4 (density 1.00) diluted to 100 ml with water.

(2) 100 μl (1) diluted to 100 ml. This gives 10 μ gm N_2H_4/ml.

F. Standardization

To approximately 6 ml of water add Standard (2) and 2 ml Reagent and make up to 10 ml. Read at 15 minutes against a blank of 2 ml Reagent plus 8 ml water.

A calibration curve is appended. The maximum sensitivity is 1.0 micrograms N_2H_4 in 20 ml of absorbing solution.

G. Procedure

Collect sample in scrubber containing 20 ml water, dilute as necessary add 2 ml Reagent, make up to 10 ml with water, and read after 15 minutes against a blank of 2 ml Reagent plus 8 ml water using Klett colorimeter (#44 filter and 1/2" test tube). Obtain micrograms N_2H_4 from Klett reading using calibration curve.

H. Calculation

For a 20 ml sample:

$$\text{ml } N_2H_4/\text{sec} = \frac{(3.3 \times 10^{-4})(\mu\text{gm } N_2H_4 \text{ measured})}{(\text{min. spl. time})(\mu\text{l sample used})}$$

To calculate Aerozine-50 leakage from hydrazine data multiply ml N_2H_4/sec by 2.17.

I. Interferences

Unsymmetrical dimethylhydrazine does not interfere when present in concentrations of up to 500 times that of hydrazine. MMH, if present, would be measured.

HYDRAZINE ANALYSIS CALIBRATION CURVE

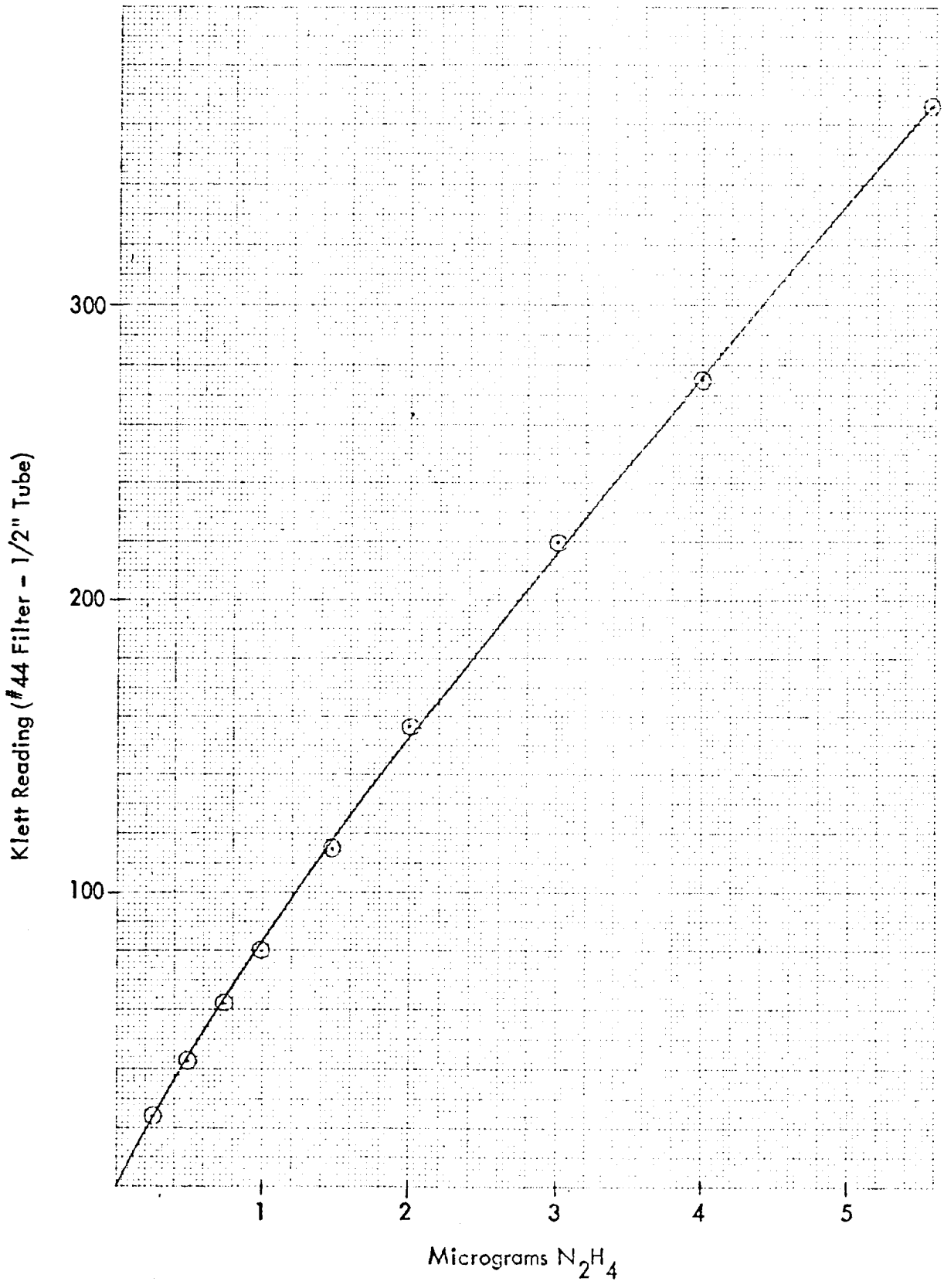

IV. ETHYLENE GLYCOL

A. Introduction

Ethylene glycol in aqueous solutions is determined colorimetrically by periodate oxidation to formaldehyde, reduction of excess oxidant with arsenous acid, and reaction of the formaldehyde with 4, 5-dihydroxy-2,7-naphthalenedisulfonic acid, disodium salt (chromotropic acid) in sulfuric acid solution to form a colored complex.

B. Reference

Belcher, "Submicro Methods of Organic Chemistry", Elsevier Publishing Co., Amsterdam, 1966.

C. Equipment

Beckman Instrument Company DK-2 Ultraviolet and Visible Spectrophotometer.

D. Reagents

1. Chromotropic Acid

   Dissolve 1.0 gm of chromotropic acid (Eastman #P230) in 100 ml of distilled water, and filter. Mix 300 ml of concentrated sulfuric acid and 150 ml of distilled water and add to above solution, and then dilute to 500 ml with concentrated sulfuric acid. Store in brown bottle for maximum of two weeks.

2. Sodium Periodate, 0.05N. Dilute 5.35 gm Reagent Grade $NaIO_4$ to 1 lt. with distilled water.

3. Arsenous Acid Solution; 0.05N. Dissolve 0.618 gm C.P. $NaAsO_2$ in 10 ml 1N NaOH, make faintly acid with H_2SO_4, and dilute to 250 ml.

E. Standards

1. Dilute 100 mg of C.P. ethylene glycol to 1000 ml in a volumetric flask. This gives 100 μgm/ml.

2. Dilute solution (1) to give concentrations of 1, 2, 5, 10 μgm/ml.

F. Standardization

Mix 5.0 ml of standard with 0.25 ml of sodium periodate solution and allow to stand 15 minutes. Add 2.0 ml of arsenous acid solution and allow to stand 15 minutes. Add 5.0 ml each of chromotropic acid solution and concentrated sulfuric acid, and heat 1 hour at 98°C. Read the absorbance at 570 mμ against a reagent blank, and plot a calibration curve.

G. Procedure

Wash the tip of the experimental leak with a jet of distilled water, collect the washings in a 100 ml volumetric flask, and dilute to the mark. Analyze 5.0 ml of the solution as described under standardization, diluting if necessary. Read the glycol concentration from the calibration curve.

H. Calculation

$$\text{Glycol Leak Rate } (\mu\text{gm/minute}) = \frac{100 \cdot (\text{glycol concentration measured}) \cdot (\text{dilution factor})}{(\text{minutes sampling time})}$$

ETHYLENE GLYCOL ANALYSIS CALIBRATION CURVE

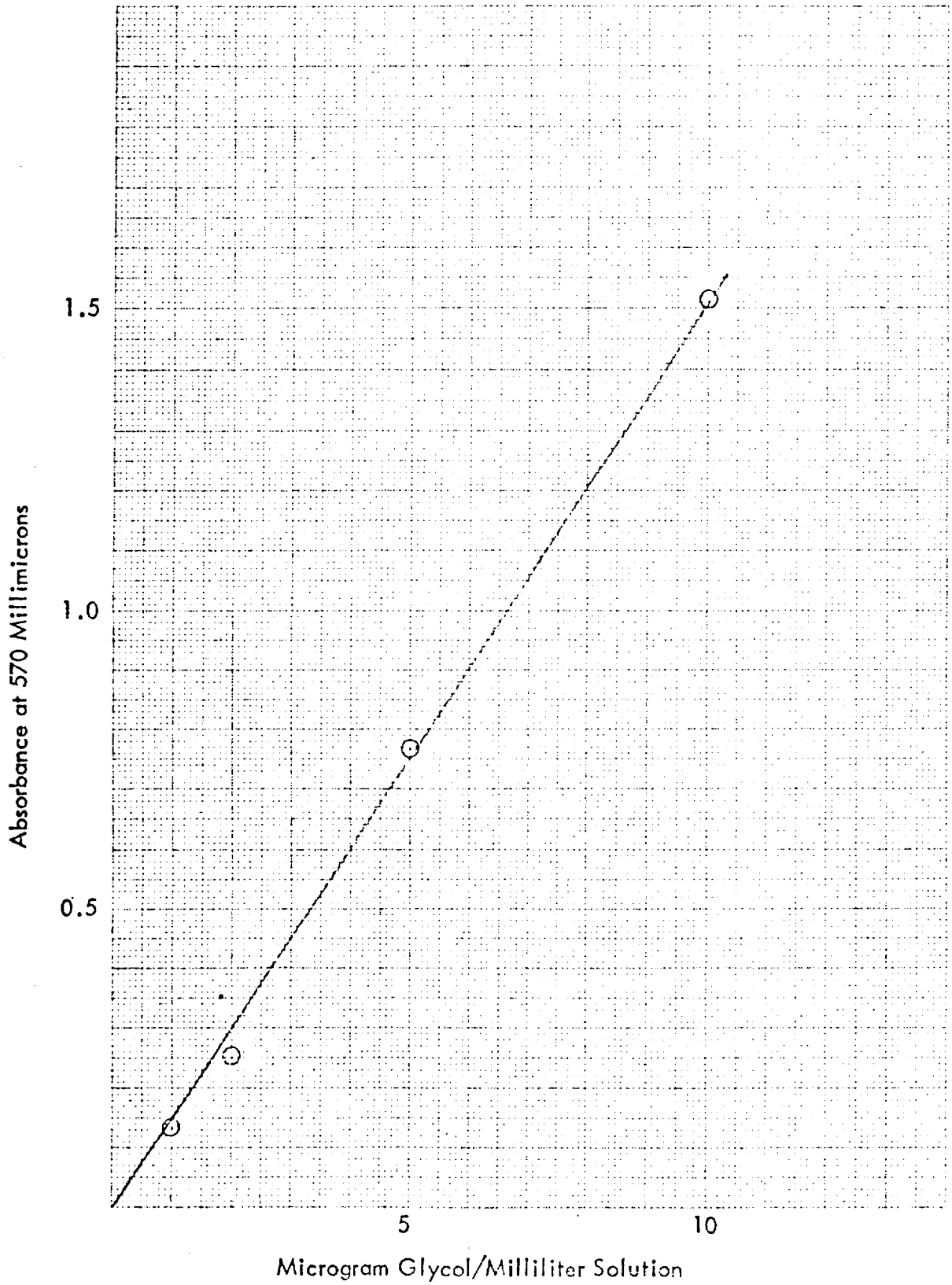

LIMITATIONS

This document is controlled by Materials & Processes, 2-7860

All revisions to this document shall be approved by the above noted organization prior to release.

ACTIVE SHEET RECORD

SHEET NUMBER	REV LTR	ADDED SHEETS				SHEET NUMBER	REV LTR	ADDED SHEETS			
		SHEET NUMBER	REV LTR	SHEET NUMBER	REV LTR			SHEET NUMBER	REV LTR	SHEET NUMBER	REV LTR
1	A					41					
2	A					42					
3						43					
4						44					
5						45					
6						46					
7						47					
8						48					
9						49					
10						50					
11						51					
12	A					52					
13	A					53					
14						54					
15						55					
16						56					
17						57					
18						58					
19						59					
20						60					
21						61					
22						62					
23						63					
24						64					
25						65					
26						66					
27						67					
28						68					
29						69					
30						70					
31						71					
32						72					
33						73					
34						74					
35						75					
36						76					
37						77					
38						78					
39						79					
40						80					

ACTIVE SHEET RECORD

SHEET NUMBER	REV LTR	ADDED SHEETS				SHEET NUMBER	REV LTR	ADDED SHEETS			
		SHEET NUMBER	REV LTR	SHEET NUMBER	REV LTR			SHEET NUMBER	REV LTR	SHEET NUMBER	REV LTR
80						120					
81						121					
82						122					
83						123					
84						124					
85						125					
86						126					
87						127					
88						128					
89						129					
90						130					
91						131					
92						132					
93						133					
94						134					
95						135					
96						136					
97						137					
98						138					
99						139					
100						140					
101						141					
102						142					
103						143					
104						144					
105						145					
106						146					
107						147					
108						148					
109						149					
110						150					
111						151					
112						152					
113						153					
114						154					
115						155					
116						156					
117						157					
118						158					
119						159					

ACTIVE SHEET RECORD

SHEET NUMBER	REV LTR	ADDED SHEETS				SHEET NUMBER	REV LTR	ADDED SHEETS			
		SHEET NUMBER	REV LTR	SHEET NUMBER	REV LTR			SHEET NUMBER	REV LTR	SHEET NUMBER	REV LTR
160											
161											
162											
163											
164											
165											
166											
167											
168											
169											
170											
171											
172											
173											
174											
175											
176											
177											
178											
179											
180											
181											
182											
183	A										
184											
185	A										
186	A										

REVISIONS

LTR	DESCRIPTION	DATE	APPROVAL
A	Pages 1, 2, 12, 13 for contractual clarification	8-20-68	J. M. Carter 5-2940